Biochemical and X-ray crystallographic studies on the energy transducing protein TonB and the TonB-dependent siderophore receptor FhuA from *Escherichia coli*

A dissertation submitted to the
UNIVERSITY OF KONSTANZ
for the degree of
DOCTOR OF NATURAL SCIENCES

presented by
JIRI FRANZ KÖDDING

Konstanz 2004

Dissertation der Universität Konstanz
Tag der mündlichen Prüfung: 15.12.2004

Referent: Prof. Dr. Wolfram Welte
Referent: Prof. Dr. Peter Kroneck

This work is dedicated to

my dear Mother who passed away in 2002

Table of contents

Table of contents

List of Figures

List of Tables

This PhD thesis is based on the following publications:

Ferguson, A.D., **Ködding, J**., Walker, G., Bös, C., Coulton, J.W., Diederichs, K., Braun, V., and Welte, W. (2001) Active transport of an antibiotic rifamycin derivative by the outer-membrane protein FhuA. *Structure* **9**, 707 – 716

Koedding, J., Howard, S.P., Kaufmann, L., Polzer, P., Lustig, A., and Welte, W. (2004) Dimerization of TonB is not essential for its binding to the outer membrane siderophore receptor FhuA of Escherichia coli. *J. Biol. Chem*. **279**, 9978 – 9986

Koedding, J., Polzer, P., Killig, F., Howard, S.P., Gerber, K., Seige, P., Diederichs, K., and Welte, W. (2004) Crystallization and preliminary X-ray analysis of a C-terminal TonB fragment from Escherichia coli. *Acta Cryst*. **D60**, 1281 - 1283

Koedding, J., Killig, F., Polzer, P., Howard, S.P., Diederichs, K., and Welte, W. (2004) Crystal structure of a 92-residue long C –terminal fragment of TonB from Escherichia coli reveals significant conformational changes compared to structures of smaller TonB-fragments. *J. Biol. Chem. (in press)*

1. Zusammenfassung

Die Zellwand gram–negativer Bakterien beinhaltet viele Proteine die für den Transport lebenswichtiger Substanzen verantwortlich sind. Vor allem die Äußere der beiden Lipidmembranen erfüllt eine wichtige Schutzfunktion, die besondere Anforderungen an die Transportsysteme der äußeren Membran stellt. Die direkte Aufnahme von Eisen stellt ein besonderes Problem dar, da die Konzentration an freien Eisenionen in wässriger Lösung sehr gering ist. Bakterien haben dieses Problem durch spezifische Transportwege für eine ganze Anzahl von chemisch verschiedenen Siderophoren gelöst. Siderophore sind Moleküle von etwa 600 Da, die Eisenionen aus der Umgebung der Zelle komplexieren und zum Teil von den Bakterien selbst synthetisiert und sekretiert werden. Eines dieser Siderophore ist Ferrichrome das pilzlichen Ursprungs ist und in *Escherichia coli* durch das Transportprotein FhuA (ferric hydroxamate uptake system) über die äußere Membran ins Periplasma aufgenommen wird. Einige Phagen wie T1, T5, Φ80 und UC-1 nutzen FhuA als Bindeprotein an *E. coli*. Auf der anderen Seite stellt FhuA auch einen wichtigen Aufnahmeweg für einige Antibiotika dar, wie für das chemisch dem Ferrichrom verwandte Albomyzin oder für das strukturell ganz anders aussehende Rifamycin Derivat CGP 4832. Die Energie, die für diese spezifische Aufnahme durch FhuA gebraucht wird, stammt von der chemischen Potentialdifferenz an der inneren Bakterienmembran, hervorgerufen durch einen H^+-Konzentrationsradienten. Die Übertragung der Energie von der inneren Membran auf FhuA erfolgt durch den Proteinkomplex ExbB/ExbD/TonB. Alle drei Proteine sind in der inneren Membran verankert, wobei der größte Teil von TonB ins Periplasma ragt und mit seiner C-terminalen Domaine den eigentlichen Kontakt zu FhuA herstellt. Da TonB eine große Anzahl homologer Außenmembran-Transporter mit der nötigen Energie versorgt, wird diese Klasse von Proteinen, im Gegensatz zu den ABC-Transportern, als „TonB-abhängige“ Transporter bezeichnet.

Die dreidimensionalen Röntgenstrukturen von einigen TonB-abhängigen Transportproteinen sind mittlerweile bekannt. Für die vorliegende Arbeit ist die Struktur von FhuA (Ferguson et al., 1998) von besonderer Bedeutung. Ebenfalls bekannt sind einige Strukturen von FhuA mit verschiedenen Liganden wie Ferrichrome, Phenylferrichrome, Albomyzin und Rifamyzin CGP 4832. Die Strukturlösung des FhuA-CGP 4832 Komplexes ist Teil der vorliegenden Arbeit (Kapitel 3).

TonB, das aus 239 Aminosäuren besteht, wurde erstmals nur als Fragment der letzten 85 C-terminalen Aminosäuren kristallisiert (Chang et al., 2001). Dieses TonB-85 Fragment zeigt ein Homodimer, dessen funktionelle Rolle im Prozess der Energieübertragung unbekannt blieb.

Im Verlauf der vorliegenden Arbeit wurden unterschiedlich lange C-terminale Fragmente von TonB aus *E. coli* überexprimiert und gereinigt, bestehend aus 77, 86, 88, 90, 92, 94, 96, 106, 116 und 126 Aminosäuren. Die Kristallisation und Strukturanalyse konnte für zwei TonB Fragmente erfolgreich durchgeführt werden: TonB-77 zeigt eine Dimerenstruktur, identisch mit der von TonB-85 (Kapitel 4). TonB-92 bildet dagegen eine signifikant andere Struktur (Kapitel 5 und 6). Diese unterschiedlichen Strukturen sind im Einklang mit dem Verhalten dieser Fragmente in Lösung: Die kürzeren Fragmente liegen als Dimere und die längeren Fragmente als Monomere vor. Für ein weiteres Verständnis der FhuA-TonB Wechselwirkung wurde die Fähigkeit der TonB Fragmente untersucht, *in vitro* an FhuA zu binden. Es stellte sich heraus, daß die gleichen Fragmente, die in der Lage sind FhuA zu binden, auch die Ferrichromaufnahme *in vivo* blockieren und die Zellen vor dem Angriff durch Bakteriophagen Φ80 schützen (Kapitel 4).

Alle Versuche, die gereinigten Proteinkomplexe aus FhuA und den C-terminalen TonB-Fragmenten zu kristallisieren, waren bisher erfolglos.

2. General Introduction

2.1. Abstract

A large number of proteins are involved in the transport of essential compounds across the cell wall of gram-negative bacteria. The very low concentration of free iron ions in aqueous solutions makes the use of specific uptake systems necessary. One transport system of the outer membrane of *Escherichia coli* is the protein FhuA (uptake of ferric hydroxamate). FhuA is a specific transporter for the iron chelating molecule ferrichrome. Several low molecular weight compounds called siderophores that scavange iron from the external environment have already been reported in the literature. The 3D-structures of both FhuA alone and in complex with its siderophore were solved by A. Ferguson in 1998 (Ferguson et al., 1998b). FhuA also serves as the primary receptor for several antibiotics like the rifamycin derivative CGP 4832 that is structurally not related to hydroxamate–type siderophores. We have solved the crystal structure of FhuA in complex with CGP 4832 (Ferguson et al., 2001). The energy required for the transport process is provided by the proton motive force of the cytoplasmic membrane and is transmitted to FhuA by the protein TonB. TonB forms a large protein complex with ExbB and ExbD. The structure of full length TonB is not known, however, the structure of the last 86 C-terminal amino acid residues of TonB is available in the literature (Chang et al., 2001). TonB–86 crystallized as an intertwined homodimer. The functional role of this dimer in the process of energy transduction remains completely unknown.

During the course of my Ph.D. thesis I purified several C-terminal fragments of TonB from *E. coli* consisting of 77, 86, 88, 90, 92, 94, 96, 106, 116 and 126 amino acid residues, respectively, and tried to crystallize them. TonB-77 was successfully crystallized and its 3D-structure could be determined. The structure of TonB-77 presents a homodimer, very similar to the recently published TonB-86 structure (Koedding et al., 2004a). We were also able to crystallize TonB–92 and to collect a native X –ray diffraction data-set at 1.09 Å resolution (Koedding et al., 2004b). The selenomethionine–substitution method was used to obtain the phase information needed for a successful determination of the 3D structure of TonB–92. A comparison of TonB–92 with TonB–86 shows significant differences between the two structures (Koedding et al., 2004c). This finding is in agreement with my previous results concerning the behaviour of the purified TonB-fragments in solution. The shorter fragments behave dimeric, whereas the longer fragments behave monomeric in solution. For a more detailed understanding of the FhuA-TonB interaction I analysed the ability of the truncated C-

terminal TonB-fragments to bind to the outer membran receptor FhuA. TonB-fragments that bind to FhuA *in vitro* also inhibit ferrichrome uptake via FhuA *in vivo* and protect cells against attack by bacteriophage Φ80 (Koedding et al., 2004a).
All attempts to crystallize purified FhuA–TonB protein complexes failed to this day.

2.2. Cell wall of gram-negative bacteria

The cell wall of gram-negative bacteria consists of two lipid bilayers, the outer membrane and the cytoplasmic membrane, enclosing the periplasmic space. The cytoplasmic membrane is a symmetric phospholipid bilayer that separates the cytoplasm from the periplasmic space (reviewed in Kadner, 1996). A lot of proteins are embedded in the cytoplasmic membrane and are involved in energy-dependent transport of metabolites, electron transport, protein and carbohydrate translocation, transmembrane signalling, cell motility and chemotaxis. The electron transport system and the production of ATP at the cytoplasmic membrane is directly linked to a charge separation across the membrane. This process leads to an accumulation of H^+ - ions in the periplasm, resulting in the generation of a pH gradient and an electrochemical potential across the cytoplasmic membrane. This energized state of the membrane is called the proton motive force (pmf) and is used as the main source of energy for several specific uptake systems located in the outer membrane. The energy transduction from the cytoplasmic membrane to the outer membrane is mediated by the ExbB/ExbD/TonB protein complex (Bradbeer, 1993; Larsen et al., 1999; Postle and Kadner, 2003).
The periplasm is a gel–like region of 12 – 15 nm in diameter build by peptidoglycan macromolecules. Peptidoglycan is a polysaccharide composed of alternating repeats of acetylglucosamine and acetylmuramic acid with the latter in adjacent layers cross-linked by short peptides. A lot of binding proteins in the periplasm regulate the transport of substrates from the outer membrane to the cytoplasmic membrane (reviewed by Ames, 1988).

An asymmetric bilayer forms the outer membrane of gram-negative bacteria (reviewed by Nikaido,1996) and is the first barrier between the environment and the cell. The extracellular leaflet of the bilayer is comprised entirely of lipopolysaccharide molecules (LPS or endotoxin). LPS is composed of three covalently linked domains differring by their genetic organization, biosynthetic pathways, chemical structures and biological features (reviewed by Raetz, 1996). These domains are
1) lipid A, a glycolipid acting as an amphiphilic anchor in the OM,
2) the core, a variable non-repeating hetero-oligosaccharide, and

3) the O-antigen, an immunogenic and highly variable polysaccharide that extends into the external medium.

The three dimensional structure of LPS from the bacterial strain *E.coli* K-12 in complex with the outer membrane protein FhuA by X-ray crystallography (Ferguson et al., 2000a). The *E.coli* K-12 strain has a gene defect resulting in an LPS chemotype lacking the O-antigene. LPS plays an important role in stimulating the innate (non–clonal) immune response. Furthermore, high doses of LPS can cause excessive release of inflammatory mediators and might lead to septic shock (reviewed by Medzhitov and Janeway,1997).

2.2. Outer membrane transporter

The outer membrane protects the bacterial cell from detrimental influence of antibiotics, degradative enzymes and other deleterious agents from the external environment (reviewed by Hancock, 1997). On the other hand, a lot of essential compounds have to be transported into the cell. To solve this permeability dilemma, gram-negative bacteria have developed different transport mechanisms carried out by three classes of channel-forming proteins that reside in the outer membrane (reviewed by Postle, 1990 „specific transporter“, Welte et al., 1995 „porins“ and Nikaido, 1996):

1. non –specific, so –called general diffusion, porins, which facilitate the diffusion of small solutes;
2. specific diffusion porins, which enhance the rate of diffusion by specific interaction;
3. energy-dependent specific receptors, which mediate the active transport of compounds that are found in very low concentrations in the environment.

Non –specific porins

The non–specific porins represent the major protein component of the outer membrane. They are water-filled channels that facilitate the passive diffusion of ions and other hydrophilic compounds with a typical exclusion limit of 600 Da. The non–specific porins show differences in the permeability of anions and cations. The expression of non –specific porins is often regulated by environmental conditions. For example, under phosphate –limiting conditions *E.coli* cells expresses the anion selective porin PhoE which mediates the diffusion of phosphate and phosphorylated compounds into the periplasm (Korteland et al., 1982).

The three dimensional structures of several non –specific porins have been determined by X-ray crystallography. Two of these are OmpF and PhoE from *E.coli* (Cowan et al., 1992). All

these structures assume a similar fold, a homotrimer that is formed by a 16-stranded antiparallel β-barrel. Each monomer forms a single transmembrane channel with 7 by 11 Å in diameter. A large extracellular loop, known as the „constriction loop“, folds into the barrel and reduces the free cross section of the channel to an extend that hydrated ions cannot pass it freely any longer (Welte et al., 1995). The distribution of charged residues inside the channel causes the ion selectivity. Two rings of aromatic amino acid residues with their side chains on the external side of the barrel mark the membrane-embedded surface of the protein. These two aromatic girdles are found in all porins and can be used for structure prediction of porins (Welte et al., 1991).

Specific porins

Some nutrients are too large to diffuse through non–specific porins. For this case, gram-negative bacteria have evolved specific porins to accelerate the rate of diffusion across the outer membrane. For example, in *E. coli*, LamB, Tsx and ScrY mediate the uptake of maltose, nucleosides and sucrose. These solutes diffuse passively through specific porins. The presence of a specific ligand-binding site leads to a Michaelis-Menten saturation kinetics at high solute concentrations (Benz et al., 1987).

Three dimensional structures of several specific porins have already been solved, for example LamB (Schirmer at al., 1995) and ScrY (Forst et al., 1998). Analogously to non–specific porins, LamB and ScrY form stable homotrimers in the outer membrane. Each monomer is formed by an 18-stranded antiparallel β-barrel. Longer extracellular loops and shorter periplasmic turns connect adjacent β-strands. The surface–exposed loops are involved in ligand–binding and transport (Anderson et al., 1999).

High-affinity receptors

Outer membrane receptors are used for the uptake of compounds that are found at exceedingly low concentrations in the external medium. These concentrations are too low for a sufficient – uptake rate by passive diffusion. Specific receptors bind their cognate ligand with high affinity and specificity ($K_D \sim 0.1\ \mu M$) followed by the transport of the ligand into the periplasm. This specific transport requires energy which comes from the proton motive force of the cytoplasmic membrane. The microbial iron acquisition is based on high-affinity receptors. The mechanism of energy–transduction for these processes is part of this thesis.

2.3. Iron acquisition of gram-negative bacteria

Iron as a cofactor plays an essential role in central metabolic processes including RNA synthesis and electron transport (Briat, 1992). Iron exists in two oxidized forms Fe^{2+}/ Fe^{3+} with a wide range of redox potentials from –300 to +700 mV, depending on the iron ligands and the environment. All organisms, with the exception of certain lactobacilli, take advantage of this unusually wide range of electron transport capacity. Despite its relative abundance in nature, iron is difficult to acquire by most organisms. Under oxic conditions and at the physiological pH of 7, the concentration of free ferric ions in equilibrium with the ferric hydroxide polymer is in the order of 10^{-18} M (Neilands et al., 1987). This very low concentration of free iron ions makes the use of special uptake mechanisms necessary. Therefore bacteria either synthesize and secrete iron-chelating compounds, called siderophores, and take up the ferric siderophores via highly efficient transport systems, or they take up iron chelated by compounds of their environment (reviewed by: Braun et al., 1991; Braun et al., 1998; Clarke et al., 2001). The iron siderophores with a molecular mass of 700 to 1000 Da are too large to diffuse through open porin channels.

Escherichia coli K-12 synthesizes six distinct siderophore-mediated ferric iron transport systems, each of them recognizing a single type of ferric siderophore (Figure 2.1). However, *E.coli* K-12 synthesizes only one siderophore, enterobactin (cyclic trimer of 2,3-dihydroxybenzoylserine). Figure 2.1 presents an overview of the proteins involved in ferric siderophore and vitamine B_{12} uptake across the outer membrane, the periplasm and the cytoplasmic membrane of *E.coli*.

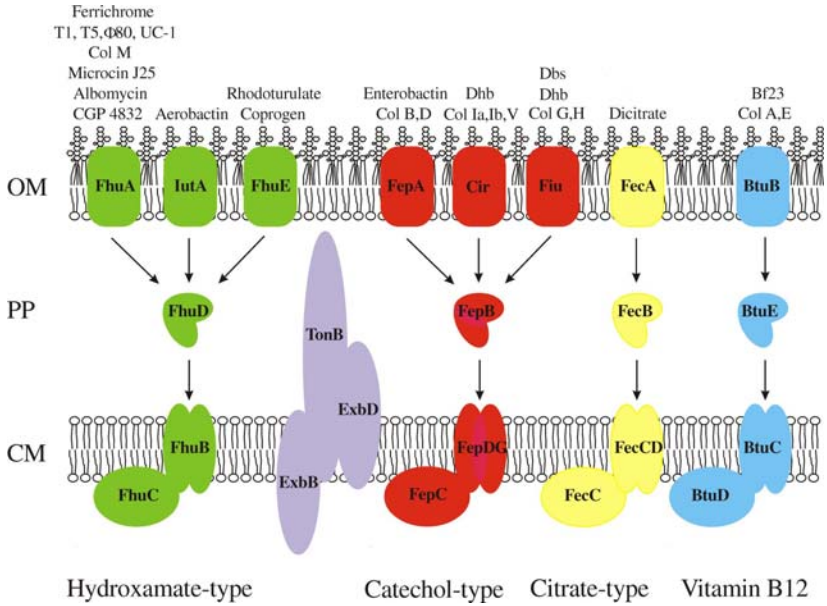

Figure 2.1. *Selected TonB-dependent uptake systems located in the cell wall of E.coli. Abbreviations: T1, T5, ϕ80 and UC-1 are bacteriophages; Col colicin; Dhb dihydroxybenzoate; Dbs dihydroxybenzoylserine; OM outer membrane; PP periplasm; CM cytoplasmic membrane.*

The specific outer membrane transport system for the siderophore enterobactin (also called enterocholin) is the protein FepA (Lundrigan and Kadner,1986). There are two transport systems for the biosynthetic precursors of enterobactin, Cir for the siderophore 2,3-dihydroxybenzoic acid (Curtis et al.,1985) and Fiu for the siderophore 2,3-dihydroxybenzoylserine (Nau and Konisky, 1989). Citrate is an exogenous siderophore for iron uptake that is not formed by *E.coli*. FecA is the ferric citrate transporter (Pressler et al., 1988). Two other siderophores are from fungal origin, ferrichrome transported by FhuA (Coulton et al., 1986) and coprogen transported by FhuE (Sauer et al., 1990).

Pathogenic *E.coli* strains frequently synthesize aerobactin and an aerobactin-specific transport protein IutA (Krone et al., 1985). All these water soluble compounds are coordinating Fe^{3+} -ions in an octahedral complex of high affinity and can be arranged into three classes depending

on their chemical structures: catechol - type, citrate – type and hydroxamate – type, including ferrichrome, coprogene and aerobactin, respectively.

The siderophores scavange Fe^{3+} -ions from the external medium or from host proteins and are bound by their distinct receptors, followed by their translocation into the periplasm by an energy dependent mechanism. The outer membrane does not maintain an electrochemical gradient. The energy comes from the proton motive force of the cytoplasmic membrane and is mediated by the protein complex ExbB/ExbD/TonB. TonB plays the role of the energy – transducing protein and combines the outer membrane receptor with the cytoplasmic membrane. Therefore all these uptake processes are called „TonB-dependent“ mechanisms. There are no experimental data available showing how the energy transduction –process occurs and for which molecular event the energy is needed. Most likely, the outer membrane transport proteins form closed channels and the energy –dependent step is the opening of the channel. The uptake of cyanocobalamine (vitamin B_{12}) is also TonB-dependent and is similar to the siderophore transport (Kadner and Heller, 1995). The vitamin B_{12} receptor in the outer membrane of *E.coli* is BtuB (Heller and Kadner, 1985).

Periplasmic binding proteins shuttle the siderophores across the periplasm to specific ABC-transporters in the cytoplasmic membrane: FhuD for hydroxamate-type siderophores (Koster and Braun, 1990; Clarke et al., 2002), FepB for the catechol-type siderophores (Stephens et al., 1995; Sprencel et al., 2000), FecB for the citrate-type siderophores (Hussein et al., 1981) and BtuE for vitamin B_{12} (deVeaux et al., 1986). The transport across the cytoplasmic membrane is less specific than across the outer membrane. Unlike the number of the different outer membrane receptors (seven or eight) there are only four different periplasmic binding proteins belonging to four different ABC –transporters in the cytoplasmic membrane (Nikaido and Hall, 1998) (Figure 2.1).

It is assumed that after transport of the siderophore into the cytoplasm, Fe^{3+} is released from the siderophore by being reduced to Fe^{2+}, which has a much lower affinity than Fe^{3+} to the siderophore (Koster, 1991). For this transition, a lot of siderophore reductase activity have been detected *in vitro* (Fischer et al., 1990). The cytoplasmic protein FhuF of *E. coli* containing a [2Fe-2S] center is involved in the process of iron reduction (Müller et al., 1998; Matzanke et al., 2004).

The three dimensional structures of several TonB-dependent outer membrane receptors of *E.coli* were determined by X-ray crystallography (reviewed by Ferguson and Deisenhofer, 2002): FhuA (Ferguson et al., 1998b, Locher et al., 1998), FepA (Buchanan et al., 1999), FecA (Ferguson et al., 2002) and BtuB (Chimento et al., 2003). All these structures show similar

molecular architecture composed of a β-barrel-domain and a globular domain (plug or cork) filling the barrel interior. The β-barrel is formed by 22 antiparallel β-strands connected by short periplasmic turns and longer extracellular loops.
The structurally best characterized transport system so far is the cobalamin uptake by BtuB in *E. coli* (reviewed by Locher and Borths, 2004). Recently the structure of the inner membrane ABC transporter BtuCD (Locher et al., 2002) and of the periplasmic binding protein BtuF (Borths et al., 2002) have also been solved.

2.4. The outer membrane siderophore receptor FhuA of *E.coli*

FhuA is an outer membrane receptor for ferric hydroxamate uptake, an integral membrane protein composed of 714 amino acid residues (Coulton et al., 1986). In addition to binding of the ferric siderophore ferrichrome-iron, FhuA also serves as the primary receptor for several bacteriophages (T1, T5, Φ80 and UC-1), the bacteriotoxin colicin M and the antibiotics albomycin, microcin J25 and CGP 4832. The binding of ferrichrome-iron to FhuA induces conformational changes (Moeck et al., 1996) signalling the ligand-loaded status of the receptor. This signal seems to be a requirement for TonB-dependent energy transduction (Moeck et al., 1997). The crystal structures of unliganded FhuA and of FhuA in complex with ferrichrome (Ferguson et al., 1998b; Locher et al., 1998) allow a deep insight into the molecular architecture of TonB-dependent receptors as well as into their mechanism of ligand binding. The structure of FhuA presents a monomeric integral membrane protein organized into two domains that behave autonomously with distinct unfolding temperatures of 65 and 75°C, respectively (Bonhivers et al., 2001). The C-terminal domain, including residues 161 – 714, forms a 22-stranded antiparallel β-barrel that spans the outer membrane. Two girdles of aromatic residues located at the outer surface of the barrel extend into the lipid bilayer and delineate the border between the hydrophobic chains and the polar headgroups of the lipids. These aromatic girdles are found in all outer membrane porins. In the crystal structure of FhuA solved by Ferguson et al. in 1998 (Ferguson et al. 1998) a single LPS–molecule is non – covalently associated with the membrane–embedded surface of the protein giving us an image of the extent of the lipid bilayer (see Figure 2.2). This was the first crystal structure of a protein–lipopolysaccharide complex (Ferguson et al., 2000a). The hydrogen–bonds and electrostatic interactions between FhuA and the LPS are provided by eight positively charged residues of FhuA.

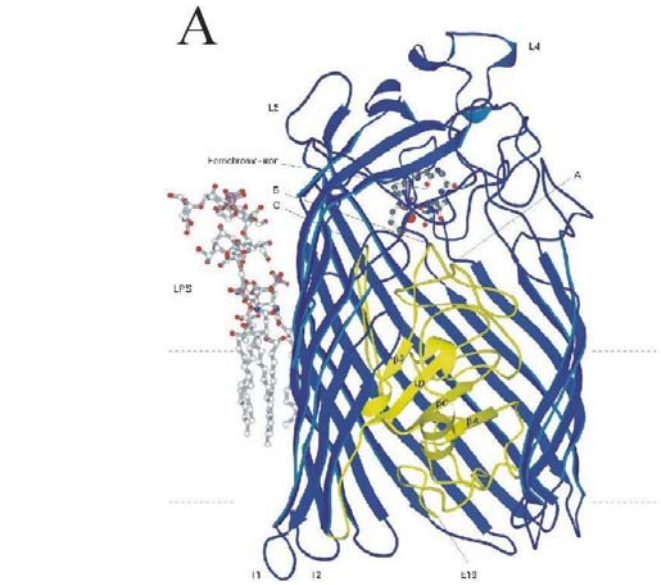

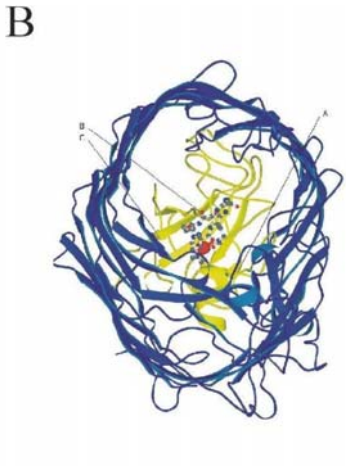

Figure 2.2. *Overall structure of the FhuA – ferrichrome – LPS complex as published by Ferguson et al., 1998b. The β-barrel is shown in blue and the cork–domain in yellow. The LPS and ferrichrome molecules are represented as ball-and stick models with the iron-ion as a larger red sphere. A, B and C mark the position of the residues Arg^{81}, Gln^{100} and Tyr^{116} of the cork–domain involved in ligand binding. (A) side–view onto FhuA with the LPS molecule. The two large surface - located loops are indicated with L4 and L5, respectively. The dotted lines show the position of the aromatic girdles. (B) View onto FhuA from the external environment.*

Adjacent β-strands are connected by 11 solvent–accessible loops at the external membrane surface and 10 short turns directed toward the periplasm. Residues 236 – 248 of loop 3 belong to the ferrichrome–binding site, whereas loop 4 (residues 318 – 339) plays a role in targeting the ligand from the environment to its binding site.

The C-terminal domain of FhuA (residues 1 – 160), the so called cork–domain, fills the barrel interior and closes the channel. As seen in Figure 2.2 the cork domain mainly consists of a mixed four–stranded β sheet (βA to βD). Residues of the external loops, the barrel and the cork domain (see regions A, B and C in Figure 2.2) form a large pocket filled with a single ferrichrome molecule in the ligand – loaded structure. These residues are strongly conserved in the sequence alignment of ferrichrome–iron receptors from *E.coli*, *Pantoea agglomerans*, *Salmonella paratyphi* and *Salmonella typhimyrium* (Killmann et al., 1998).

At the periplasmic side of the cork domain resides another peptide motif (residues 7 –11) that is highly conserved among all TonB–dependent receptors (DTITV in FhuA, DALTV in FecA, DTIVV in FepA, and DTLVV in BtuB). This motif plays an important role in the receptor–TonB interaction and is called the TonB–box (Larsen et al., 1997; Cadieux and Kadner 1999). This direct interaction of TonB with the outer membrane receptor was first demonstrated by cross– linking studies using FepA. When treated with formaldehyde, FepA can be chemically cross– linked to TonB in the absence of ferric enterobactin (Skare et al., 1993). Similar cross–linking experiments have been carried out with FhuA both in presence and in absence of ferrichrome (Moeck et al., 1997). The formation of the FhuA–TonB complex is dependent upon the binding of ferrichrome to FhuA and could not be detected in the absence of the siderophore *in vivo*. Direct physical interactions between the TonB-box of the receptor and TonB was also examined by site-directed disulfide cross–linking experiments. Cysteine residues introduced at successive positions within the TonB-box of BtuB form disulfide bridges with a single cysteine residue inserted at or near to position 160 of TonB (Cadieux and Kadner, 1999).

The TonB–box is not visible in the electron density map of the FhuA structures. Considering that seemingly invariant TonB-box residues can be mutated without affecting function, it is likely that it is the conformation rather than the primary structure of the TonB-box that is required for efficient energy transduction (Ogierman and Braun, 2003). Accordingly, point mutations presumably distort the conformation of the TonB-box or adjacent regions of TonB–dependent receptors, such that specific protein – protein interactions with TonB are impaired. Close to the TonB–box of FhuA, resides a short α - helix (residues 24 – 29) called switch – helix only observed in the unliganded form of FhuA. In the structure of FhuA in complex with

ferrichrome this short α-helix is unwound and the residue Glu^{19} is placed 17 Å away from the position it had in the unliganded structure (Figure 2.3, Panel A compared to Panel C). These conformational changes were also observed in the fluorescence pattern of Trp^{22} that decrease after addition of ferrichrome iron (Locher and Rosenbusch, 1997). The „switch–helix“ is also found in the structure of FecA (Ferguson et al., 2002) but it is not a conserved structure motif among all TonB–dependent receptors, since neither BtuB nor FepA possesses one (Chimento et al., 2003).

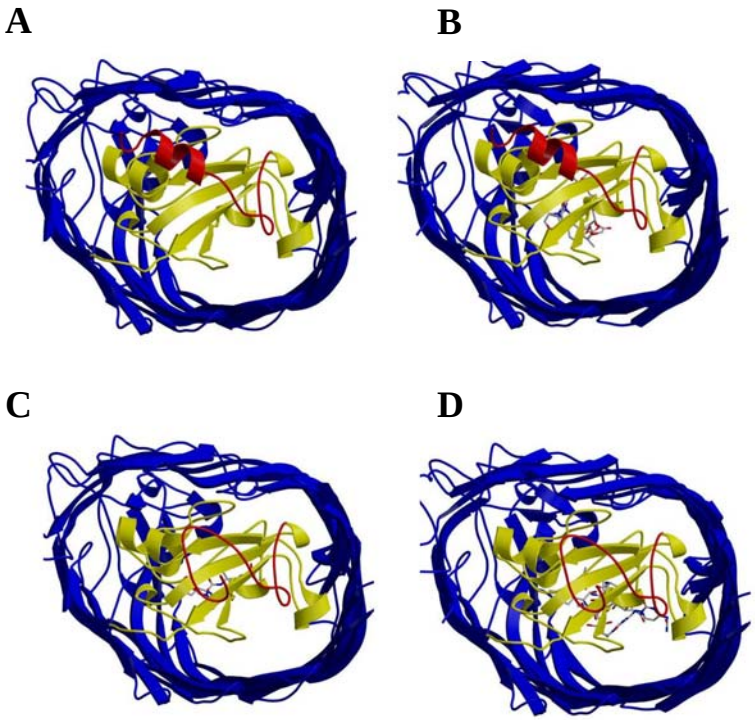

Figure 2.3. *Periplasmic view onto the three dimensional structure of FhuA with different compounds in the external binding site, Panel A: unliganded Fhu. Panel B: FhuA in complex with CGP 4832. Panel C: FhuA in complex with its siderophore ferrichrome. Panel D: FhuA in complex with albomycin. The barrel domain of FhuA is coloured in blue and the cork–domain is shown in yellow. The N–terminus containing the switch–helix (residues 24 – 29) is shown in red.*

The crystal structure of FhuA in complex with the ferrichrome–related antibiotic albomycin presents an unwound conformation of the switch–helix (Ferguson et al., 2000b). The behaviour of the switch–helix is strongly influenced by the kind of the molecular interaction the ligand forms with FhuA. The antibiotic CGP 4832 is chemically unrelated to albomycin but is also transported into the bacterial cell via FhuA. The switch–helix remains intact after complex formation of CGP 4832 with FhuA and is discussed in chapter 3 (Ferguson et al., 2001). Figure 2.3 shows a comparison of FhuA in complex with different ligands viewed from the periplasmic side. A superposition of the ligand–free and the ligand–loaded structure of FhuA reveals two differences: Large conformational changes at the periplasmic side of the cork domain and a transition of all loops of this domain towards the ferrichrome–binding site. On the other hand, the barrel–domain and the four stranded β-sheet of the cork remain stationary. These conformational changes were proposed to be a mechanism for signalling the ligand–loaded status of the receptor to the periplasmic TonB. A mechanism of ferrichrome transport through the FhuA channel into the periplasm and the possible interaction with TonB cannot be seen in the crystal structures and remains completely unclear.

2.5. Active transport of antibiotics by the outer membrane receptor FhuA of *E.coli*

Apart from the ferrichrom–uptake across the outer membrane FhuA also serves as the primary receptor for antibiotics (Braun and Braun, 2002). The binding of two antibiotics, albomycin and rifamycin CGP 4832 to FhuA, has been studied recently: Albomycin is a broad–spectrum antibiotic with a minimal inhibitory concentration for *E.coli* K-12 that is 100-fold lower than that of ampicillin (minimal inhibitory concentration of 0.005 μg/ml, compared to 0.1 μg/ml for ampicillin; Pugsley et al., 1987). Albomycin is composed of a trihydroxamate that binds Fe^{3+}, a peptide linker and a thioribosyl pyrimidine moiety that confers the antibiotic activity (see Figure 3.8 and 3.3b). The structural similarity of albomycin to the natural siderophore ferrichrome is responsible for the specific uptake via FhuA across the outer membrane, the affinity to the periplasmic binding protein FhuD and the transport across the cytoplasmic membrane via the FhuB/C system. After transport into the cytoplasm, iron is released from albomycin and the antibiotically active thioribosyl pyrimidine group has to be cleaved by peptidase N (Braun et al., 1983). The three dimensional structure of a FhuA – albomycin complex is available and was the first crystal structure of an antibiotic protein transporter (pdb-accession code 1qkc; Ferguson et al., 2000b).

This complex structure is very similar to the structure of FhuA with bound ferrichrome (pdb-accession code 1fcp; Ferguson et al., 1998b) with the difference of an albomycin molecule instead of ferrichrome in the external binding site.

Another antibiotic compound that is actively transported into the periplasm by FhuA is the semisynthetic rifamycin–derivative CGP 4832 (Ciba Geigy Product) (see 3.8. figure 3.3a). The chemically related antibiotic rifampicin is at least 200 times less active than CGP 4832 against *E.coli* and related bacteria. The increased activity of CGP 4832 correlates with its ability to be specifically transported into the periplasm by FhuA (Pugsley et al., 1987). In contrast to albomycin, CGP 4832 is not actively transported across the cytoplasmic membrane by FhuBCD (Pugsley et al., 1987). The periplasmic binding protein FhuD and the cytoplasmic embedded permease FhuBD effectively discriminate between rifamycin CGP 4832 and the diverse hydroxamate–type siderophores and antibiotics that are transported by this system (Braun et al., 1998). Since the chemical structure of this rifamycin derivative differs markedly from that of ferric hydroxamates or albomycin, we determined the three dimensional crystal structure of FhuA in complex with rifamycin CGP 4832 (Ferguson et al., 2001). The structure shows rifamycin CGP 4832 located at the same ligand–binding site of FhuA as ferrichrome or albomycin. These specific interactions in the ligand–binding site between FhuA and CGP 4832 answer the question why the rifamycin derivative CGP 4832 can be transported via FhuA.

2.6. The energy transducing protein TonB of *E.coli*

The energy for the specific uptake systems in the outer membrane comes from the proton motive force of the cytoplasmic membrane and is mediated by the protein complex ExbB, ExbD and TonB (Bradbeer, 1993; Letain and Postle, 1997; Larsen et al., 1999; Postle and Kadner, 2003; Larsen et al., 2003). ExbB/D is located in the cytoplasmic membrane whereas TonB is attached to the membrane by an N–terminal hydrophobic anchor (Postle, 1993). The ratio of the copies of each protein in the protein complex TonB : ExbD : ExbB was found to be 1 : 2 : 7 (Higgs et al., 2002a/b). The major part of TonB spans the periplasmic space to reach the outer membrane receptor.

The TonB protein of *E.coli* is composed of 239 amino acid residues with 17 % proline residues mainly located between residues 75 and 107, a region predicted to span the periplasmic space to link the outer membrane to the cytoplasmic membrane (Postle and Skare, 1988). The elongated conformation of this proline–rich region has been demonstrated by NMR studies (Evans et al., 1986; Brewer et al., 1990). However, cells expressing a deletion mutant of TonB

(TonBΔ66 – 100) display near wild-type levels of TonB-dependent activity (Larsen et al., 1993). These results indicate that the proline–rich region is not essential for TonB–dependent function. Two other significant regions can be distinguished and were contributed in distinct ways to the function of TonB as an energy transducer (Traub et al., 1993):

1) A hydrophobic region at the N–terminus (residues 1 – 32) anchoring TonB to the cytoplasmic membrane (Postle and Skare, 1988). Residues 12 to 32 are postulated to assume an α-helical conformation. Four residues of this transmembrane helix Ser^{16}, His^{20}, Leu^{27} and Ser^{31}, are highly conserved and form the so called „SHLS – motif". This motif was found to be essential for the interaction with the membrane embedded protein ExbB (Larsen and Postle, 2001).

2) The C – terminal domain (residues 102 – 239) forming contact to the outer membrane receptor. Site–directed disulfide cross–linking experiments between TonB and BtuB were successful with cysteine residues mutated at or near position 160 of TonB (Cadieux and Kadner, 1999; Merianos et al., 2000). This region of TonB, specifically residues 160 to 167, most likely mediates a conformation–dependent interaction with TonB–dependent receptors (Günther and Braun, 1990). This finding was supported by the observation that synthetic nonapeptides with sequence identity to the amino acid region between residues 150 and 166 of TonB are able to inhibit the capacity of FhuA to transport ferrichrome *in vivo* (Killmann et al., 2002). Residues 199 – 216 were predicted to form an amphipathic α-helix (Larsen et al., 1993). This structure prediction was confirmed by the first three dimensional crystal structure of a truncated TonB–fragment containing the last 86 C–terminal amino acid residues (residues 155 – 239) (Chang et al., 2001). As seen in Figure 2.4 the structure reveals a cylinder shaped dimer. Each monomer contains three β-strands and a short α-helix arranged in a dimer so that the six β-strands build a large antiparallel β-sheet. The first 10 amino acid residues of this fragment are not visible in the electron density map due to their flexibility. We were able to solve the structure of a shorter C-terminal fragment of TonB containing 77 amino acid residues (chapter 4: Koedding et al., 2004a).

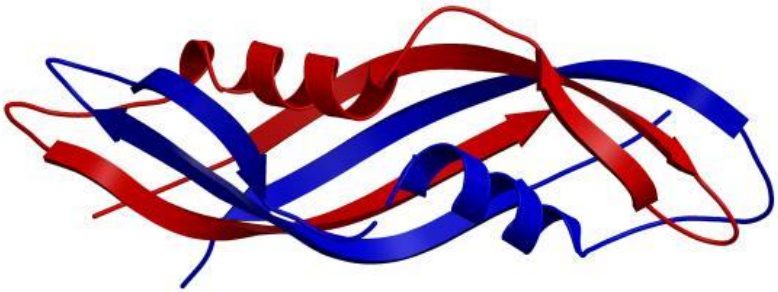

Figure 2.4. *Ribbon diagram of the C-terminal fragment of TonB (TonB-86) from Chang et al., 2001, showing an intertwined dimer. One monomer is shown in red and the other one in blue. The atomic coordinates are from the Protein Data Bank (acession code: 1IHR).*

In the absence of ExbB and ExbD bacterial cells retain a residual level of TonB–dependent activity that results from the presence of the protein complex TolQ/TolR, a functional analogue of the ExbB/ExbD–complex of *E.coli* (Braun, 1989). TolQ and TolR are embedded in the cyroplasmic membrane and are associated with a membrane anchored protein TolA that mediates a contact to the outer membrane across the periplasm, similar to TonB. (Koebnik, 1993). The biological function of the Tol Q/R/A-complex, however, is still unclear. Although the primary structures of TonB and TolA are not homologous, their predicted secondary structures and ultimately their 3D-structures were predicted to be similar (Braun and Herrmann, 1993; Cascales et al., 2001). This similarity was not confirmed by the crystal structure of the C-terminal domain of TolA from *E.coli* in complex with the bacteriophage coat protein g3p that has recently been determined (Lubkowski et al., 1999). In contrast to TonB-86 and TonB-77 the C-terminal domain of TolA presents a monomeric structure forming a three–stranded antiparallel β-sheet that is flanked by four α-helices positioned on one side of the β-sheet. This three dimensional arrangement was confirmed by the crystal structure of a C-terminal domain of TolA from *Pseudomonas aeruginosa* that has been solved recently (Witty et al., 2002). In spite of a sequence identity of only 20 % (Lalign server) to the corresponding domain of TolA from *E. coli*, the structures of the two TolA molecules are remarkably similar (see Figure 2.5).

A structure-based alignment of the C-terminal domains of TolA from *P.aeruginosa* with TonB from *E.coli* leads to sequence identity of 18 % (Witty et al., 2002). Residues in the loop between β-strands β1 and β2 are highly conserved among all available TolA and TonB homologues and form the so called PDG – loop (Pro^{184} – Asp^{185} – Gly^{186} in TonB from *E.coli*). A specific function of the PDG-loop has not yet been observed. Both TolA and TonB possess the secondary structure pattern β-β-α-β but they differ topologically and their structural relationship is not apparent at first sight. A more detailed description of the structural relationship is given in chapter 4 of this thesis (Koedding et al., 2004a). We were able to crystallize and to solve the structure of a new C-terminal fragment of TonB (TonB-92). The structure of TonB-92 presents a dimer with a different fold compared to TonB-77 and TonB-86, however each monomer shares structural homologies to TolA (chapter 6, Koedding et al., 2004c).

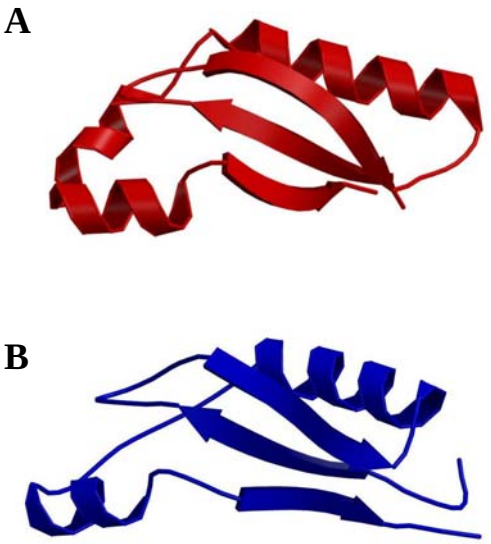

Figure 2.5 *Panel A: Ribbon diagram of the C-terminal domains of TolA from (panel A, coloured in red) Pseudomonas aeruginosa (Witty et al., 2002). Panel B: Ribbon diagram of the C-terminal domains of TolA from E. coli (Lubkowski et al., 1999). TolA from E. coli was solved in complex with the phage g3p protein that is not shown here.*

3. Active transport of an antibiotic rifamycin derivative by the outer membrane protein FhuA

Andrew D Ferguson[1,2,3], Jiri Ködding[1], Georg Walker[4], Christoph Bös[4], James W Coulton[3], Kay Diederichs[1], Volkmar Braun[4] and Wolfram Welte[1*]

1 Fakultät für Biologie, Universität Konstanz, M656, D-78457 Konstanz, Germany

2 Howard Hughes Medical Institute, Department of Biochemistry, University of Texas Southwestern Medical Center, 5323 Harry Hines Boulevard Y4-206, Dallas, Texas 75390-9050 U.S.A.

3 Department of Microbiology and Immunology, McGill University, 3775 University Street, Montréal, Québec, Canada H3A 2B4

4 Lehrstuhl Mikrobiologie / Membranphysiologie, Universität Tübingen, Auf der Morgenstelle 28, D-72076 Tübingen, Germany

published in Structure (2001) Vol. 9, 707 – 716

3.1. Summary

Background

FhuA, an integral membrane protein of *Escherichia coli*, actively transports ferrichrome and the structurally related antibiotic albomycin across the outer membrane. The transport is coupled to the proton motive force, which energizes FhuA through the inner-membrane protein TonB. FhuA also transports the semisynthetic rifamycin derivative CGP 4832, although the chemical structure of this antibiotic differs markedly from ferric hydroxamates.

Results

X-ray crystallography revealed that rifamycin CGP 4832 occupies the same ligand-binding site as ferrichrome and albomycin, demonstrating a surprising lack of selectivity. However, deviant from the complexes of FhuA with hydroxamate-type ligands, binding of rifamycin CGP4832 does not result in the unwinding of the switch helix but only in its destabilization as reflected by increased B-factors. Unwinding of the switch helix is proposed to be required for efficient binding of TonB to FhuA, and to couple the proton motive force of the cytoplasmic membrane with energy-dependent ligand transport. Transport data from cells expressing mutant FhuA proteins indicated conserved structural and mechanistic requirements for the transport of both types of compounds.

Conclusions

We conclude that binding of rifamycin CGP 4832 destabilizes the switch helix and promotes the formation of a transport-competent FhuA-TonB complex, albeit with lower efficiency than ferrichrome. Active transport of this rifamycin derivative explains the 200-fold increase in potency compared to rifamycin, which is not a FhuA-specific ligand and permeates across the cell envelope by passive diffusion only.

3.2. Introduction

Uptake of antimicrobial agents across the outer membrane of Gram-negative bacteria is mediated by a family of transport proteins employing a variety of mechanisms. Small hydrophilic solutes, primarily ions and sugars, are taken up into the periplasm by passive diffusion through nonspecific and substrate-specific porins. The structural architecture of bacterial porins with their apparent exclusion limit of approximately 600 Da, and the electrostatic arrangement of charged side-chains lining porin channels, contribute to the exclusion of antibiotics from the cell interior [Welte et al., 1995]. Essential molecules (> 600 Da) present only at low concentrations, including siderophores and vitamin B_{12}, are actively transported across the cell envelope. With the exception of the Donnan potential, no permanent electrical or chemical potential difference can be maintained across the outer membrane. Moreover, no source of energy has been localized in the periplasm. The chemical energy needed to drive these energy-dependent transport processes is provided by the electrochemical proton gradient maintained across the cytoplasmic membrane [Bradbeer, 1993]. The energy-transducing TonB-ExbB-ExbD complex couples the proton motive force of the cytoplasmic membrane to a family of diverse outer membrane proteins, the TonB-dependent transporters. In *Escherichia coli*, the ferric hydroxamate uptake receptor, FhuA, actively transports the siderophores ferrichrome and ferricrocin, the cyclic peptide antibiotic microcin J25, the siderophore-antibiotic conjugate albomycin, and the bacterial toxin, colicin M, across the outer membrane [Braun et al., 1998]. FhuA also functions as the primary receptor for bacteriophages T1, T5, Φ80 , and UC-1.

The determination of the three-dimensional structure of FhuA was an important step towards understanding the intricate structure-function relationships of this receptor and its energy-dependent transport mechanism [Ferguson et al., 1998b; Locher et al., 1998; Ferguson et al., 2000b]. FhuA is composed of two domains. A 22-stranded β-barrel (residues 161-714) spans the outer membrane; longer extracellular loops and shorter periplasmic turns connect adjacent antiparallel transmembrane β-strands. Part of the barrel interior is occluded by the cork domain, an amino terminal globular domain (residues 1-160) composed of a mixed four-stranded β-sheet and a series of short α-helices. The residues that compose the ligand-binding site are located within a non-occluded portion of the β-barrel, which is accessible from the external solvent.

FhuA possesses high-affinity but limited structural specificity for hydroxamate-type siderophores including ferrichrome, a cyclic hexapeptide composed of three δ-*N*-acetyl-L-δ-*N*-hydroxyornithine and three glycine residues. Structural alteration of the iron-chelating portion of this siderophore abrogates receptor-specific recognition [Jurkevitch et al., 1992]. In contrast, structural analogues of ferrichrome that possess identical iron-chelating and distinct hydrophobic peptide linkers, including ferricrocin and albomycin, are bound and transported by FhuA. Because albomycin is actively transported across both the outer and cytoplasmic membranes, it is one of the most potent antibiotics against *E. coli* [minimal inhibitory concentration (MIC) of 0.005 µg/ml]. The three-dimensional structure of FhuA in complex with albomycin [Ferguson et al., 2000b] confirmed that this antibiotic occupies the same ligand-binding site as ferrichrome, ferricrocin, and phenylferricrocin. This similarity extends to the set of residues involved in ligand binding, which are essentially conserved between these hydroxamate-type siderophores, thereby providing a structural explanation for high-affinity binding.

In 1987, Wehrli *et al*. [Wehrli et al., 1987] described a semisynthetic rifamycin derivative, CGP 4832, that displayed at least a 200-fold increase in antimicrobial activity against *E. coli* and *Salmonella typhimurium* compared to the clinically used drug, rifamycin (Rifampicin®). The enhanced bactericidal activity of rifamycin CGP 4832 was correlated with the ability of this antibiotic to be specifically transported into the periplasm by FhuA [Pugsley et al., 1987]. In contrast to albomycin, rifamycin CGP 4832 is not actively transported across the cytoplasmic membrane by FhuBCD [Pugsley et al., 1987], an ABC transport system [Kadner et al., 1980]. The periplasmic binding protein FhuD, and the cytoplasmic membrane-embedded permease FhuBC, effectively discriminate between rifamycin CGP 4832 and the diverse array of hydroxamate-type siderophores and antibiotics that are uniquely transported by this system [Braun et al., 1998]. As the chemical structure of this rifamycin derivative shares no structural similarities with ferrichrome or albomycin, we wished to determine how this antibiotic is specifically recognized and transported by FhuA. To establish whether it occupies the same ligand-binding site as previously observed with hydroxamate-type siderophores, and to characterize any distinct ligand-induced conformational changes, we determined the three-dimensional structure of FhuA in complex with rifamycin CGP 4832. Furthermore, we also studied the binding of ligands to FhuA by fluorescence measurements, transport inhibition, and selection of mutants resistant against this antibiotic. Our findings reveal common structural and mechanistic requirements for the energy-dependent transport of structurally dissimilar FhuA-specific ligands. Moreover, this structural information provides a basis for the

rational design of synthetic antibiotics that are actively transported by this receptor or by its homologues. As the outer membrane of Gram-negative bacteria is inherently impermeable for polar substances >600 Da making diffusional uptake inefficient, such receptor-specific bactericidal agents may increase the efficacy of chemotherapeutic agents [Ferguson et al., 2000b].

3.3. Results

General description of the structure and the rifamycin CGP 4832-binding site

FhuA in detergent-containing solution was co-crystallized with rifamycin CGP 4832. Phases to 2.9 Å resolution were derived from the isomorphous unliganded structure (Figure 3.1 and Table 3.1) [Ferguson et al., 1998b]. After initial structural refinement a F_{obs} - F_{calc} difference map showed clear electron density for a single rifamycin CGP 4832 molecule located within the extracellular pocket of FhuA (Figure 3.1 and 3.2A). Side-chains from apices B and C of the cork domain [Ferguson et al., 1998b], and from the β-barrel domain form hydrogen bonds, charge interactions, and van der Waals contacts with the antibiotic (Figure 3.2B and Table 3.2). The addition of morpholino and N-methyl-3-piperidyl-acetoxyacetyl groups structurally distinguishes rifamycin CGP 4832 from rifamycin; the latter is not actively transported by FhuA. Previous structure-function studies [Wehrli et al., 1987], demonstrated that both chemical moieties are required for the rifamycin derivative to exert its bactericidal activity. Our analysis of protein-ligand interactions between FhuA and rifamycin CGP 4832 showed that the morpholino and N-methyl-3-piperidyl-acetoxyacetyl groups form multiple hydrogen bonds, charge interactions, and van der Waals contacts with FhuA side-chains (Figure 3.2B and Table 3.2). Chemical replacement of the morpholino moiety by a methyl-piperazinyl-iminomethyl substituent abolished the bactericidal activity of rifamycin CGP 4832 [Pugsley et al., 1987]. The structure indicated that substitution of the morpholino group would prevent formation of a critical hydrogen bond between rifamycin CGP 4832 and Y116 from apex C, thereby abrogating high-affinity binding.

Structural comparison of the ligand-binding sites of FhuA

The chemical structure of rifamycin CGP 4832 (Figure 3.3A) shows no obvious similarity with albomycin (Figure 3.3B) and ferricrocin (Figure 3.3C). Moreover, the cork domain structure in the FhuA-CGP 4832 complex differs from that found in complexes with hydroxamate-type siderophores and albomycin. By comparing side-chains involved in binding of these structurally dissimilar substrates, we identified signature residues that are involved in ligand binding (Table 3.3). The iron-chelating moiety of FhuA-specific hydroxamate-type siderophores and albomycin is formed by three δ-*N*-acetyl-L- δ-*N*-hydroxyornithine peptides. This portion of the siderophore forms multiple highly conserved interactions with side-chains from apices A, B, and C of the cork domain, as well as residues from the β-strands and extracellular loops of the barrel domain (Figures 3.3B and 3.3C). There are also contacts between the tri-peptide component of the siderophore [GGG (ferrichrome), GSG (ferricrocin), GFG (phenylferricrocin)] and the amino acetyl thioribosyl pyrimidine moiety of albomycin, and side-chains of the extracellular pocket (Table 3.3). A similar set of side-chains, also form contacts with rifamycin CGP 4832. However, there is one notable exception: R81 from apex A does not interact with the antibiotic. In the binding site for hydroxamate-type ligands, this residue forms multiple hydrogen bonds with the iron-chelating component of the siderophore. In the FhuA-CGP 4832 complex, the guanidinium group of R81 is placed 4.6 Å away from the nearest rifamycin CGP 4832 atom and thus, forms only weak charge interactions with the derivative.

Ligand-induced allosteric transitions

Structural superposition of the C_α-atoms of unliganded FhuA and FhuA liganded with rifamycin CGP 4832, ferrichrome, ferricrocin, phenylferricrocin or albomycin revealed almost perfect superposition of the β-barrel domains (0.25 Å root mean square deviation of C_α-atoms). However, comparing the C_α-atoms of the cork domain identified three distinct conformations: unliganded, the hydroxamate-type liganded conformation, and the CGP 4832-liganded conformation. The transition from the unliganded to the hydroxamate-type liganded conformation reveals the following induced fit binding mechanism [Ferguson et al., 1998b; Ferguson et al., 2000b; Locher et al., 1998]: residues 80 to 82 of apex A and 98 to 100 of apex B move by 0.7 - 2.0 Å toward the siderophore or albomycin. In the transition to the CGP 4832-liganded conformation, only residues 97 to 100 from apex B moved upward (0.5 - 1.5 Å) to interact with the antibiotic (Table 3.2). All other cork domain residues remain stationary. In the complexes with iron-hydroxamates the upward translation of apex A is propagated to all

cork domain loops between this point and the periplasmic pocket of FhuA. The translation of apex A and other cork domain loops alters the shape of the hydrophobic pocket of the switch helix (residues 24 to 29), and disrupts several hydrogen bonds formed between periplasmic turns eight and nine and this helix, thereby promoting its unwinding. As a result, all residues NH_2-terminal of R31 assume an extended conformation within the periplasmic pocket. In contrast, apex A in the FhuA-CGP 4832 complex remains fixed 4.6 Å away from the nearest ligand atom, as in the unliganded conformation. No upward movement of cork domain loops is induced, and therefore, the switch helix remains wound. However, the increase in relative B-factors of the C_α-atoms composing the switch helix suggests that this segment is destabilized upon rifamycin CGP 4832 binding (Figure 3.4). The allosteric transition induced by this antibiotic thus differs from those observed with other liganded complexes of FhuA.

To confirm these unexpected crystallographic observations, intrinsic tryptophan fluorescence measurements with detergent-solubilized FhuA were collected. In accord with Locher and Rosenbusch [Locher and Rosenbusch, 1997], we found that the addition of ferrichrome to purified, detergent-solubilized FhuA decreased the emitted intrinsic tryptophan fluorescence of the receptor. A slight decrease in tryptophan fluorescence upon binding of rifamycin CGP 4832 or desferriferrichrome was also observed (Figure 3.5A). Unexpectedly, the addition of ferrichrome to a tryptophan solution of equivalent concentration also decreased the emitted fluorescence (Figure 3.5B). However, the magnitude of the fluorescence quenching was not equivalent to that observed with FhuA. Addition of rifamycin CGP 4832 or desferri-ferrichrome to the tryptophan solution also failed to produce a similar effect (Figure 3.5B). A second biophysical method to monitor ligand-induced structural transitions in FhuA was provided by measuring fluorescence changes of fluorescein-labelled cysteine residues. This technique has the advantage that the location of the reporter is known and that data can be collected directly from viable intact cells. It was shown previously [Bös et al., 1998] that ferrichrome binding to FhuA quenched the emitted fluorescence of two fluorescein-labelled cysteines (residues 329 and 336), which according to the three-dimensional structure of FhuA are located in the fourth extracellular loop. Rifamycin CGP 4832 binding caused a similar reduction in fluorescence of both surface-exposed cysteines. However, a 100-fold higher concentration of rifamycin CGP 4832 was required to obtain a similar ferrichrome-bound spectrum (Table 3.4). The observed fluorescence quenching by rifamycin CGP 4832 was not a function of the TonB-dependent transport of this antibiotic through FhuA, as identical spectra were obtained from *tonB*-deleted background strains (data not shown). The binding of

ferrichrome to FhuA also induced a similar TonB-independent shift in fluorescence [Bös et al., 1998].

Rifamycin CGP 4832 competes with ferrichrome for binding to the ligand-binding site of FhuA

To probe the functional implications resulting from the similarity of the binding sites for rifamycin CGP 4832 and ferrichrome, transport inhibition assays were performed. Addition of 10, 30 or 100 µg/ml of rifamycin CGP 4832 produced a 50, 75 or 85% reduction in the [$^{55}Fe^{3+}$]-ferrichrome transport rate (Figure 6). These data indicate that this antibiotic competes with ferrichrome for the same binding site, and that both substrates have similar binding affinities. Competitive transport inhibition is confined to passage across the outer membrane only, because rifamycin CGP 4832 does not use the FhuBCD ferrichrome transport system across the cytoplasmic membrane [Pugsley et al., 1987].

Bacterial mutants resistant to rifamycin CGP 4832

To determine if the energy-dependent transport of rifamycin CGP 4832 and ferrichrome share common structural requirements, we assessed the sensitivity for the antibiotic of cells expressing FhuA proteins with known point mutations in their TonB boxes (residues 6 to 11) which all exhibit impaired TonB-related FhuA activity [Schöffler and Braun, 1989]. Plasmid-encoded *fhuA* genes were used to transform *E. coli* UL3, which does not synthesize a wild-type FhuA protein. In contrast to cells expressing wild-type FhuA, those producing FhuA mutants (I9P) or (V11D) showed resistance to 0.4 - 10 µg/ml of rifamycin CGP 4832. The antibiotic sensitivity of mutant and wild-type cells for rifamycin CGP 4832 and rifamycin were equivalent at high concentrations (>100 µg/ml); the latter compound is not actively transported by FhuA and presumably permeates through the outer membrane by passive diffusion only.

3.4. Discussion

Ligand binding and concomitant allosteric conformational transitions

In contrast to rifamycin, the semisynthetic derivative CGP 4832 binds to FhuA. Competition of ferrichrome transport by CGP 4832, as shown in this paper, indicates a common binding site for both substrates, and the concentration dependence of CGP 4832 inhibition suggests a rather high affinity of CGP 4832 to FhuA (K_D for ferrichrome is < 0.1 μM [Braun et al., 1998]). It was mere coincidence that screening rifamycin derivatives against *E. coli* and related Gram-negative bacteria identified this antibiotic, which fits snugly into the common binding-site of FhuA and is actively transported across the outer membrane. The crystal structure of FhuA in complex with rifamycin CGP 4832 showed that high-affinity binding results from the addition of morpholino and N-methyl-3-piperidyl-acetoxyacetyl moieties to rifamycin. These additional groups form most of the specific interactions with side-chains found in the extracellular pocket of FhuA. Most transport proteins display high-affinity for their cognate ligands; however, they rarely covalently modify their substrates, thereby imposing stringent geometric constraints on those side-chains lining the binding-site. For this reason, transporters tolerate larger structural diversity than enzymes, as observed in the FhuA-CGP 4832 complex.

Binding of ferrichrome or albomycin to FhuA induces a short NH_2-terminal segment designated the switch helix (residues 24 to 29) to unwind displacing E19 approximately 17 Å from its unliganded C_α-position to a site designated the 'putative channel-forming segment' [Ferguson et al., 1998b; Ferguson et al., 2000b; Locher et al., 1998]. These crystallographically determined TonB-independent conformational transitions are in accord with *in vivo* and *in vitro* data collected from intact cells and detergent-solubilized FhuA. Specifically, ligand binding reduced the efficiency of binding of monoclonal antibodies that are sensitive to the conformation of residues 21 to 59 [Moeck and Coulton, 1996]; enhanced the formation of a chemically cross-linked FhuA-TonB complex [Moeck et al., 1997]; decreased the intrinsic tryptophan fluorescence of FhuA [Locher and Rosenbusch, 1997]; and caused fluorescence quenching of fluorescein-maleimide bound to a genetically introduced cysteine residue in the fourth extracellular loop [Bös et al., 1998]. The translation of W22 (which in unliganded conformation is buried together with the switch helix within a hydrophobic pocket) by approximately 17 Å across the periplasmic pocket of FhuA upon binding of hydroxamate-type siderophores or albomycin, may substantially contribute to tryptophan quenching. FhuA in complex with rifamycin CGP 4832 possesses a conformation

that lies between the unliganded and hydroxamate-bound conformations of FhuA. Apex B moves upward to the antibiotic and causes a similar relocation of the neighbouring cork domain segments as observed with hydroxamate-type ligands. In contrast to the hydroxamate-bound conformation of FhuA, apex A does not interact with rifamycin CGP 4832, and thus, the switch helix remains wound in the CGP 4832-liganded conformation. Nevertheless, the movement of apex B does allosterically affect the hydrophobic pocket in which the switch helix resides, as judged by the increase in relative B-factors of the C_α-atoms. This data suggests that the switch helix may temporarily unwind, albeit with lower probability than in the hydroxamate-type liganded conformation.

Interaction of TonB with FhuA and its functional consequences

The pronounced allosteric transition observed upon hydroxamate-type ligand binding presumably serves to recruit the energy-transducing protein TonB to its principal site of known interaction with TonB-dependent transporters, the TonB box. Relocation of this highly conserved segment is likely required to efficiently couple TonB with FhuA. This NH_2-proximal region of FhuA is localized in the periplasm and by genetic and biochemical means has been shown to interact physically with a region of TonB at or near residue 160 [Schöffler and Braun, 1989; Günther and Braun, 1990]. The failure to visualize this segment of FhuA (residues 6 to 11) in any of the currently available electron density maps [Ferguson et al., 1998b; Ferguson et al., 2000b; Locher et al., 1998] agrees with its apparent flexibility. However, the solution of the three-dimensional structure of the ferric enterobactin receptor FepA [Buchanan et al., 1999] revealed that the TonB box assumes an extended structure.

By *in vivo* disulphide cross-linking, direct physical interactions between the TonB box of the outer membrane vitamin B_{12} transporter BtuB, and a segment of TonB around residue 160 have been demonstrated [Cadieux and Kadner, 1999]. Site-directed spin labelling and electron paramagnetic resonance assays also indicated that in the unliganded conformation, the TonB box of BtuB may be localized adjacent to a helix that forms specific interactions with side-chain residues from the periplasmic turns of the β-barrel domain of the receptor [Merianos et al., 2000]. Binding of vitamin B_{12} converted this segment into an extended, disordered and highly dynamic structure that likely extends into the periplasm to interact physically with TonB. Collectively, these findings support the proposal that the unwinding of the switch helix promotes the formation of the FhuA-TonB complex *in vivo*, and this may be an essential mechanistic requirement to couple the proton motive force of the cytoplasmic membrane with receptor-mediated ligand transport across the outer membrane.

Considering the TonB-dependence of rifamycin CGP 4832 transport as shown in [Pugsley et al., 1987] and the data presented here, FhuA may assume two conformations that are in equilibrium. The majority of FhuA molecules have wound switch helices, however, a small fraction contain unwound switch helices. Under crystal growth conditions this equilibrium may be skewed towards the helical conformation, however, *in vivo* a small percentage of FhuA proteins may be sufficient to form transport-competent complexes with TonB, and thereby sustain the observed transport rate. Alternatively, the physical interaction of TonB with the destabilized switch helix may allow for an induced fit and yield a productive complex at a sufficient rate. Finally, the direct physical interaction of the TonB box of FhuA with TonB may not be essential for the transport of rifamycin CGP 4832, indicating the presence of at least one additional site of interaction between FhuA and TonB. The latter interpretation is supported by the finding that removing the entire cork domain from the β-barrel (including the TonB box) generated a mutant FhuA protein (FhuAΔ5-160) with residual TonB-dependent transport activity, including the uptake of rifamycin CGP 4832 [Braun et al., 1999]. When the cork domain is genetically excised, interactions between the barrel domain of FhuA and TonB may be sufficient to induce a structural transition within the barrel, such that the ligand is released from its residual binding site [Braun et al., 1999]. To further probe the functional role of the TonB box in the transport of rifamycin CGP 4832, a series of bacterial strains with known point mutations in their TonB boxes [Schöffler and Braun, 1989] were assessed; all FhuA-mediated TonB-dependent transport activities were impaired in these strains. The sensitivities of these cells to the bactericidal effects of rifamycin CGP 4832 were equivalent to rifamycin that is not actively transported by FhuA, and presumably permeates through the outer membrane by passive diffusion only. These genetic data indicate that the conformation of the TonB box and its physical interaction with TonB are involved in the uptake of rifamycin CGP 4832.

A proposed transport mechanism

By integrating the available biochemical, genetic and structural data, the following model of TonB-dependent ligand transport can be proposed. First, the binding of the hydroxamate-type siderophores or albomycin to the extracellular pocket of FhuA causes a TonB-independent conformational change that is propagated through the outer membrane and displayed by select periplasmic segments of the receptor, primarily the switch helix and the TonB box. The unwinding of the switch helix and the accompanying translocation of the TonB box or possibly a change in the conformation of the TonB box itself, alone or in combination with

conformational changes of periplasmic segments, may serve to recruit TonB to its site of interaction with FhuA.

Upon forming a productive complex with FhuA, TonB transduces conformational energy to the transporter. This event triggers a TonB-dependent conformational change in FhuA such that the ligand-binding site is disrupted, and the binding affinity is reduced. Disruption of the binding site may be affected by a small shift of apices A, B and C towards the periplasm. This may transiently alter the arrangement of aromatic side-chain residues lining the extracellular pocket, specifically those found on the fourth extracellular loop [Bös et al., 1998]. Furthermore, the transduction of energy causes a high-conductance channel to open within FhuA. This channel may be physically and electrically similar to that formed upon the irreversible adsorption of bacteriophage T5 to FhuA, as mediated by the straight tail fibre protein pb5 [Bonhivers et al., 1996, Plançon et al., 1997]. Although the open channel conformation of FhuA remains to be determined structurally, we speculate that subtle conformational changes in the loops of the cork domain between apex B and the periplasmic pocket may be involved in channel formation. When viewed along the barrel axis of unliganded FhuA and its liganded complexes, the extracellular pocket is connected to the periplasmic pocket in one segment of the barrel cross-section by a 10 Å aqueous channel, the putative channel-forming segment. Once released from their binding sites, ligands may enter this region and reach the periplasmic pocket by directed diffusion along a string of low-affinity binding sites. These transient ligand-binding sites could be provided by a set of strictly conserved side-chain residues lining the interior barrel wall of the putative channel-forming segment from the ligand-binding site to the periplasmic pocket of FhuA [Ferguson et al., 1998b, Killmann et al., 1998].

The observed switch helix destabilization upon rifamycin CGP 4832 binding suggests that it may briefly unwind or allow complex formation with TonB by an induced fit mechanism at a low rate. We suggest that this small yield of productive complexes among the rifamycin CGP 4832-loaded FhuA molecules may establish the transport of antibiotic molecules across the outer membrane at a rate sufficient to inhibit RNA polymerase activity [Hartmann et al., 1985]. Collectively, these results provide a structural-basis for the superior bactericidal activity of CGP 4832 against *E. coli* (MIC of 0.02 µg/ml) compared to rifamycin (MIC of 4.0 µg/ml).

Evolution of TonB-dependent receptors

Bacterial cells that synthesize the deletion derivative FhuAΔ5-160 retain a diminished level of TonB-dependent activity [Braun et al., 1999], suggesting that the barrel domain together with TonB can constitute a functional transport system. We therefore speculate that ancient Gram-negative bacteria possessed a channel-forming protein similar to FhuA Δ5-160. A string of low-affinity binding sites spanning the outer membrane may have facilitated the uptake iron-containing siderophores, as observed with glycoporin-mediated carbohydrate uptake [Schirmer et al., 1995; Forst et al., 1998].

3.5. Biological Implications

TonB-dependent receptors bind their cognate ligands with high-affinity, and thereby accelerate the passage of sparse essential nutrients through the outer membrane. These energy-dependent transport systems also display broad ligand selectivity, a feature that can be exploited in the rationale design of novel receptor-specific antibiotics. This work describes the three-dimensional structure of the FhuA-CGP 4832 complex, a semisynthetic antibiotic that is both chemically and functionally different from the natural substrates of FhuA. The composition of the rifamycin CGP 482-binding site is remarkably similar to those defined for ferric hydroxamates, demonstrating the plasticity of the ligand-binding site. Distinct conformational changes are induced in the cork domain of FhuA upon binding of rifamycin CGP 4832; however, an NH_2-terminal segment (switch helix) thought to signal the occupancy of the receptor remains wound. Genetic, biophysical, and crystallographic data are used to identify common structural and mechanistic requirements for the active transport of dissimilar substrates by FhuA, and provide a platform to increase the efficacy of antibiotics by designing receptor-specific bactericidal agents that are actively pumped across the outer membrane by FhuA or by its homologues.

3.6. Experimental Procedures

Crystallization, data collection and structure determination

Using the hanging drop vapour diffusion technique, FhuA was co-crystallized with rifamycin CGP 4832 by mixing equal volumes (5µl) of FhuA [10 mg/ml, 0.80% N,N-dimethyldecylamine-N-oxide (DDAO), 10 mM ammonium acetate (pH 8.0), 1% *cis*-inositol, and 1 mM rifamycin CGP 4832] and reservoir solution [12% polyethylene glycol (PEG) 2,000 monomethyl ether, 0.1 M sodium cacodylate (pH 6.4), 20% glycerol, and 3% PEG 200]. Rifamycin CGP 4832 was generously provided by Dr. Reto Naef, Novartis-Pharma, Switzerland. FhuA-CGP 4832 co-crystals grew within seven days to a final size of 300 by 300 by 220 µm at 18°C. Crystals were mounted in cryoloops and flash frozen by direct immersion into liquid nitrogen. Diffraction data were collected at 100 K using a cryostream apparatus with synchrotron radiation at the X-ray diffraction beam line at ELETTRA (Table 3.1). X-ray diffraction data were processed and reduced using the program XDS [Kabsch, 1988]. Initial phases for the FhuA-CGP 4832 complex were calculated using the FhuA coordinates (1QFG) as an initial model. A model for the FhuA-CGP 4832 complex was built into an experimental electron density map with the program O [Jones et al., 1991]. The model was refined with the program CNS using molecular dynamics and the maximum likelihood target [Brünger et al., 1998]. Following rounds of model building and structural refinement the final model contains residues 19 to 714, 1 lipopolysaccharide molecule, 1 rifamycin CGP 4832 molecule, 1 DDAO molecule, and 178 ordered water molecules. The crystallographic coordinates (FhuA in complex with rifamycin CGP 4832) and structure factor amplitudes have been deposited in the Protein Data Bank with the accession code **1FI1**.

Isolation and characterization of rifamycin CGP 4832-resistant bacterial mutants

To assess the sensitivity of defined FhuA mutants to rifamycin CGP 4832 we used *E. coli* UL3 [Bös et al., 1998] that was transformed with plasmid-encoded *fhuA* genes with point mutations in their TonB boxes [Schöffler and Braun, 1998]. Plasmid pHK763 encoding wild-type FhuA served as a control. Wild-type and mutant *fhuA* genes were cloned on the same pT7-5 plasmid. Twenty microliter aliquots of a ten-fold dilution series of rifamycin CGP 4832 (stock solution 0.5 mg in 1 ml of 50% methanol) and rifamycin were spotted in parallel onto nutrient agar plates seeded with 10^8 cells of *E. coli* UL3. Diameters of the zones of growth inhibition were recorded.

Transport inhibition assays using rifamycin CGP 4832

E. coli AB2847 cells were grown overnight on TY nutrient agar plates. This *E. coli* strain has a mutation in *aroB,* a gene required for synthesis of the only endogenous siderophore, enterobactin. If appropriate precursors are not provided, *E. coli* AB2847 will transport exogenously added siderophores. Colonies were suspended in 0.5 ml of M9 minimal media salts supplemented with 0.4% glucose, and grown to an optical density of 0.55 at 578 nm [Miller, 1972]. Nitrilotriacetate (8.8 µl of a 10 mM solution) was added to 0.35 ml of cell suspension. Following a two-minute incubation period, 3.5 µl aliquots of rifamycin CGP 4832 (1, 3 and 10 mg/ml dissolved in 50% methanol) were added to the cell culture. Three minutes later, transport was initiated by the addition of a mixture of 2.35 µM radiolabelled [$^{55}Fe^{3+}$]-ferrichrome and 5 µM desferriferrichrome. The cell suspension was shaken and 50 µl samples were withdrawn after one and four-minute intervals, for a total of 21 minutes. The samples were subsequently filtered, washed twice with 5 ml of 0.1 M LiCl, dried, and the [$^{55}Fe^{3+}$]-isotope signal measured with a liquid scintillation counter at 37°C. *E. coli* UL3 does not synthesize a wild-type FhuA protein, and there is no polar effect on the expression of the *fhuCDB* genes, which are located downstream of *fhuA*.

Protein expression, purification and intrinsic tryptophan fluorescence measurements

A recombinant FhuA protein was constructed by inserting a hexahistidine-tag plus five additional linker residues (SSHHHHHHGSS) into the *fhuA* gene after residue 405 [Moeck et al., 1994]). FhuA was expressed and purified as previously described [Ferguson et al., 1998a]. The intrinsic tryptophan fluorescence of FhuA and its complexes with rifamycin CGP 4832, ferrichrome or desferriferrichrome [dissolved in 6 mM KH_2PO_4 (pH 7.0), 0.15 M NaCl, and 0.06% N,N-dimethyldodecylamine-N-oxide] were measured in 1.1 µM FhuA solutions and as a control in 10 µM tryptophan solutions. 1.1 µM of FhuA (~79 kDa with nine tryptophan residues) was considered equivalent to a 10 µM tryptophan solution. All data were collected at 20°C with a Fluoromax-2 spectrophotometer (Jobin Yvon-Spex Instruments S.A. Inc.) and processed using the GRAMS/386 software package. A single excitation wavelength (280 nm) was used for all fluorescence measurements. Two emission wavelengths were collected and they correspond to the fluorescence maxima of FhuA (335 nm) and tryptophan (355 nm).

Figures

Figures 3.2A and 3.3 were prepared using the programs O [Jones et al., 1991] and ISIS Draw. All other colour figures were prepared using MOLSCRIPT [Kraulis, 1991] and Raster3D [Merrit and Bacon, 1997].

Acknowledgements

We gratefully acknowledge M Degano at the X-ray diffraction beam line at ELETTRA for his assistance during data collection and R Naef at Novartis-Pharma for providing rifamycin CGP 4832. We appreciate the technical assistance of C Herrmann and H Wolff. The Deutsche Forschungsgemeinschaft (to VB and WW) and Natural Sciences and Engineering Research Council, Canada (to JWC) supported this work. ADF was the recipient of a Deutscher Akademischer Austauschdienst Grant for Study and Research, and Medical Research Council of Canada Doctoral Research Awards.

3.7. Tables

Table 3.1. Data collection and refinement statistics of FhuA in complex with Rifamycin CGP 4832. Brackets indicate the highest resolution shell.

FhuA in complex with rifamycin CGP 4832		
Data collection and reduction		
Space group		$P6_1$
Unit cell	a (Å)	172.82
	b (Å)	172.82
	c (Å)	87.91
Number of molecules per asymmetric unit		1
Number of measured reflections		161.168
Number of unique reflections		33.363
Completeness (%)		99.9 (99.8)
Resolution (Å)		2.90
R_{sym} (%)		6.2 (29.8)
R_{meas} (%)		7.0 (33.5)
$R_{merge\text{-}F}$ (%)		7.2 (24.6)
$<I>/\sigma I$		17.2 (4.2)
Structural refinement		
R_{work} (%)		23.3
R_{free} (%)		27.5
Root mean square deviation		
	Bond lengths (Å)	0.008
	Bond angles (°)	1.5
	Dihedral angles (°)	25.9
	Improper angles (°)	0.9

Table 3.2. Interactions of FhuA with rifamycin CGP 4832. Listed are the residue-atom, location, distance, and type of interaction formed between all FhuA side-chain residues within 4 Å of rifamycin CGP 4832 atoms. See Figure 3a for structural details of the hydrogen bonding pattern and charge interactions between side-chains and rifamycin CGP 4832.
(„v. d. W." stays for van der Waals)

Residue-Atom	Location	Distance	Type of Interaction
E98-OE2	Apex B	3.7 Å	Charge interactions with O8 carbonyl atom of the N-methyl-3-piperidyl-acetoxyacetyl group
E98-O	Apex B	3.8 Å	Charge interactions with O20 carbonyl atom of the N-methyl-3-piperidyl-acetoxyacetyl group
G99-NH	Apex B	3.7 Å	Charge interactions with O20 carbonyl atom
Q100-OE1	Apex B	3.5 Å	v. d.W. contact with the C5 methyl group
S101-OG	Apex B	3.5 Å	Hydrogen bond with O20 carbonyl atom
F115-O	Apex C	3.0 Å	v.d. W. contact with C55 atom of the piperidyl group
Y116-OH	Apex C	3.2 Å	Hydrogen bond with O18 of the morpholino group
Y244-OH	L3	3.9 Å	Charge interactions with N6 atom
W246-CZ2	L3	3.6 Å	v. d.W. contact with the aromatic ring system (distance is given for the O17 atom)
Y313-OH	β7	3.6 Å	Charge interactions with N4 atom
Y315-OH	L4	2.8 Å	Hydrogen bond with O1 carbonyl atom of the aromatic ring system
K344-CD	β8	3.4 Å	v. d.W. contact with C24 methyl group
F391-CE2	β9	3.0 Å	v. d.W. contact with O18 atom of the morpholino group and the C31 and C32 methyl groups
G392-O	β9	3.2 Å	v. d.W. contact with C24 methyl group
Y423-OH	β10	3.3 Å	v. d.W. contact with the C31 and C32 methyl groups
Q505-NE2	L7	3.0 Å	Hydrogen bond with the O8 carbonyl atom of the N-methyl-3-piperidyl-acetoxyacetyl group
F693-CE1	L11	3.5 Å	v. d.W. contact with the aromatic ring system (distance is given for the C40 atom)
Y696-OH	L11	3.0 Å	Hydrogen bond with the O2 hydroxyl atom

Table 3.3. Interactions of FhuA with its cognate ligands bound to the extracellular pocket. Listed are all side-chains within 4 Å of ligand atoms: ferricrocin [Ferguson et al., 1998b]; phenylferricrocin [Ferguson et al., 2000b]; albomycin extended (*****) and compact (†) conformational isomers [Ferguson et al., 2000b]; or rifamycin CGP 4832.

Side chain residues	**Ferricrocin**	**Phenyl-ferricrocin**	**Albomycin***	**Albomycin†**	**Rifamycin CGP 4832**
R81 from apex A	+	+	+	+	-
Y87 from a cork domain loop	-	+	-	-	-
E98 near apex B	-	-	-	-	+
G99 near apex B	+	+	+	+	+
Q100 from apex B	+	+	+	+	+
S101 from a cork domain loop	-	-	-	-	+
F115 near apex C	-	+	-	+	+
Y116 from apex C	+	+	+	+	+
Y244 from L3	+	+	+	+	+
W246 from L3	+	+	+	+	+
Y131 from β7	+	+	+	+	+
Y315 from L4	+	+	+	-	+
K344 from β8	-	-	+	-	+
F391 from β9	+	+	+	+	+
G392 from β9	-	-	-	-	+
Y393 from L5	-	-	+	+	-
Y432 from β10	-	-	-	+	+
Q505 from L7	-	-	-	+	+
F557 from L8	-	-	+	-	-
F558 from L8	-	-	+	-	-
F693 from L11	+	+	+	+	+
Y696 from L11	-	-	-	-	+

Table 3.4. Ligand-induced fluorescence quenching of fluorescein-maleimide labelled cells. *E. coli* UL3 cells expressing the following plasmids; pfhuA4 (C318S), pfhuA5 (C329S), pfhuA6 (D336C), and pfhuA8 (wild-type FhuA) were labelled as described previously [Bös et al., 1998]. Mean relative fluorescence value prior to and following preincubation with 1 µM rifamycin CGP 4832 or 10 nM ferrichrome. -ΔF (%) indicates the ligand-induced decrease in relative fluorescein-maleimide labelling for cells not preincubated with 1 µM rifamycin CGP 4832 or 10 nM ferrichrome [σ (n-1)=10%].

	Relative fluorescence (mean value)		
FhuA	Not preincubated withCGP 4832	Preincubated with 1 µM CGP 4832	-ΔF (%)
Wild-type	16.6	16.5	0
C329S (C318)	25.9	23.9	8
C318 (C329)	43.3	34.1	21
D336C	94.7	62.7	34

	Relative fluorescence (mean value)		
FhuA	Not preincubated with Ferrichrome	Preincubated with 10 nM Ferrichrome	-ΔF (%)
Wild-type	16.6	6.3	0
C329S (C318)	26.4	24.0	9
C318 (C329)	43.1	33.7	22
D336C	94.3	70.7	26

3.8. Figures

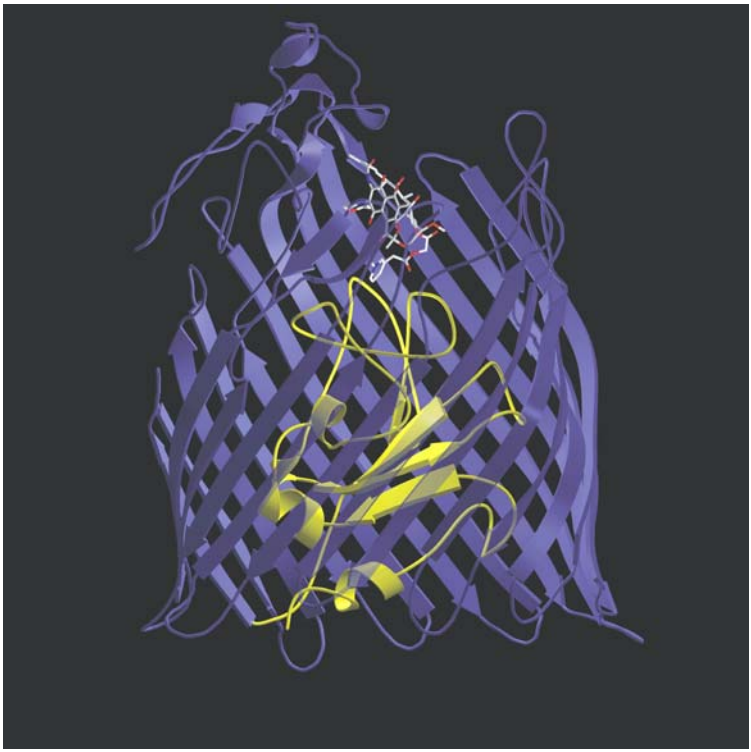

Figure 3.1. FhuA-CGP 4832 complex. The view is perpendicular to the barrel axis. To provide an unobstructed view of the cork domain, the β-strands that form the front of the barrel domain have been rendered semitransparent. The barrel domain is coloured blue and the cork domain, yellow. The rifamycin CGP 4832 molecule is shown as a bond model with carbon atoms white, oxygen atoms red, and nitrogen atoms blue.

(a)

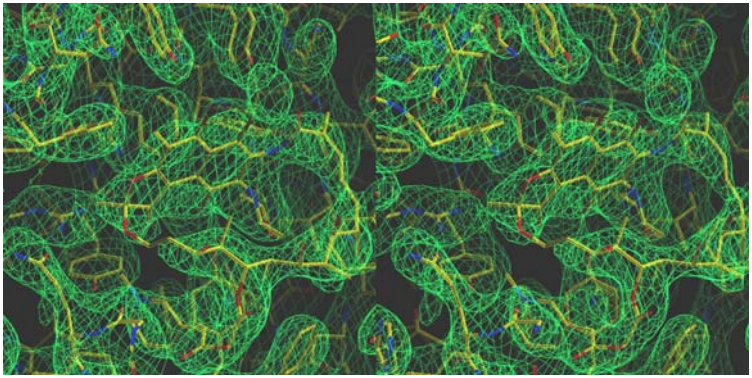

(b)

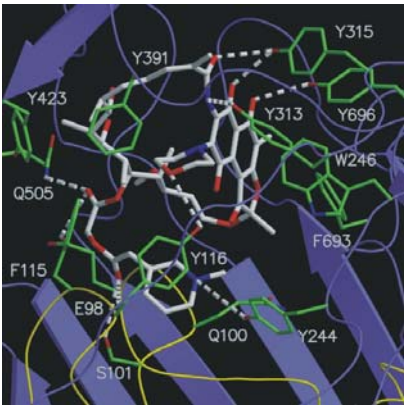

Figure 3.2. The FhuA Rifamycin CGP 4832 binding site. (**a**) Representative section of the electron density map for the FhuA-CGP 4832 complex. Stereoview of the final simulated annealing omit electron density map (green) at a resolution of 2.90 Å is contoured at 1.2 σ, showing the rifamycin CGP 4832-binding site. The rifamycin CGP 4832 molecule and select side-chain residues are shown with carbon atoms yellow, oxygen atoms red, and nitrogen atoms blue. (**b**) The FhuA rifamycin CGP 4832-binding site. Those side-chains that form hydrogen bonds or van der Waals contacts with rifamycin CGP 4832 atoms are labelled and shown in green. The rifamycin CGP 4832 molecule is presented as a bond model with carbon atoms white, oxygen atoms red and, nitrogen atoms blue.

(a)

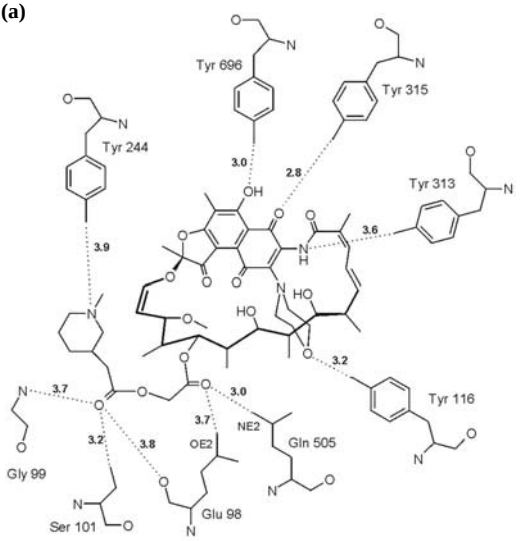
Tyr 696
Tyr 315
Tyr 244
Tyr 313
Tyr 116
Gln 505
Gly 99
Ser 101
Glu 98
3.0
2.8
3.6
3.9
3.7
3.2
3.8
OE2
NE2

(b)

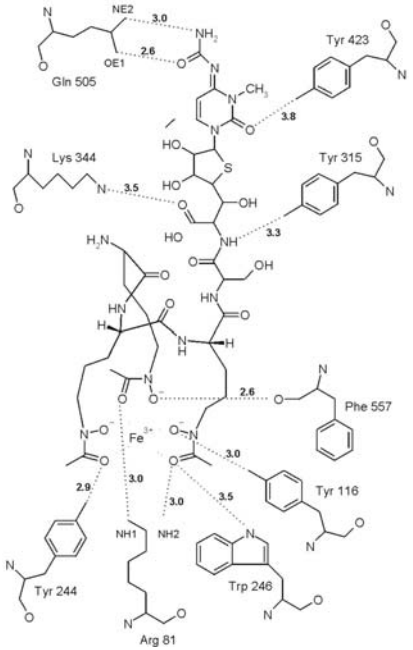
Gln 505
NE2
OE1
Tyr 423
Lys 344
Tyr 315
Phe 557
Tyr 116
Tyr 244
Trp 246
Arg 81
NH1
NH2
Fe
3.0
2.6
3.8
3.5
3.3
2.9
3.5

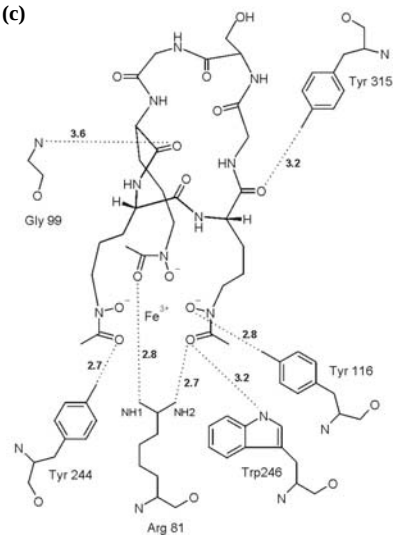

Figure 3.3. Ligand binding to FhuA. Schematic comparison of the hydrogen bonding pattern and charge interactions of (**a**) rifamycin CGP 4832, (**b**) albomycin (extended conformational isomer) [Ferguson et al., 2000b], and (**c**) ferricrocin with side-chain residues of the FhuA ligand-binding site [Ferguson et al., 1998b]. The chemical structures of ferricrocin, albomycin, and rifamycin CGP 4832 are shown with hydrogen bonds and charge interactions with side-chains as dotted lines (distances are given in Å). See Table 3.2 for details of additional van der Waals contacts between side-chains and rifamycin CGP 4832.

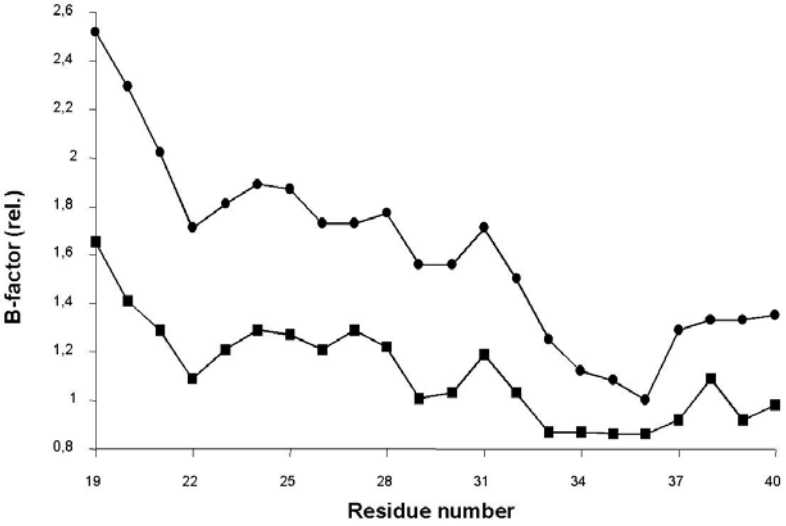

Figure 3.4. Destabilization of the Switch-Helix upon Binding of CGP 4832. Relative B-factors of the first 21 C_α atoms of unliganded FhuA (■) and FhuA liganded with the rifamycin CGP 4832 (●). Relative B-factors are B-factors divided by the mean B-factor of all C_α atoms of the respective structure, which are 63 $Å^2$ (σ = 13.6) for unliganded FhuA and 48 $Å^2$ (σ = 14.0) for FhuA in complex with rifamycin CGP 4832. Residues 24 to 29 compose the switch helix.

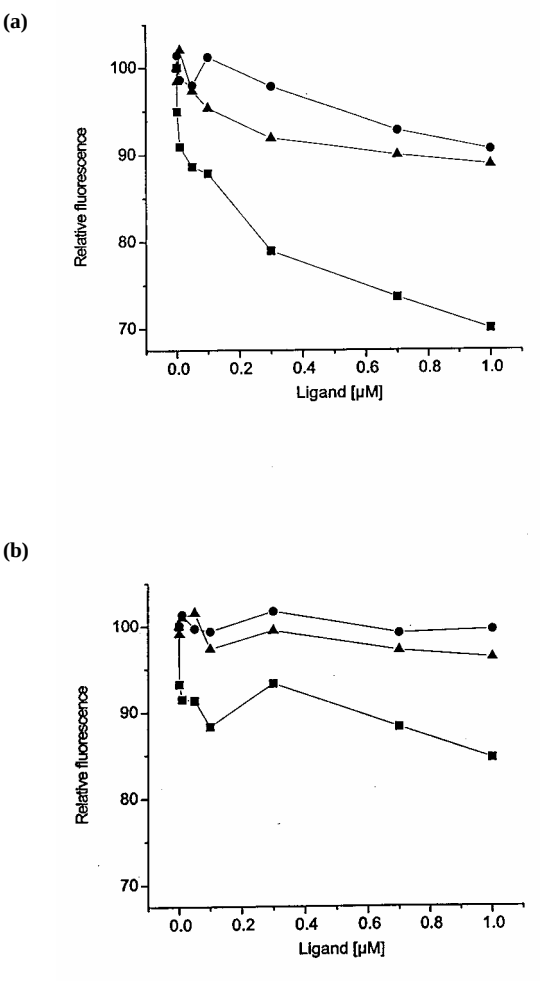

Figure 3.5. Ligand-induced fluorescence quenching [ferrichrome (■), desferriferrichrome (●), and rifamycin CGP 4832 (▲)] of the emitted tryptophan fluorescence of (**a**) FhuA, and (**b**) tryptophan containing solutions. The given tryptophan fluorescence values were averaged from three independent experiments in which each spectrum was collected three times. The background fluorescence spectra of all buffers (without added ligand) were subtracted from the collected experimental spectra. The emitted tryptophan fluorescence of FhuA was taken as 100%.

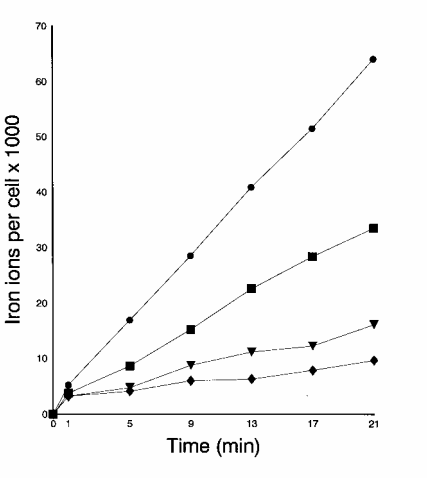

Figure 3.6. Transport inhibition assays using rifamycin CGP 4832. Transport of radiolabelled [$^{55}Fe^{3+}$]-ferrichrome (2.35 μM) into *E. coli* AB2847 cells in the absence (●), and presence of 10 μg/ml (■), 30 μg/ml (▼) and 100 μg/ml (♦) of rifamycin CGP 4832.

4. Dimerization of TonB is not essential for its binding to the outer membrane siderophore receptor FhuA of *E.coli*

Jiri Koedding[1], Peter Howard[2], Lindsay Kaufmann[2], Patrick Polzer[1], Ariel Lustig[3], and Wolfram Welte[1]

[1]Department of Biology, University of Konstanz, 78457 Konstanz, Germany, [2]Department of Biology, University of Regina, Regina, Saskatchewan, Canada, [3]Department of Biophysical Chemistry, Biozentrum Basel, Switzerland

published in *J. Biol. Chem*. (2004) Vol. 279, 9978 - 9986

4.1. Abstract

FhuA belongs to a family of specific siderophore transport systems located in the outer membrane of *Escherichia coli*. The energy required for the transport process is provided by the proton motive force of the cytoplasmic membrane and is transmitted to FhuA by the protein TonB. Although the structure of full length TonB is not known the structure of the last 77 residues of a fragment composed of the 86 C-terminal amino acids was recently solved and shows an intertwined dimer (Chang, C., Mooser, A., Pluckthun, A., and Wlodawer, A. (2001) J. Biol. Chem. 276, 27535-27540). We analysed the ability of truncated C-terminal TonB-fragments of different lengths (77, 86, 96, 106, 116 and 126 amino acid residues, respectively) to bind to the receptor FhuA. Only the shortest TonB-fragment, TonB-77, could not effectively interact with FhuA. We have also observed that the fragments TonB-77 and TonB-86 form homodimers in solution, whereas the longer fragments remain monomeric. TonB fragments that bind to FhuA *in vitro* also inhibit ferrichrome uptake via FhuA *in vivo* and protect cells against attack by bacteriophage Φ80.

4.2. Introduction

The cell wall of gram-negative bacteria consists of two lipid bilayers, the outer membrane and the cytoplasmic membrane enclosing the peptidoglycan layer. A number of different transport pathways regulate the uptake of essential compounds into the cell. One class of outer membrane transporters is connected to the cytoplasmic membrane by the TonB protein, therefore they are called TonB-dependent receptors. The three dimensional structure of a short C-terminal fragment of TonB is available in the literature (Chang et al., 2001). One of these receptors in *E. coli* is the ferric hydroxamate uptake system containing the integral outer membrane protein FhuA (Coulton et al., 1986), that serves as a receptor for the iron siderophore ferrichrome (Fc), the antibiotics albomycin and rifamycin CGP 4832, colicin M, microcin J25 and the phages T1, T5 and Φ80. Other TonB-dependent iron transporters of the outer membrane include FecA for ferric dicitrate (Cit) uptake (Pressler et al., 1988), FepA for enterobactin uptake (Lundrigan and Kadner, 1986) and BtuB for vitamin B_{12} uptake (Heller and Kadner, 1985).

The transport of all of these ligands requires energy which is provided by the electrochemical potential of the proton gradient across the cytoplasmic membrane (proton motive force) and is mediated by the protein complex ExbB, ExbD and TonB (Bradbeer, 1993; Larsen et al., 1999; Postle and Kadner, 2003). ExbB/D is located in the cytoplasmic membrane whereas TonB is attached to the membrane by an N-terminal hydrophobic anchor (Postle, 1993). The major part of TonB spans the periplasmic space to reach the outer membrane receptors.

The crystal structure of FhuA reveals a two-domain architecture (Ferguson et al., 1998b; Locher et al., 1998): a β-barrel consisting of 22-antiparallel strands and a globular domain at the N-terminus (residues 1–160), called the cork or plug domain filling most of the interior of the barrel. Stability studies using differential scanning calorimetry experiments have shown the autonomous behaviour of the cork and the β-barrel that unfold at different temperatures (Bonhivers et al., 2001). The interactions between the cork-domain and the β-barrel consist of nine salt bridges and more than 60 hydrogen bonds (Locher et al., 1998). Located at the periplasmic side of FhuA there is a short α-helix, the so called "switch-helix" (residues 24 – 29). This α-helix has been found to unwind during or following ligand binding, indicating that this structural change might be a signal for TonB to bind FhuA (Ferguson et al., 1998b; Locher et al., 1998). This unwinding was observed in the crystal structures of FhuA with bound ferrichrome (Ferguson et al., 1998b) or albomycin (Ferguson et al., 2000b). On the other hand,

the crystal structure of FhuA with the rifamycin derivative CGP 4832 demonstrates that ligand binding causes destabilisation rather than unwinding of the switch helix (Ferguson et al., 2001). These structures present a specific ligand binding site that is exposed to the external medium and determined by specific hydrogen bonds between the substrate and residues of both the cork and the β-barrel domain. The crystal structures of FepA (Buchanan et al., 1999), FecA (Ferguson et al., 2002) and BtuB (Chimento et al., 2003) show similar molecular architectures. The presence of a switch-helix has only been observed in the structures of FhuA and FecA but not in FepA and BtuB, implying that this structure element is not essential for TonB recognition in general. The pathway of the ligand from the binding site to the periplasm and the mechanism of its transport have not yet been elucidated. Two possibilities are discussed in the literature: 1) conformational change of the cork-domain opens up a channel large enough for the siderophore to slide through (Ferguson et al., 1998b; Ferguson et al., 2002) or 2) the cork-domain leaves the barrel together with the bound siderophore (Usher et al., 2001).

A highly conserved motif among all TonB-dependent siderophore receptors is the TonB-box (residues 7 – 11: DTITV in FhuA) which plays an important role in the receptor-TonB interaction (Larsen et al., 1997; Cadieux and Kadner, 1999). The TonB-box is located at the periplasmic side of the cork-domain close to the switch-helix. Furthermore, the globular domains of FhuA and FepA are exchangeable without loss of substrate specificity. For example, a mixed mutant consisting of a FhuA-barrel and a FepA-cork retains the specificity for ferrichrome, the natural substrate for FhuA (Scott et al., 2001). Different cork-barrel combinations from several bacterial strains led to the same results (Killmann et al., 2001). Complexes between *wt* FhuA or *wt* FepA with the periplasmic domain of TonB were characterized *in vitro* (Moeck and Letellier, 2001). However, up to now there has been no in vitro evidence for interactions between the receptor lacking the cork-domain and the TonB protein, and new investigations of FepA indicated that the barrel domain alone could not behave as an active transporter (Vakharia and Postle, 2002).

The TonB protein of *E. coli* is composed of 239 amino acids of which 17 % are proline residues. Most of these are located between residues 75 and 107, spanning the periplasmic space to link the outer membrane receptor with the cytoplasmic (Postle and skare, 1988). The elongated conformation of this proline-rich region has been demonstrated by NMR studies (Evans et al., 1986). This region is not essential for the process of energy transduction (Larsen et al., 1994). Two other significant regions can be distinguished: 1) a hydrophobic region at the N-terminus (residues 1 – 32) anchoring TonB to the cytoplasmic membrane. The amino

acids between Ser-16 and His-20 were found to be essential for the interaction with the membrane embedded proteins ExbB/D (Larsen and Postle, 2001). 2) a C-terminal domain that forms the contact to the outer membrane receptor. The 3D-structure of a C-terminal fragment (residues 155 – 239) reveals a cylinder shaped dimer (Chang et al., 2001). Each monomer contains three β-strands and a short α-helix arranged in a dimer so that the 6 β-strands build a large antiparallel β-sheet. The first 10 N-terminal amino acids of this fragment are not visible in the electron density map because of their flexibility.

The structure of another energy transducing protein, TolA from *Pseudomonas aeruginosa*, has been solved recently (Witty et al., 2002). In spite of a sequence identity of only 24% (Lalign server) the crystal structure of the periplasmic domain of TolA shows a similar structure and topology, however without dimer formation. The importance of the dimer formation for the mechanism of energy transduction is thus not yet understood. However, it has been shown that a region of TonB contributing the critical interaction with the receptor is located arround amino acid 160 (Günter and Braun, 1990). This finding was supported by the observation that synthetic nonapeptides with sequence identity to the amino acid region between residues 150 to 166 of TonB are able to inhibit the capacity of *wt* FhuA to transport siderophores (Killmann et al., 2002).

To understand the role of the C-terminal domain of TonB in the interaction with FhuA, we have investigated FhuA-TonB interactions using purified C-terminal TonB fragments of different lengths shown in Fig. 4.1 (consisting of 77, 86, 96, 106, 116 or 126 amino acid residues, respectively). All TonB-fragments except TonB-77 were able to form a complex with FhuA. Analytical ultracentrifugation experiments and tryptophan fluorescence measurements also showed that the fragments with 86 or more amino acid residues behave differently than TonB-77. In parallel, we analysed the ability of these TonB fragments to inhibit ferrichrome (Fc) and ferric citrate (Cit) uptake *in vivo* and to protect cells against attack by bacteriophage Φ80.

4.3. Experimental Procedures

Construction of plasmids encoding TonB proteins

All constructions, with the exception of pBADTonB118, were created using PCR and the products were first cloned into an intermediate vector ($pSKII^+$ or $pKSII^+$). The oligodeoxynucleotides used are listed in Table 4.1. The plasmid pCSTonB30 (Howard et al., 2001), which encodes residues 33-239 of the periplasmic domain of TonB cloned into pET30a (Novagen), was used as a template to generate the four smaller tonB fragments. Standard PCR conditions were used, with US10-US12 and US26 being the forward primers unique for each fragment as indicated, each one giving a *PstI* cut site on the 5'-end of the fragment, and US5 as the return primer, creating a *HindIII* restriction site on the 3'-end of the fragment. In combination with US5, oligo US10 was used to create pBADTB86, oligo US11 for pBADTB77, oligo US12 for pBADTB96 and oligo US26 for pBADTB106. Each fragment encodes the final number of amino acids of the periplasmic domain of TonB as specified by the TonB fragment number, i.e. pBADTB77 encodes the final 76 amino acids of the periplasmic TonB domain plus a Methionine as the first amino acid. The *PstI-HindIII* digested product was then electrophoresed and the TonB fragment isolated and cloned into *PstI-HindIII* digested pBAD/gIII. The construct pBADBTB118 was obtained by digesting pMFTLP (Howard et al., 2001) with *PstI* and *HindIII*, and cloning the fragment into *PstI-HindIII* digested pBAD/gIII. Each of these recombinant clones codes for an 18 amino acid (54 base pair) signal sequence provided by the vector. Cloning the TonB fragment into the *PstI* site of pBAD/gIII downstream of this sequence also adds an 8 amino acid linker at the N-terminal side. For pTB77 to pTB126, UR134, UR135, and UR141 to UR144 were the forward primers for each fragment as indicated, each one creating an *Nde1* site on the 5'-end of the fragment, and UR136 was the return primer, which hybridizes to the pET30a vector just downstream of the multiple cloning site and contains a *Bpu1102I* site. Cloning of the resulting PCR fragment back into pCSTonB30 created the plasmids pTB77 – pTB126, which in each case expresses the indicated TonB fragment without a signal sequence.

Bacterial strains, plasmids and growth conditions

The strains and plasmids used in this study are shown in Table 4.2. The media used were tryptone yeast extract (2xYT), nutrient broth (NB) (Difco) and Luria-Bertani media (LB). The growth temperature was 37^{o}C for all experiments. Ampicillin was used at a concentration of

100 µg/mL (Ap100). Strain AB2847Δara was created by P1 transduction of *leu*::Tn*10* and Δ*ara*714 from LMG194 (Invitrogen) into AB2847 (Hantke and Braun, 1978).

Purification of FhuA

FhuA405.H_6 was expressed in *E. coli* strain AW 740 [*ΔompF zcb: Tn10 ΔompC fhuA31*] (Ingham et al., 1990) on plasmid pHX 405 with a his_6-tag inserted between residue 405 and 406 (Moeck et al., 1994). The protein was purified as described in the literature (Ferguson et al., 1998a) with the following changes: for binding experiments the purification was stopped before the detergent exchange from LDAO to DDAO. Fractions containing FhuA were concentrated to 10 mg/ml and dialyzed ON against 50 mM ammonium acetate pH 8.0 with 0.05 % LDAO (N,N-dimethydodecylamine-N-oxide/ FLUKA).

Purification of the C-terminal TonB fragments

C-terminal fragments of TonB (77, 86, 96, 106, 116 and 126 residues, respectively) were over-expressed in *E. coli* BL21(DE3) cells containing the plasmids pTB77 to pTB126 (shown in Table 4.2) and induced at OD600=0.7 by addition of 0.4 mM IPTG (isopropyl-β-D-thiogalactopyranoside, BioVetra). Protein expression was maintained at 37°C for 2 hours. The pellets from 4 x 500 ml cell culture (2xYT/Kan^{50}) were resuspended in buffer A (20 mM Tris-HCl pH 8.0/ 100 mM NaCl/ 1 mM EDTA) and the cells were broken by french press (4000 PSIG/ 3 passes). After centrifugation at 15,000 g for 30 min the supernatant was loaded on an SP sepharose cation-exchange column (Amersham Biosciences) and was then washed with buffer A. TonB was eluted from the column with a NaCl gradient at a salt concentration of about 300 mM NaCl. The eluate was then desalted on a Sephadex G25 column (Amersham Biosciences) before loading onto another strong cation-exchange column (Source 15s /Amersham Biosciences). The eluted TonB protein containing about 250 mM NaCl was again desalted on a Sephadex G25 column with buffer A (no EDTA) and yielded protein at a concentration of ca. 4 mg/ml. The mobility of the fragments on 15% SDS-PAGE corresponded to their theoretical molecular masses (Figure 4.2). The purification was carried out within one day to avoid protein degradation. For analytical ultracentrifugation and crystallization experiments an additional gel filtration step was added. The protein was concentrated up to 10 mg/ml (Amicon spin-column with YMCO 5,000) and glycerol was added to a final concentration of 10%. The TonB sample was then loaded onto a gel filtration column (Superose 12 HR 60/10, Amersham Biosciences). Binding experiments with FhuA were done

with TonB fragments that were purified without this gel filtration step but mixed with 0.05% LDAO immediately before the incubation with FhuA.

Purification of the FhuA405.H_6/TonB-complexes

Protein solutions containing FhuA (10 mg/ml) and TonB fragment (4 mg/ml), respectively, were mixed in a weight ratio of 1:2 resulting in a large molar excess of TonB in the samples. The protein mixture was then incubated ON in the presence of 60 µM ferrichrome (M_r=740, Biophore Research). Glycerol was subsequently added to the protein solution to a final concentration of 10%. The sample was then applied to a Superose 12 HR 60/10 column (Amersham Biosiences), equilibrated and eluted with the following buffer: 20 mM Tris pH 8.0/ 50 mM NaCl/ 0.05% LDAO. The flow rate was kept at 0.1 ml/min. The protein containing fractions were analyzed by 15% SDS-PAGE and stained with coomassie blue (Fig. 4.3). For western blots to detect TonB we used anti-TonB antiserum from rabbit as previously described (Howard et al., 2001).

Crystallization, data collection and structure solution

The C-terminal TonB-77 fragment was crystallized under the following conditions: TonB-77 was purified as described above and concentrated to 20 mg/ml (centricon YM 5,000). Hanging drop crystallization plates were used with 1 ml reservoir solution containing 2.0 M sodium formate and 0.1 M sodium citrate pH 5.6, mixing 2 µl reservoir solution with 2 µl protein solution in the drop. Crystals of the size 120 x 120 x 120 μm^3 grew at 18°C within 2 weeks (Fig. 4.4). For diffraction data collection single TonB-77 crystals were soaked in cryobuffer: reservoir solution with 20% glycerol for 1 minute and were then flash-frozen in liquid nitrogen. X-ray diffraction data were collected at beamline ID14-4 at the ESRF in Grenoble/France. The crystals diffracted to a resolution of 2.5 Å. Raw data were processed with the program package XDS (Kabsch, 1993) to a final resolution of 2.7 Å. Higher resolution shells were omitted from the refinement process because of very high R-values (>50%). The space group was determined to be $P6_422$ with the following unit cell parameters: a=61.58 Å, b=61.58 Å, c=121.95 Å, α=90°, β=90°and γ=120°. The structure of TonB-77 was solved using molecular replacement with the program MOLREP (Vagin and Teplyakov, 1997) and REFMAC5 (Murshudov et al., 1997) from the program package CCP4 (Collaborative Computational Project, Number 4). The search model consisted of all protein atoms of the published model of TonB-86 (PDB entry 1IHR, (Hanahan, 1983)). Chain tracing and model building was done with the graphical interface 'O' (Jones et al., 1991). The program LSQCAB

from CCP4 (Collaborative Computational Project, Number 4) was used to calculate the rms deviation for the C_α atoms between TonB-77 and the existing structure 1IHR of TonB-86.

Analytical Ultracentrifugation

The purified C-terminal fragments of TonB (77, 86, 96 and 116, respectively) were analyzed by sedimentation velocity and sedimentation equilibrium experiments using an AN 60-Ti rotor 316 in a Beckmann XL-A Optima equipped with an optical absobance system (Ariel Lustig, Biozentrum Basel, Switzerland). All protein solutions were freshly purified and gel filtrated. The buffer was 20 mM Tris pH 8.0 and 100 mM NaCl in all experiments. Velocity sedimentation data were obtained from 0.5 mg/ml protein solutions and a rotor speed of 54,000 rpm at room temperature obtaining the sedimentation coefficient ($s_{20,w}$). Sedimentation equilibrium experiments were done at different concentrations between 0.5 and 2 mg/ml and a rotor speed of 24,000 and 28,000 rpm at RT. The partial specific volume (ν) of the proteins was calculated on the basis of the amino acid distribution (Edelstein and Schachman, 1973) and was near the mean value of globular proteins 0.73 cm^3/g. These experiments were used to determine the molecular mass (M_r), hydrodynamic radius (R_H) and the frictional ratio (f/f_0) (Lebowitz et al., 2002) of the purified TonB-fragments. The calculations were done with the computer program SEGAL (http-reference) based on the numerical fitting of the sedimentation equilibrium pattern to one or two exponential functions.

Tryptophan fluorescence of the C-terminal TonB-fragments

Fluorescence spectra were measured from TonB-77, TonB-86, TonB-96 and TonB-116, respectively, at an excitation wavelength of 295 nm over the range from 320 to 400 nm (Perkin Elmer, L550B). The fragments were purified as described above and used at a final concentration of 0.1 mg/ml.

Assay of Bacteriophage susceptibility

Susceptibility to bacteriophage $\phi 80\lambda i^{21}$ was measured by dropping 5 μl aliquots of 10-fold dilutions of the phage onto freshly poured overlays (100 µl containing ca. 10^8 cells of the various strains added to 3 ml LB soft agar and poured onto LB plates). The LB soft overlay, LB plates and bacterial cultures each contained the indicated concentration of arabinose when measuring the effect of the arabinose induction level on the susceptibility of the cells to bacteriophage. The susceptibility was recorded as the –log of the highest dilution of phage which gave a confluent lysis zone of the bacterial lawn.

Assay of siderophore dependent growth and iron transport

The ability of the strains to gain iron from either ferrichrome (FC) or ferric citrate (Cit) was assayed on NB agar plates (Howard et al., 2001). To limit the free iron available to the cells, dipyridyl was added to both the agar plates and NB soft overlay at a final concentration of 250 μM. When measuring the effect of the arabinose induction level on the ability of the cells to transport iron, the various indicated levels of arabinose were added. Sterile paper discs (6 millimeter diameter) were saturated with 10 µl of either 1 mM FC, 10 mM Na citrate, or 100 mM Na citrate and left to dry. The discs were then placed onto the overlays, which consisted of ca. 10^8 bacteria added to 3 ml NB soft agar. The plates were incubated overnight at 37^{o}C and the diameter of rings of growth around each siderophore disc was measured (in millimeters), including the diameter of the disc. No growth was recorded as 6 mm.

4.4. Results

Analysis of FhuA/TonB interaction in vitro

Several uptake processes across the outer membrane of Gram negative bacteria are energized by the proton motive force of the cytoplasmic membrane. TonB from *E. coli* is the protein that transduces the energy from the inner membrane to the outer membrane transporter. One of the transporters is the ferric hydroxamate receptor FhuA of *E. coli*. The amino acid region around residue 160 of TonB is known to interact with the periplasmic side of this outer membrane (Günter and Braun, 1990; Killmann et al., 2002). For a detailed analysis of the interaction of FhuA with TonB we prepared protein complexes of FhuA with C-terminal fragments of TonB. Gel filtration (Superose 12 column) of protein mixtures containing FhuA and the C-terminal fragment of TonB led to an elution profile with two well separated peaks, that were monitored on a 15% SDS-PAGE gelstained with Coomassie-blue (Fig. 4.3). If a protein complex was present in the sample, the first elution peak contained both FhuA and the TonB fragment (Fig. 4.3 lane B1, C1, D1, E1 and E3). The second elution peak consisted only of TonB (Fig. 4.3 lane A2, B2, C2, C4, D2, E2 and E4). In the case of the shortest fragment TonB-77, the first elution peak contained only FhuA (Fig. 4.3, lane A1), whereas all longer fragments of TonB coeluted with FhuA from the gel filtration column. The formation of the FhuA/Fc/TonB-complex was only observed in the presence of ferrichrome which also colors the solution of the first peak yellowish (data not shown). Obviously FhuA is able to form a complex with the

longer C-terminal fragments of TonB (86, 96, 106, 116 and 126). We also noticed that NaCl had to be present in the buffer at a concentration of at least 50 mM for the FhuA/Fc/TonB-106 complex to be stable over a pH range from 4.6 to 8.0. In order to stabilize the complex we tried 10% glycerol, 1% glucose, 100 mM glycine or 1% betaine hydrochloride, respectively. Except for betaine none of these additives led to a significant alteration in the behaviour of the proteins in these binding experiments. The presence of 1% betaine in the buffer abolished complex formation between FhuA and the TonB fragments. Moreover we have shown that this purified FhuA/Fc/TonB-96 complex could be disrupted by the addition of 1% betaine. In the subsequent gel filtration step with 1% betaine in the elution buffer the first peak contained FhuA alone (Fig. 4.3, lane C3), while the second peak contained TonB-96 (Fig. 4.3, lane C4). This FhuA fraction was colorless, whereas fractions containing FhuA with bound ferrichrome had a yellowish color, suggesting that ferrichrome had dissociated from the receptor after the addition of betaine. It is possible that betaine replaces ferrichrome in the FhuA binding site and thereby induces the release of the TonB-fragment.

Analytical Ultracentrifugation of the C-terminal TonB-fragments

The crystal structures of TonB-88 (Chang et al., 2001) and of TonB-77 (this work) show identical dimers. This led us to investigate the aggregation state of the C-terminal TonB-fragments (TonB-77, TonB-86, TonB-96 and TonB-116) in solution by analytical ultracentrifugation. Sedimentation coefficients were determined by sedimentation velocity analyses and yielded increasing values from 1.54S to 1.98S for the fragments TonB-77 and TonB-86, respectively. The TonB-fragments 96 and 116 showed significantly lower sedimentation values of 1.39S and 1.37S, respectively. The radii calculated from the sedimentation coefficients were thus much smaller for the two longer fragments than for the two shorter ones. The frictional ratio was larger than 1.2, the typical value for spherical globular proteins, suggesting that the conformation is more elongated for these longer TonB fragments. The molecular mass of the fragments was assessed from sedimentation equilibrium (see 4.3. Experimental Procedures). Molecular masses of 8.5 kDa and 12 kDa for the fragments TonB-96 and TonB-116, respectively, correspond very well with the theoretically calculated masses based on the amino acid sequences of these proteins being 10.8 kDa for TonB-96 and 12.8 kDa for TonB-116. The masses of the shorter fragments, TonB-77 and TonB-86, of 15 kDa and 18.3 kDa respectively correspond well with the theoretical masses of the homo-dimers of 17.4 kDa for TonB-77 and 19.5 kDa for TonB-86. In both cases no monomeric protein were detectable in the sedimentation equilibrium profiles at 0.25, 0.5 and

1.0 mg/ml protein concentration. The results from analytical ultracentrifugation are summarized in Table 4.3.

Trp-fluorescence of the C-terminal TonB-fragments

Another way to test the aggregation state of the TonB fragments is to measure their tryptophan fluorescence. This method is based on the fact that the molecular neighborhood of tryptophan influences its fluorescence characteristics. Each of the C-terminal TonB-fragments used in this study contains only one tryptophan (W213, see Figure 4.1) that projects its indole group into the hydrophobic core of the TonB-77 dimer (Chang et al., 2001 and this study). The intensity maximum of the fluorescence spectra of the two dimers TonB-77 and TonB-86 is similar at λ_{max}= 343 nm and at λ_{max}= 340 nm, respectively. The maximum for the TonB-fragments 96, 106, 116 and 126 is also similar, but shifted to a shorter wavelength of λ_{max}= 333 nm. We are not able to explain this blue shift because we have no information about the environment of Tryptophane 213 in the monomeric form of TonB. The fact that the fluorescence spectra of the shorter and the longer fragments is in agreement with the results of the analytical ultacentrifugation analyses indicating that the C-terminal fragments of TonB with a length of 77 and 86 amino acids, respectively, form homodimers in solution whereas the longer fragments TonB-96 and TonB-116 remain monomeric .

TonB fragments shorter than 96 amino acids inhibit TonB function in vivo very weakly

It has previously been demonstrated that the entire periplasmic C-terminal domain of TonB can inhibit the function of native TonB *in vivo* (Howard et al., 2001). Various carboxyl-terminal fragments of TonB were produced as periplasmic proteins by expression as a fusion protein with the signal sequence of FecA (Howard et al., 2001). The periplasmic C-terminal domain was shown to inhibit both ferrichrome and ferric citrate transport as well as growth on iron-limited media when iron was provided as ferrichrome or ferric citrate. In addition, induction of the periplasmic TonB fragment was shown to rescue the producing cells from the lethal effects of colicin M and bacteriophage Φ80, both of which depend on TonB for uptake. In those studies, the smallest fragment of TonB to be assayed and shown to be inhibitory was that produced by pMFTLP, which contained the last 118 amino acids of TonB. Here, we similarly assayed fragments containing the last 77, 86, 96, and 106 amino acids of TonB, again when produced as periplasmic proteins. In this case due to the very slight inhibitions observed with some of the fragments (see Tables 4.4 and 4.5), we expressed the fragments as fusion proteins with the signal sequence of the GeneIII protein of the filamentous phage fd from the

vector pBAD/gIII. This vector allowed higher expression than was obtained for the FecA signal sequence/TonB fusions produced by the pMalc2G vector used earlier (data not shown). As a control, we also created a Gene III signal sequence fusion to the "LP" fragment encoding the last 118 amino acids of TonB and assayed it as well. Cells containing the plasmids were grown in varying concentrations of arabinose to induce the fusion proteins and plated on iron deficient media containing discs soaked in ferrichrome or Na citrate, and were also challenged with serial dilutions of bacteriophage Φ80. As before, the LP fragment containing the last 118 amino acids of TonB was capable of inhibiting siderophore dependent growth, such that at inducer concentrations of 0.02% or higher, growth on ferrichrome or ferric citrate was completely inhibited (Table 4.4). In addition the synthesis of this fragment in the presence of 0.002% arabinose or greater was capable of rescuing the cells from the Φ80 challenge (Table 4.5). As can also be seen in Tables 4 and 5, very similar inhibition and rescue results were observed for the carboxyl terminal 96 and 106 amino acid TonB fragments. In contrast, there was no inhibition of siderophore dependent growth by the carboxyl terminal 77 amino acid TonB fragment, even when induced with 0.2% arabinose. The carboxyl terminal 86 amino acid fragment inhibited growth only on ferrichrome and only at concentrations of 0.02% arabinose or higher (Table 4.4). Cells expressing the TonB-77 fragment were only poorly rescued from the Φ80 challenge, even at the highest inducing concentration of 0.2% arabinose (Table 4.5). Again the cells expressing the TonB-86 fragment showed an intermediate phenotype, being rescued more than the cells expressing the TonB-77 fragment but substantially less than those containing the TonB-96, TonB-106 and TonB-118 fragments.

Crystal structure of the TonB-77 fragment

Model building and refinement ended with a final R-factor of 26.7% and an R-free of 27.1%. The data collection and refinement statistics are summarized in Table 6. The 3D structure of TonB-77 presents a dimer shown in figure 5, and is very similar to the structure of TonB-86 (Chang et al., 2001). Effectively, the TonB-86 model comprises only 76 amino acids in the electron density map because of the high flexibility of the first 10 N-terminal amino acids. These additional amino acids apperently do not influence dimer formation and the crystal structure of the protein. The C_α atom positions of the two TonB models can be superimposed with a rms deviation of 0.745Å. These results are in agreement with our experiments showing that TonB-77 and TonB-86 both behave as dimers in solution.

4.5. Discussion

The mechanism of energy transduction between the cytoplasmic membrane and the outer membrane via the TonB-ExbB-ExbD system is still unclear. We know, however, that the outer membrane siderophore receptors FhuA and FecA from *E. coli* form a complex with TonB mediating the transport of siderophores through the membrane. With respect to the crystal structure of FhuA, alone and in complex with the siderophore (Ferguson et al., 1998b), it is assumed that the conformational changes of the receptor caused by the siderophore create a TonB binding site at the periplasmic side of the receptor. Our *in vitro* results correlate with this model. In the absence of the siderophore ferrichrome we observed only a very weak complex formation between FhuA and TonB, correlating with results of earlier studies (Moeck and Letellier, 2001). We also found that ferrichrome can be displaced by betaine in a purified FhuA-ferrichrome-TonB-complex. This exchange of the ligand is followed by a dissociation of TonB underlining the necessity of the specific FhuA-ferrichrome interaction for effective binding of FhuA to TonB.

Recently it has been shown that a C-terminal fragment of TonB (TonB-86) crystallizes as a dimer (Chang et al., 2001). We were able to confirm this dimer structure by solving the structure of TonB-77 in a different crystal form. Based on these crystallographic data, it was proposed that the dimer formation of TonB is of critical importance for the mechanism of the energy transduction. Our analytical ultracentrifugation experiments support the existence of a TonB-77 dimer in solution indicating that this observation is not a crystallization artefact (Tables 4.3 and 4.7). On the other hand, we found no complex formation between TonB-77 and FhuA *in vitro* (Fig. 4.3, lane A1). This observation correlates with the failure of TonB-77 to inhibit both ferrichrome uptake via FhuA and ferric citrate uptake via FecA *in vivo* (Table 4.4). In addition infection of the cells by bacteriophage Φ80 is only very weakly influenced by TonB-77 (Table 4.5). TonB-86 was found to be dimeric in solution as well (Table 4.7). This fragment, however, is able to bind to FhuA *in vitro* (Fig. 4.3, lane B1) and to interfere with ferrichrome uptake *in vivo* (Table 4.4). These findings indicate the special role of the additional amino acid residues in TonB-86 compared to TonB-77 for binding to FhuA. On the other hand these residues do not influence the dimeric structure of TonB, as shown in both the crystal structure of TonB-86 and our analysis of in vitro complex formation. The addition of 10 further amino acid residues or more at the N-terminus led to stable monomers in solution as we observed in case of the longer C-terminal fragments: TonB-96, TonB-106 and TonB-116 (Table 4.7). It was also possible to correlate these results with the *in vivo* inhibition studies

since each of the fragments that were monomeric *in vitro* strongly inhibited siderophore and bacteriophage Φ80 uptake (Tables 4.3 and 4.4). Our observations agree with the results obtained for the whole periplasmic domain of TonB (residues 33-239). Sedimentation analyses showed this fragment to be monomeric in solution (Moeck and Letellier, 2001), while *in vivo* studies showed this fragment to be inhibitory for all TonB-dependent functions assayed (Howard et al., 2001). It was also shown that this fragment binds to FhuA as a monomer (Moeck and Letellier, 2001). Sauter et al., 2003 came to similar conclusions *in vivo* using a bacterial two-hybrid system. TonB-76 formed dimers or multimers in these experiments, while TonB-207 did not. Full-length TonB, containing the transmembrane part, also showed dimer formation or multimer formation.

Based on the data presented here we propose that the dimer formation of the short C-terminal TonB fragments (TonB-77 and TonB-86) is an exception and not the energetically favoured oligomer of native TonB. The stability of the TonB-77 dimer is supported by the formation of a 6-stranded β-sheet with 3 β-strands from each monomer (Fig. 4.6A). We suppose that a C-terminal TonB-fragment longer than 96 amino acid residues can form a 4-stranded β-sheet by itself so that it is monomeric in solution (Fig. 4.6C). This hypothesis is supported by a secondary structure prediction for the longer TonB-fragments which indicates an additional zone of β-strand around amino acid 148 (Fig. 4.1). The shortest TonB-fragment harboring this region is TonB-96. The additional β-strand might fold between β-strand number 1 and 3 (Fig. 4.6C). In the TonB-77 dimer this strand of the β-sheet is filled by the β-strand number 3 of a second TonB molecule (Chang et al., 2001).

A monomeric form of this proposed topology was also found in the crystal structure of TolA, a protein functionally related to TonB from the TolA-TolQ-TolR protein complex (Braun and Herrmann, 1993). The 3D-structure of the C-terminal domain of TolA from *E. coli* in complex with g3p (Lubkowski et al., 1999) shows a very similar fold to the 3D-structure of the same domain of TolA from *P. aeruginosa* (Witty et al., 2002) despite an amino acid sequence identity of only 20%. Both TolA structures are composed of 3 β-strands and two α-helices in the order β-β-α-α-β forming a 3 stranded antiparallel β-sheet (Fig. 4.6B). A similar structure is achieved by the dimeric TonB-77 through β-strand swapping (Witty et al., 2002; Liu and Eisenberg, 2002). The domain-swapped TonB-77 can be generated by connecting the helix from one monomer with the β-strand number 3 of the other monomer (Fig. 4.6A and 4.6B). We hypothesize that the monomeric fragment TonB-96 folds into a three dimensional structure similar to the domain-swapped TonB-77 dimer. Alternatively, it seems more likely

that the additional 20 N-terminal amino acid residues of a TonB-96 monomer might form a β-strand that slides between β-strands 1 and 3 (Fig. 4.6C), building a 4 stranded β-sheet.

A comparison of the dimerization state of the C-terminal TonB-fragments and their ability to bind to FhuA (Table 4.7) demonstrates that the C-terminal amino acid sequence of the TonB-fragments and not their aggregation state determines their binding behaviour. The C-terminal fragment TonB-77, a stable dimer in solution (Tables 4.7), cannot effectively interact with the membrane receptor protein FhuA (Fig. 4.3, lane A1). This finding correlates with the observation that the TonB sequence around amino acid residue 160 might contribute critical interactions to the binding of the cork-domain of FhuA (21, 33). This amino acid region is missing in TonB-77 (Fig. 4.1). On the other hand TonB-86, which forms a dimer as does TonB-77, contains the major part of the sequence around residue 160 for binding to FhuA (Fig. 4.1) and is able to effectively interact with the receptor molecule (Fig. 4.3, lane B1). In the crystal structure, these residues could not be resolved, probably due to disorder. Since the longer TonB-fragments are monomeric in solution and inhibit TonB-dependent transport far more effectively than do shorter ones, we cannot find any evidence that TonB functions as a dimer in the energy transduction process.

Acknowledgements

We are grateful to the following persons from the University of Konstanz: Dietmar Schreiner for helping us with the protein purifications, André Schiefner for X-ray diffraction data collection, Milena Roudna for helping us with the tryptophan measurements and Kinga Gerber for helpful discussions.

4.6. Tables

Table 4.1. Oligodeoxynucleotides used in creation of pBADTonB and pTB recombinant clones.

Oligodeoxy-nucleotide	Sequence (5' to 3')
US 5	GAA TTC AAG CTT TTA CCT GTT GAG TAA TAG TCA
US10	CTG CAG CAT TAA GCC GTA ATC AGC C
US11	CTG CAG CAC CGG CAC GAG CAC AGG CA
US12	CTG CAG CAC CGG TTA CCA GTG TGG CTT CA
US26	CTG CAG CAT CAA GTA CAG CAA CGG CTG CA
UR134	CAT ATG GCA TTA AGC CGT AAT CAG CC
UR135	CAT ATG CCG GCA CGA GCA CAG GCA
UR136	GCT AGT TAT TGC TCA GCG G
UR141	CAT ATG CCG GTT ACC AGT GTG GCT TCA
UR142	CAT ATG TCA AGT ACA GCA ACG GCT GCA
UR143	CAT ATG TTT GAA AAT ACG GCA CCG GCA C
UR144	CAT ATG AAA CCC GTA GAG TCG CGT C

Table 4.2. Strains of *E. coli* K-12 and plasmids used.

Strains		***Source***
AB2847	*aroB tsx malT thi*	Hantke 1978
AB2847 Δara	*aroB tsx malT thi* Δ*ara714 leu*::Tn*10*	This study
XL Blue	*recA1 endA1 gyrA96 thi-1 hsdR17 supE44 relA1 lac*	
	[F' *proAB lacI*^{q}*ZDM15*::Tn*10*] St^{r}	Stratagene
W3110	IN(*rrnD-rrnE*)1 *rph*-1	Jensen, 1993
LMG194	F^{-}Δ*lac*X74 *gal* E *thi rps*L Δ*pho*A (*Pvu* II)	
	Δ*ara*714 *leu*::Tn*10*	Invitrogen
DH5α	Δ(*argF lac*)U169 *endA1 recA1 hadR17*	
	supE44 thi1 gyrA1 relA1 (F' ϕ80 *lacZ*ΔM15)	Hanahan, 1983

Plasmids		***Source***
pCSTonB30	*tonB* fusion in pET30a	Howard, 2001
pSK^{+}T/pKS^{+}T	ColE1 *ori*, lac*Z*, Ap^{r}	Stratagene
pBAD/gIII/B	pBR322 *ori*, *ara*BAD promoter, *araC*, Ap^{r}	Invitrogen
pMFTLP	*fecA' 'tonB* fusion in pMALc2G	Howard, 2001
pTU3	*cma* and *cmi* in pUC19	Pilsl H, 1993
pTB77	*tonB* fragment in pET30a	This study
pTB86	*tonB* fragment in pET30a	This study
pTB96	*tonB* fragment in pET30a	This study
pTB106	*tonB* fragment in pET30a	This study
pTB116	*tonB* fragment in pET30a	This study
pTB126	*tonB* fragment in pET30a	This study
pBADBTonB77	*tonB* fragment in pBAD/gIII/B	This study
pBADBTonB86	*tonB* fragment in pBAD/gIII/B	This study
pBADBTonB96	*tonB* fragment in pBAD/gIII/B	This study
pBADBTonB106	*tonB* fragment in pBAD/gIII/B	This study
pBADBTonB118	*tonB* fragment in pBAD/gIII/B	This study

Table 4.3. Data from the sedimentation velocity and sedimentation equilibrium experiments done with the C-terminal TonB-fragments 77, 86, 96 and 116. All fragments were freshly purified (see 4.3. Experimental Procedures). The partial specific volume necessary for radius and weight determination was calculated based on the amino acid composition of the fragments. The actual molecular weight (given in kilo-Daltons) of each TonB-fragment was measured by analytical ultacentrifugation (see 4.3. Experimental Procedures) and is compared here to the theoretical molecular weight calculated by the Swissprot server (www.expasy.ch).

TonB-fragment	**TonB-77**	**TonB-86**	**TonB-96**	**TonB-116**
sedimentation coefficient [S]	1.54	1.71	1.39	1.37
partial specific volume [ml/g]	0.743	0.740	0.740	0.736
frictional ratio	1.42	1.34	1.08	1.38
radius	2.32	2.23	1.46	2.09
molecular weight [kDa]	15.0	16.0	8.5	12.0
molecular weight [kDa] (theoretical)	8.68	9.74	10.80	12.80

Table 4.4. Summary of results with the TonB fragments. Correlation between the ability of the C-terminal TonB-fragments to bind to the FhuA-ferrichrome complex in vitro, their state of aggregation and in vivo inhibition of siderophore uptake. The aggregation state was determined by analytical ultracentrifugation (see 4.3. Experimental Procedures). The structure of of the dimeric TonB-77 and TonB-86 fragments has been solved.

TonB-fragment	**TonB-77**	**TonB-86**	**TonB-96**	**TonB-106**	**TonB-116**	**TonB-126**
in vitro binding to FhuA/Fc	-	-	+	+	+	+
aggregation state	dimeric	dimeric	monomeric	*	monomeric	*
λ_{max} of Trp-fluorescence [nm]	343	343	333	333	333	333
in vivo binding to FhuA/Fc	-	+	+	+	*	*

* Asterisks, samples not measured

Table 4.5. *For legend see next page.*

STRAIN & SOLUTION (nm)	**GROWTH ON ARABINOSE AT (%): 0**	**0.002**	**0.02**	**0.2**
AB2847Δara(pBADB)				
FC (1)	34	35	34	31
Cit (10)	18	15	14	14
Cit (100)	26	26	24	25
AB2847Δara(pBADB/TonB118)				
FC (1)	34	6*	6	6
Cit (10)	15	19	6	6
Cit (100)	25	27	6	6
AB2847Δara(pBADB/TonB77)				
FC (1)	32	31	30	33
Cit (10)	18	19	13	13
Cit (100)	25	26	25	22
AB2847Δara(pBADB/TonB86)				
FC (1)	32	32	6	6
Cit (10)	18	16	12	13
Cit (100)	25	25	23	22
AB2847Δara(pBADB/TonB96)				
FC (1)	32	32	6	6
Cit (10)	15	16	6	6
Cit (100)	24	25	6	6
AB2847Δara(pBADB/TonB106)				
FC (1)	33	6°	6	6
Cit (10)	15	16	6	6
Cit (100)	25	26	6	6

° In one of the three experiments, a very faint full-sized growth ring was observed around the discs for these assay conditions.

Table 4.5. Growth of *E. coli* AB2847Δara transformants on NB medium containing ampicillin (100 μg/mL) and dipyridyl (250 μM). 6 mm filter discs were saturated with 10 μL of 1 mM ferrichrome (FC), 10 mM or 100 mM sodium citrate (Cit) as indicated, left to dry, and placed onto a lawn of the bacteria on media containing the indicated concentration of arabinose to induce the TonB fragments. After ON incubation the growth zone was measured (in millimeteres), and includes the diameter of the filter disc (6 mm). Therefore a measurement of "6" indicates no visible growth around the disc. Typical results from one of three experiments are shown. * In one of the three experiments, a very faint full-sized growth ring was observed around the discs for these assay conditions.

Table 4.6. Susceptibility of *E. coli* AB2847Δara transformants to phage ϕ80λ**i**[21].

5 μL of serial 10-fold dilutions of a phage lysate were dropped onto a lawn of the bacteria shown, on media that contained the indicated concentrations of arabinose to induce the expression of the TonB fragments. Results are given as the -log of the highest dilution of the phage lysate which gave a confluent lysis zone of the bacterial lawn. Results given in brackets indicate that there was confluent lysis, but the zones were cloudy. Typical results from one of three experiments are shown.

	STRAIN SUSCEPTIBILITY AT ARABINOSE (%)			
STRAIN AND TREATMENT	**0**	**0.002**	**0.02**	**0.2**
AB2847Δara (pBADB)	6	6	6	6
AB2847Δara (pBADBTonB118)	6	1	1	1
AB2847Δara (pBADBTonB77)	6	5	5	5
AB2847Δara (pBADBTonB86)	6	4	4	4
AB2847Δara (pBADBTonB96)	6	2	2	1
AB2847Δara (pBADBTonB106)	6	2	2	1

Table 4.7. Data collection and refinement statistics for the TonB-77 homodimer. Values in parentheses refer to the highest resolution shell (2.8-2.7 Å).

Resolution range (Å)	26.4-2.7
Space group	$P6_422$
Unit cell parameters	a = b = 61.58 Å, c = 121.95 Å,
	$\alpha = \beta = 90°$, $\gamma = 120°$
No. of molecules per ASU	1
No. of observations	39238
No. of unique reflections	4053 (409)
Completeness (%)	97.5 (97.6)
Solvent content (%)	68.2
R_{merge} for all reflections (%)	4.9 (46.3)
Average I/σ(I)	19.32 (3.56)
R, R_{free} values (%)	26.7, 27.1

4.7. Figures

Figure 4.1. Amino acid sequence of the C-terminal TonB-fragments used in our studies. The location of the site arround residue 150 to 161 known to be involved in binding to FhuA is shown in boldface (Killmann et al., 2002). Structural elements derived from the crystal structure of TonB-77 are indicated (Chang et al., 2001). The amino acid sequence region predicted to form a β-sheet is shown underlined.

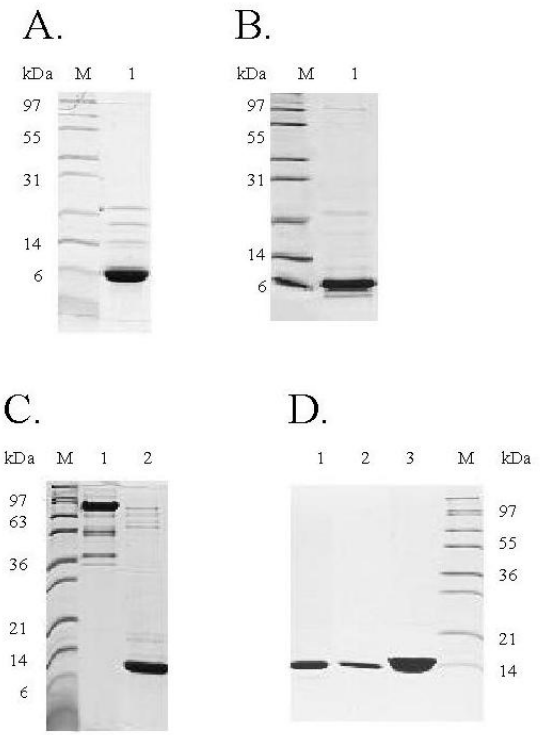

Figure 4.2. Purification of FhuA405.H_6 and of the C-terminal TonB-fragments. The proteins were purified as described under "4.3. Experimental Procedures". Their purity was tested by 15% SDS-PAGE followed by Coomassie staining. Apparent molecular masses (in kilo Daltons) are given on the left. (A) TonB-77. (B) TonB-86. (C) FhuA405.H_6 (lane 1), TonB-96 (lane 2). (D) TonB-106 (lane 1), TonB-116 (lane 2), TonB-126 (lane3).

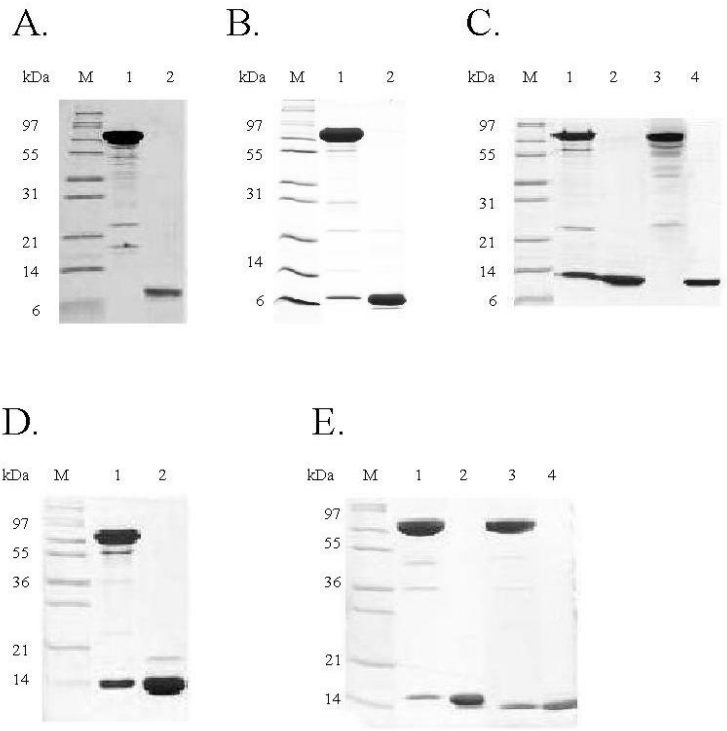

Figure 4.3. Size exclusion chromatography of FhuA405.H_6/FC/TonB protein complexes. Complex formation of C-terminal TonB-fragments of different length and FhuA405.H_6 was tested by 15% SDS-PAGE following the gel filtration step. Panels A-E show the elution peaks of the gel filtration experiments. Lane 1 corresponds to peak 1 and lane 2 corresponds to peak 2. (A) FhuA405.H_6 (lane 1), TonB-77 (lane 2). (B) FhuA405.H_6 and TonB-86 (lane 1), TonB-86 (lane 2). (C) FhuA405.H_6 and TonB-96 (lane 1), TonB-96 (lane 2). The elution peak 1 containing the FhuA/FC/TonB-96 complex shown in lane 1 was incubated with 1% betaine and purified by gel filtration again. Peak 1 from this purification step contains FhuA405.H_6 (lane 3), peak 2 contains TonB-96 (lane 4). (D) FhuA405.H_6 and TonB-116 (lane 1), TonB-116 (lane 2). (E) FhuA405.H_6 and TonB-126 (lane 1) , TonB-126 (lane 2), FhuA405.H_6 and TonB-106 (lane 3) , TonB-106 (lane 4).

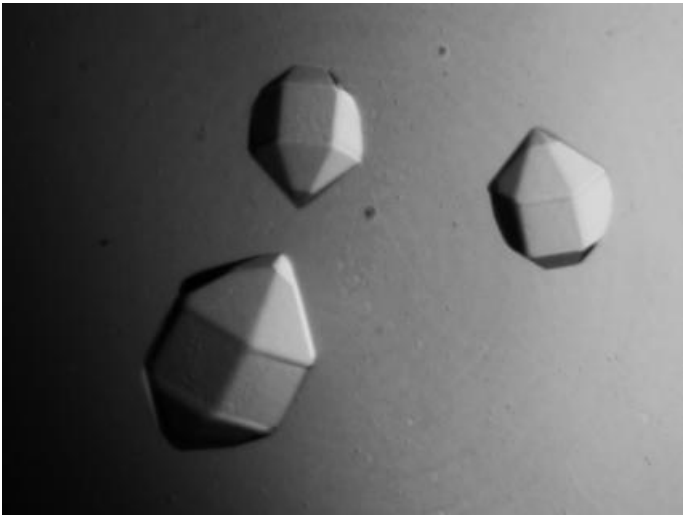

Figure 4.4. Three single TonB-77 crystals grown in 2 M sodium formiate and 0.1 M sodium citrate pH 5.6.

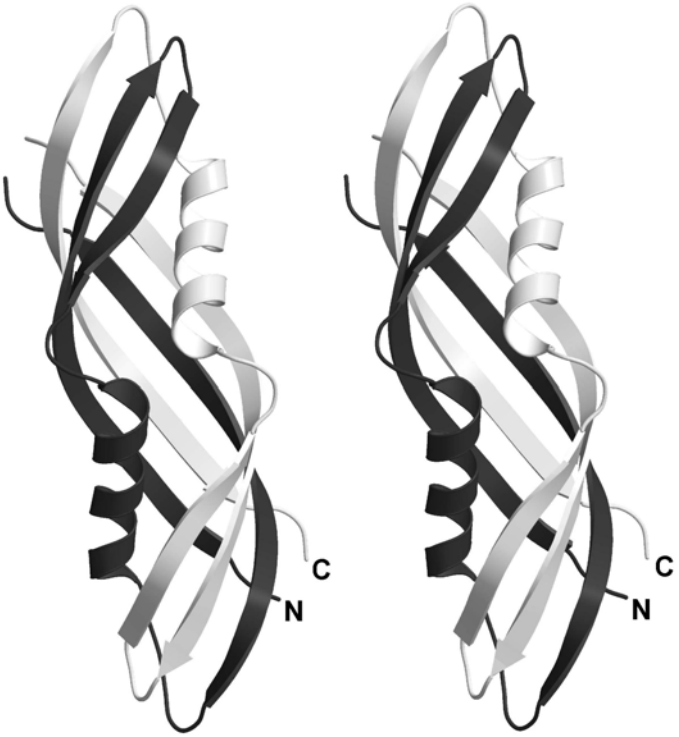

Figure 4.5. Stereo ribbon diagram of the C-terminal fragment TonB-77, showing the intertwined dimer. One TonB-77 molecule is shown in black and the other one in grey. The atomic coordinates have been deposited in the Protein Data Bank (accession code 1QXX).

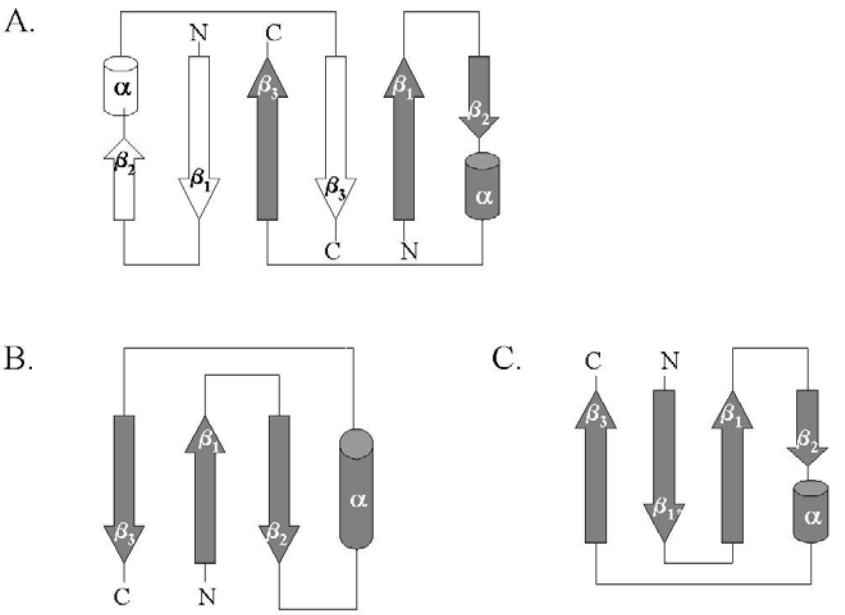

Figure 4.6. Topological diagrams derived from the structures of C-terminal TonB and TolA fragments. The arrows represent β-strands and cylinders represent α-helices. Panel A corresponds to the structure of the C-terminal fragment TonB-86 and TonB-77 from *E. coli* (Chang et al., 2001 and this study). Panel B shows the C-terminal domain of TolA from *P. aeruginosa* (Witty et al., 2002) that is very similar to the structure of TolA from *E. coli* (Lubkowski et al., 1999). Panel C shows a putative topology for the C-terminal domain of TonB-96 derived from the structure of the TonB-77 monomer with an additional N-terminal β-strand consisting of 20 amino acid residues.

5. Crystallization and preliminary X-ray analysis of a C-terminal TonB-fragment from *Escherichia coli*

Jiri Koedding[1§], Patrick Polzer[1], Frank Killig[1], S. Peter Howard[2], Kinga Gerber[1], Peter Seige[1], Kay Diederichs[1] and Wolfram Welte[1]

[1]Department of Biology, University of Konstanz, 78457 Konstanz, Germany, [2]Department of Microbiology and Immunology, University of Saskatchewan, Saskatoon, Saskatchewan Canada S7N 5E5, § To whom correspondence should be addressed

published in *Acta Cryst.* (2004) Vol. D60, 1281 – 1283

5.1. Abstract

The TonB protein located in the cell wall of gram-negative bacteria mediates the proton motive force from the cytoplasmic membrane to specific outer membrane transporters. We have purified and crystallized a C-terminal fragment of TonB of *Escherichia coli* consisting of amino acid residues 147 – 239 (TonB–92). Crystals grew in space group $P2_1$ to a size of about 1.0 x 0.12 x 0.12 mm. A native data set has been obtained at 1.09 Å resolution.

5.2. Introduction

The cell wall of gram-negative bacteria consists of two lipid bilayers, the outer membrane and the cytoplasmic membrane, enclosing the peptidoglycan layer. All essential compounds have to be transported across the outer membrane by diffusion or specific transport pathways. Specific transporters like the iron siderophore receptors FhuA, FepA and FecA or the vitamin B_{12} transporter BtuB are known to be TonB dependent because they are connected to the cytoplasmic membrane by the TonB protein. TonB mediates the chemical potential of the proton gradient across the cytoplasmic membrane (proton motive force) to the specific outer membrane receptors. TonB belongs to a protein complex together with ExbB and ExbD (Bradbeer, 1993; Larsen et al., 1999; Postle and Kadner, 2003) which are both located in the cytoplasmic membrane. TonB consists of 239 amino acid residues with the first 33 residues forming a hydrophobic anchor (Postle, 1993) attaching TonB to the cytoplasmic membrane. The major part of TonB spans the periplasmic space to reach the outer membrane receptors. This function is achieved by a flexible proline-rich region between residues 75 and 107 (Postle et al., 1988) that is not essential for the process of energy transduction (Larsen et al., 1994).

The C-terminal domain of TonB forms the contact to the outer membrane receptor but almost nothing is known about this interaction. It has been shown that a region of critical importance for this protein-protein interaction is located around amino acid residue 160 (Günter et al., 1990). The 3D-structures of two C-terminal fragments of TonB, TonB–86 (residues 155 - 239, Chang et al., 2001) and TonB–77 (residues 164 - 239, Koedding et al., 2004a), respectively, have already been determined. These two TonB fragments crystallized under different conditions and in different space groups. Despite these differences both structures are similar and reveal a cylinder shaped dimer. Each monomer contains three β-strands and a short α-helix arranged in a dimer so that the 6 β-strands can build a large antiparallel β-sheet.

The structure of another energy transducing protein, TolA from *Pseudomonas aeruginosa*, has been solved recently (Witty et al., 2002). TolA belongs to the TolA/Q/R system, a system analogous to the TonB/ExbB/ExbD complex, involved in nutrient import (Braun and Herrmann, 1993). In spite of a sequence identity of only 24% (Lalign server) the crystal structure of the periplasmic domain of TolA shows a

similar topology, however without dimer formation. The importance of dimer formation for the mechanism of energy transduction is thus not yet understood. It has been shown that C-terminal fragments of TonB with more than 90 amino acid residues behave monomeric in solution (Koedding et al., 2004a). However, Sauter et al. (2003) could show that the periplasmic part of TonB is able to dimerize in vivo. Complex formation between monomeric C–terminal fragments of TonB and FhuA has been observed in vitro (Moeck and Letellier, 2001). On the other hand, recently a stoichiometry of 2:1 has been found for TonB–FhuA complexes in vitro (Khursigara et al., 2004).

Here we present the expression, purification and crystallization of TonB–92, a C-terminal fragment of TonB from *Escherichia coli* consisting of the amino acid residues 149-239. Currently we are trying to crystallize TonB–92 with the selenomethionine-substitution method (Doublie, 1997).

5.3. Materials and methods

Expression and purification

The C–terminal fragment of TonB (TonB–92) containing the last 92 amino acid residues of the TonB protein was over-expressed in *Escherichia coli* BL21(DE3) cells containing the plasmid pTB92. For pTB92 the forward primer was US20 (5'- CAT ATG GTG GCT TCA GGA CCA CGC GCA -3'), creating an Nde1 restriction site on the 5'- end of the fragment. The return primer was UR136 (5'- GCT AGT TAT TGC TCA GCG G -3'), which hybridizes to the pET30a vector (Novagen) just downstream of the multiple cloning site and contains a Bpu1102I restriction site. Cloning of the resulting PCR fragment into pCSTonB30 (Howard et al. 2001) created the plasmid pTB92. Cells were grown in tryptone yeast extract "2xYT" supplemented with the antibiotic kanamycin (50 mg per liter culture) at 310 K and induced at OD_{600}=0.7 by the addition of 0.4 mM IPTG (isopropyl-β-D-thiogalactopyranoside, BioVetra). Expression of the 10.2 kDa protein TonB–92 was maintained at 37°C for 2 hours. The pellets from 4 x 500 ml cell culture were resuspended in buffer A (20 mM Tris-HCl pH 8.0/ 100 mM NaCl/ 1 mM EDTA) and the cells were broken by french press (4000 PSIG/ 3 passes). After centrifugation at 15,000 g for 30 min the supernatant was

loaded on an SP Sepharose cation-exchange column (Amersham Biosciences) and was then washed with buffer A. TonB was eluted from the column with a NaCl gradient at a salt concentration of about 300 mM NaCl. The eluate was then desalted on a Sephadex G25 column (Amersham Biosciences) before loading onto another strong cation-exchange column (Source 15s /Amersham Biosciences). The eluted TonB protein containing about 250 mM NaCl was again desalted on a Sephadex G25 column with buffer A (without EDTA) and yielded protein at a concentration of ca. 4 mg/ml. The mobility of the fragments on 15% SDS-PAGE corresponded to their theoretical molecular masses. The purification was carried out within one day to avoid protein degradation. An additional gel filtration step was added. The protein was concentrated up to 10 mg/ml (Amicon spin-column with YMCO 5,000) and glycerol was added to a final concentration of 10%. The TonB sample was then loaded onto a gel filtration column (Superose 12 HR 60/10, Amersham Biosciences) and eluted with buffer A.

Crystallization and data collection

For crystallization the protein sample was concentrated to 20 mg/ml. Initial screening was performed using Crystal Screen I (Jancarik & Kim, 1991), Crystal screen II (Hampton Research) and Wizard Screens I and II (Emerald BioStructures Inc.) at 291 K in 96-well sitting-drop plates (Hampton Research). Crystals of dimensions 0.3 x 0.05 x 0.05 mm were obtained with Wizard Screen I, condition 36. Further refinement yielded crystals in 24-well hanging-drop plates (Hampton Research) with 1 ml reservoir solution [100 mM imidazole pH 8.0, 1.1 M sodium citrate, 100 mM NaCl] within 5 days (Fig. 5.1). The crystallization drop contained 3 µl protein solution (20 mg/ml) and 3 µl reservoir solution. Prior to data collection single crystals were soaked in three different cryoprotectant solutions for one minute each and were then transferred into liquid nitrogen. The cryoprotectant solutions contained reservoir solution supplemented with 5 %, 15 % and 25 % glycerol, respectively. Data collection from the native TonB-92 crystals was carried out to a resolution of 1.09 Å at the beamline X06SA at the SLS, Villigen, Switzerland. Raw data were processed using XDS (Kabsch, 1993).

5.4. Results and discussion

We have expressed a C-terminal fragment of TonB of *Escherichia coli* (TonB–92) containing the last 92 amino acid residues of the protein. TonB-92 was purified to near homogeneity as determined by SDS-PAGE analysis (data not shown) and crystallized at 20 mg/ml with the hanging-drop method (Fig. 5.1). A native data set was collected to 1.09 Å resolution and the raw data were processed with the program XDS (Kabsch, 1993). The space group was determined to be $P2_1$, with 2 molecules per asymmetric unit (Table 5.1). Further data collection statistics are given in Table 5.1. Molecular replacement with the search model 1QXX was carried out with MOLREP (Vagin et al., 1997) from the CCP4 program package (CCP4 1994). This structure represents the TonB–77 dimer (Koedding et al., 2004a) that is very similar to the TonB-86 dimer (Chang et al., 2001). Unfortunately no useful phase information was obtained using this search model either with or without side-chain atoms. Molecular replacement with a model of an isolated monomer of the TonB–77 dimer gave no sufficient phase information either (Table 5.2). Additionally a search model was created based on the putative topology model of TonB–92 (Fig. 5.2) that we proposed previously for the TonB-96 fragment (Koedding et al. 2004a). This model consists of a TonB–77 monomer with an additional β-strand on the N–terminus (shown as a white arrow in Figure 5.2) that might fold between β-strand number 1 and 3. The results of the molecular replacement showed bad packing interactions. Refinement of the data with the program REFMAC5 (Murshudov et al., 1997) failed. The fact that none of these models gave us useful phase information indicates that the structure of Tonb–92 may differ significantly from the published TonB–77 and TonB–86 dimers. We are currently working on phase determination by direct phasing methods and we are also trying to crystallize TonB–92 with incorporated selenomethionine.

Acknowledgements

We thank the staff at the SLS/ Switzerland synchrotron beamline for their support.

5.5. Tables

Table 5.1. Crystal data and X-ray data-collection statistics for a native TonB-92 crystal.

Protein concentration (mg/ml)	20
Crystallization conditions	100 mM imidazole pH 8.0
	1.1 M sodium citrate, 100 mM NaCl
Unit cell parameters	a = 22.58 Å, b = 49.32 Å, c = 72.22 Å,
	α = 90°, β = 97.985°, γ = 90°
Space group	$P2_1$
Resolution (Å)	10 - 1.09 (1.10 – 1.09)
Wavelength (Å)	0.95372 (13.0 keV)
Total measured reflection number	427365
Unique reflections	65348 (1727)
Completeness (%)	99.8 (99.0)
I/σ(I)	11.67 (1.71)
R_{meas} (%)	8.3 (59.2)

Numbers in parentheses refer to the highest resolution shell (1.10 Å -1.09 Å)

R_{meas} was calculated according to Diederichs and Karplus, 1997

Table 5.2. Results of molecular replacement.

	Results of rotation search	Results of translation search	
	[Rf/σ]	[Corr]	[Corr-2]
C-terminal TonB-fragment			
TonB-77 dimer	3.48	0.060	
TonB-77 dimer, polyalanine model	3.53	0.043	
TonB-77 monomer	3.48	0.081	0.117
TonB-77 monomer, polyalanine model	3.72	0.117	0.117

5.6. Figures

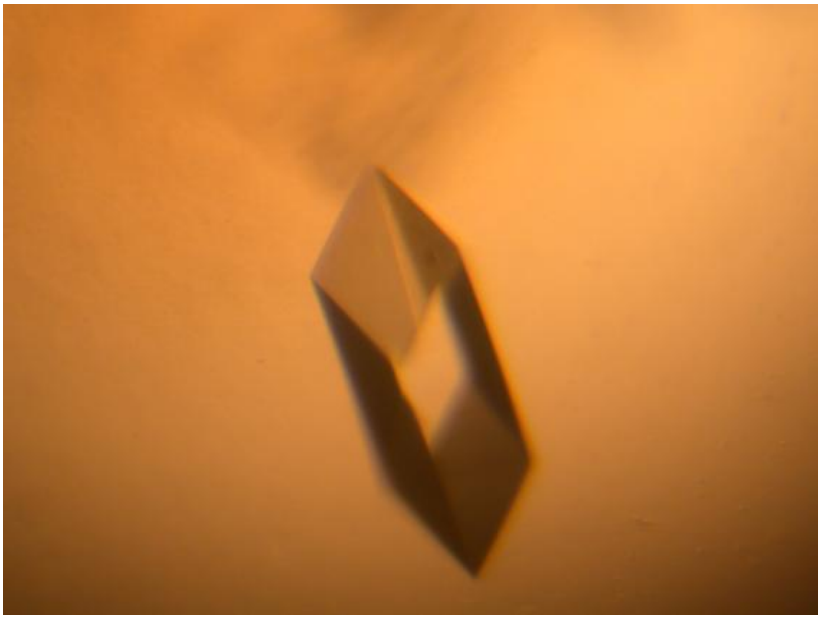

Figure 5.1. A native TonB-92 crystal of the size 1.0 x 0.12 x 0.12 mm grown in space group $P2_1$.

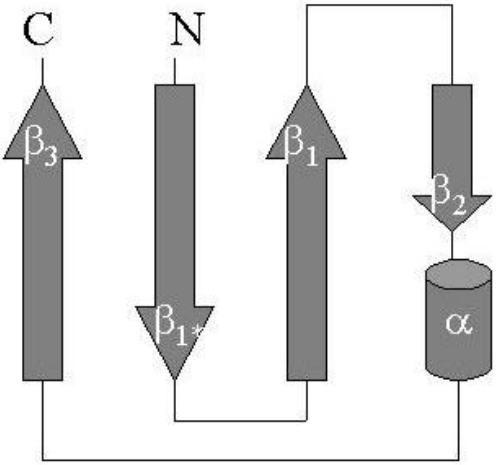

Figure 5.2. Putative topology model of TonB-92.

6. Crystal structure of a 92–residue long C–terminal fragment of TonB from *Escherichia coli* reveals significant conformational changes compared to structures of smaller TonB fragments

Jiri Koedding[1], Frank Killig[1], Patrick Polzer[1], Peter S. Howard[2], Kay Diederichs[1], and Wolfram Welte[1§]

[1]Department of Biology, University of Konstanz, Universitätsstraße 10, 78457 Konstanz, Germany, [2]Department of Microbiology and Immunology, University of Saskatchewan, Saskatoon, Saskatchewan Canada S7N 5E5, § To whom correspondence should be addressed.

(manuscript pending submission)

6.1. Abstract

TonB from *E. coli* is associated with the cytoplasmic membrane and forms a large periplasmic domain capable of interacting with outer membrane transporters. The transport systems that interact with TonB are e.g. FhuA, FecA, and FepA for siderophore uptake and BtuB for Vitamin B_{12} uptake across the outer membrane. These energy dependent uptake processes are driven by the proton motive force of the inner membrane and are mediated by the TonB protein. The receptor–binding domain of TonB is formed by a highly–conserved C–terminal amino acid sequence of approximately 100 residues. Crystal structures of two C–terminal TonB fragments composed of 77 (TonB–77) and 85 (TonB–85) amino acid residues, respectively, have been previously determined (Chang et al., 2001; Koedding et al., 2004a). In both cases the TonB fragments crystallize as dimers consisting of monomers tightly engaged with one another by exchanging a beta hairpin and a C–terminal β-strand. Here we present the crystal structure of a 92–residue long fragment of TonB (TonB–92) at 1.13 Å resolution. It shows a dimer with considerably reduced monomer–monomer interaction compared to other known TonB structures and lacks the characteristic beta–hairpin exchange.

6.2. Introduction

The cell wall of gram–negative bacteria consists of two lipid bilayers, the outer membrane and the cytoplasmic membrane, enclosing the peptidoglycan layer. A number of different transport pathways regulate the uptake of essential compounds into the prokariotic cell. Most substances are translocated through the outer membrane by diffusion porins using a concentration gradient. Substances with a molecular weight of more than 600 Da occurring at very low concentrations like iron siderophores and Vitamin B_{12} need specific uptake systems. The energy for these uptake processes comes from the proton gradient of the cytoplasmic membrane and is transported to the outer membrane by the TonB protein. Three dimensional structures of the following TonB–dependent receptors have been determined by X–ray crystallography: FhuA (Ferguson et al., 1998b; Locher et al., 1998), FepA (Buchanan et al., 1999), FecA (Ferguson et al., 2002), and BtuB (Chimento et al., 2003). All of them share the same basic architecture, a 22–stranded antiparallel β - barrel which is partially filled by an N -terminal globular domain (also called “plug” or “cork”). Exposed to the external medium resides the ligand–binding site, whereas the TonB binding site is located at the periplasmic side of the receptor. A peptide motif near the N–terminus is highly conserved among all TonB–dependent receptors: D7TITV in FhuA, D8ALTV in FecA and D6TLVV in BtuB. This conserved region is called “TonB–box” (Larsen et al., 1997; Cadieux and Kadner, 1999).

Binding of the ligand to the receptor induces conformational changes of the cork–domain. In case of the receptor FhuA, the unwinding of a short α -helix exposed to the periplasm (the so called „switch–helix“) was observed near its N–terminus (Ferguson et al., 1998b). The relocation of the switch – helix likely changes the position and the accessibility of the TonB– box on the periplasmic side of the receptor. These allosteric conformational transitions from the ligand binding site to the periplasmic side may serve to signal the ligand loaded state of the receptor.

The TonB–dependent transporters receive their energy from the proton motive force of the cytoplasmic membrane mediated by a protein complex composed of ExbB, ExbD and TonB (Bradbeer, 1993; Larsen et al., 1999; Postle and Kadner, 2003). ExbB and ExbD are located in the cytoplasmic membrane, whereas TonB is attached to it by an N–terminal transmembrane α -helix (Postle, 1993). The major part of TonB spans

the periplasmic space to reach the outer membrane receptor. Apart from the ExbB/ExbD/TonB protein complex there are two other systems in gram–negative bacteria that are known to use the proton motive force (pmf) of the cytoplasmic membrane. Despite of different biological functions, both systems share homologies with the ExbB/ExbD/TonB protein complex. One system is the stator of the flagellar motor, composed of the proteins MotA and MotB, that depends on the pmf for torque generation (DeRosier, 1998). Another similar system in gram -negative bacteria, the TolQ/TolR/TolA complex, is also involved in the uptake of macromolecules across the outer membrane, therefore being functionally more related to the Ton–system than to the flagellar motor. In this system, TolA has a function similar to TonB, TolQ to ExbB, and TolR to ExbD, respectively. In analogy to the interaction of TonB with outer membrane receptors, the C–terminal periplasmic domain of TolA interacts with the outer membrane Pal lipoprotein in a pmf–dependent manner (Cascales et al., 2000).

The TonB protein of *E. coli* is composed of 239 amino acid residues and can be divided into three domains. A hydrophobic region at the N–terminus (residues 1 to 32) anchors the TonB protein into the cytoplasmic membrane (Postle and Skare, 1988). Residues 12 to 32 are predicted to assume an α - helical conformation with four highly conserved residues, the so called „SHLS–motif“, that were found to be essential for the interaction with the integral membrane protein ExbB (Larsen and Postle, 2001). The transmembrane domain is followed by a periplasmic part consisting of a proline–rich domain and a conserved C–terminal domain, each comprising approximately 100 amino acid residues. 17 % Of the TonB sequence consists of proline residues, most of them are located between residues 75 and 107 (Evans et al., 1986, Moeck and Letellier, 2001).

Several observations indicate that the C–terminal domain of TonB (approximately residues 148 to 239) is involved in direct interactions with the TonB box of the outer membrane receptor (Heller et al., 1988; Günter and Braun, 1990). Synthetic nonapeptides corresponding to the amino acid sequence of TonB between residues 155 and 166 were found to be able to inhibit FhuA–dependent transport of ferrichrome *in vivo* (Killmann et al., 2002). Complex formation between the C–terminal domain of TonB and the outer membrane receptors FhuA or FepA, respectively, has been proven by co–purification (Moeck and Letellier, 2001; Koedding et al., 2004a).

Recently the three–dimensional crystal structures of two truncated C–terminal TonB fragments were reported. One of the fragments, TonB–85, is composed of the last 85 amino acid residues of TonB from *E. coli* (residues 155 – 239, Chang et al., 2001). The other fragment, TonB–77, is composed of the last 77 amino acid residues (residues 163 - 239, Koedding et al., 2004a). Both structures are virtually identical, since the eight additional N–terminal residues of TonB–85 are disordered and cannot be identified in the electron density map. These structures present an intertwined dimer composed of two TonB molecules. Each monomer contains three β - strands and a short α - helix in the order β - β - α - β. The arrangement of the β - strands in the dimer leads to a large 6 – stranded antiparallel β - sheet.

The three dimensional structure of the C–terminal domain of TolA, that belongs to the related TolQ/R/A system, was recently reported for TolA from *Pseudomonas aeruginosa*, alone (Witty et al., 2002) and in complex with the bacteriophage coat protein g3p for TolA from *E. coli* (Lubkowski et al., 1999). In spite of a sequence identity of only 20% between these two TolA proteins, their structures are remarkably similar. They both crystallize as monomers and consist of a three–stranded antiparallel β -sheet flanked by four α - helices positioned on one side of the β - sheet. A structure–based alignment of the C–terminal domains of TolA from *P. aeruginosa* with TonB from *E. coli* results in an amino acid sequence identity of only 18 % (Witty et al., 2002). TolA shares the secondary structure pattern β1 - β2 - α - β3 with TonB-77 and TonB-85. It lacks, however, the β1 - β2 hairpin–exchange observed in the structures of TonB–77 and TonB–85 that enables the formation of a stable dimer.

In this paper we report the crystal structure of a new C –terminal fragment of TonB from *E. coli* at 1.13 Å resolution. TonB–92 contains the last 92 amino acid residues of TonB, being only 7 residues longer than TonB–85. Its three–dimensional structure, however, differs significantly from those of TonB–85 and TonB–77. On the other hand, it shows high resemblance to TolA.

6.3. Experimental Procedures

Protein Expression and Purification

TonB–92, a C–terminal fragment containing the last 92 amino acid residues of the TonB protein of *Escherichia coli*, was over–expressed in BL21(DE3) cells containing the plasmid pTB92 and was subsequently purified to near homogeneity (Koedding et al., 2004b). Purification of the SeMet-TonB-92 was performed according to the protocol for the native TonB-92 with the following exceptions: Cells were grown in M63 minimal medium (Miller, 1972) to an OD600 of 0.6 and a selected set of amino acids was then added to the medium: lysine, phenylalanine and threonine at a concentration of 100 mg /l, leucine, isoleucine and valine at 50 mg/l and selenomethionine at 60 mg/l. 15 Min later, 0.3 mM IPTG was added to start the overexpression of SeMet-TonB-92. Purified SeMet-TonB-92 was concentrated in a 5 kDa filter (Vivaspin) and the flow-through was discarded. The final yield was 1 mg SeMet-TonB-92 per liter culture. For crystallization, SeMet-TonB-92 was used at a concentration of 20 mg/ml.

Crystallization and data collection

Crystallization and data collection of native TonB–92 at 1.13 Å resolution has been described elsewhere (Koedding et al., 2004b). Crystals of selenomethionine–substituted TonB–92 were grown in 100 mM imidazole pH 8.0, 1.1 M sodium citrate and 100 mM sodium chloride using the hanging–drop method. The crystallization drop contained 3 µl protein solution and 3 µl reservoir solution. For X–ray data collection the crystal was flash–frozen at 100 K using reservoir solution supplemented with 20% ethylene glycol as a cryoprotectant. SeMet data were collected at the Swiss Light Source (SLS) beamline X06SA to 2.0 Å resolution and measured at three wavelengths corresponding to the peak -, inflection -, and remote high–wavelength of Selen. The data were processed using XDS (Kabsch, 1993). Data collection statistics are listed in Table 6.1. The space group was determined to be $P2_1$ and the Matthews coefficient is consistent with two molecules per asymmetric unit and a solvent content of 35%.

Structure determination

Experimental phases were derived by the MAD method using a Se-Met data. Four heavy atom sites were identified by SOLVE (Terwilliger and Berendzen, 1999) corresponding to two methionines in the TonB–92 amino acid sequence and two molecules in the asymmetric unit. Initial protein phases were calculated by SOLVE. These phases were further improved by solvent flattening with RESOLVE (Terwilliger, 2000; Terwilliger, 2002) leading to a first polyalanin model of TonB–92 with 123 amino acid residues out of 184. The program also modelled the side chains of 50 amino acid residues. Because of the small number of heavy atoms, a non–crystallographic symmetry (NCS) could not be determined from the heavy atom sites. For finding the NCS, a program (K. Diederichs, unpublished) was used to identify regions with two-fold NCS from the available main-chain fragments. Three corresponding Cα-atoms from each NCS region were chosen to generate a new pseudo-heavy atom coordinate-file for input to RESOLVE. In the next run, RESOLVE found the two–fold NCS in the pseudo-heavy atom sites and used it for phase improvement, leading to a new polyalanine model with 140 amino acid residues (76% of total residues). At this time 69 side chains were modelled correctly. The resulting electron density maps were taken for further manual model building using the programs O (Jones et al., 1991) and COOT (Emsley and Cowtan, 2004). This model was refined against the high resolution data of the native TonB –92 using REFMAC5 (Murshudov et al., 1997) which is part of the CCP4 program–package (Collaborative Computational Project, Number 4). The structure was subsequently refined with SHELXL (Sheldrick and Schneider, 1997). After performing an anisotropic refinement, 201 water molecules and all hydrogen atoms have been modelled, resulting in a final R–factor of 13.4 % and an R_{free} of 18.5 %. Refinement statistics are presented in Table 6.1. Atomic coordinates have been deposited in the Protein Data Bank with the accession code: **1U07**.

Dynamic light scattering (DLS)

DLS experiments with purified TonB–92 were carried out using a DynaPro MS-16-830 instrument (Proterion Corp., High Wycome, UK). The sample volume was 12 µl of protein solution at 2 mg/ml in 20 mM Tris at pH 8.5 and 100 mM NaCl. Each sample was filtered over a 0.02 µm pore filter (Whatman, Anodisc 13) before

measurement. The time dependent intensity signal of the scattered light was evaluated with the program Dynamics Version 6 (Proterion Corp.).

Analytical Ultracentifugation

Experiments were performed on a Beckman XL-A Optima analytical ultracentrifuge equipped with an AN 60 –Ti rotor 316 and an optical absobance system. All experiments were done with freshly purified and gel – filtrated protein solution of TonB –92 at 2 mg/ml in 20 mM Tris pH 8.5 containing 100 mM NaCl. Sedimentation velocity experiments were performed at 20°C and the absorption was scanned 86 minutes after the rotor reached the top speed of 52,000 rpm.

Results of sedimentation equilibrium were obtained at protein concentrations of 0.5, 1.0 and 2 mg/ml, respectively. At 20°C and a rotor speed of 34,000 rpm, equilibrium was achieved after 20 hours. Data were analyzed using the software SEGAL 2.1 (http-reference).

In vitro binding experiments

A protein complex of TonB–92 with ferrichrome loaded FhuA was purified *in vitro* as we have described for other C–terminal TonB–fragments in a recent publication (Koedding et al., 2004a).

6.4. Results

The crystal structure of a C–terminal fragment of TonB from *E.coli* containing 92 amino acid residues (“TonB-92”, residues 148 to 239) was solved at 1.13 Å resolution. Since this fragment contains two methionine residues, we were able to gain phase information by the selenomethionine substitution method (see 6.3.Experimental Procedures). The structure refinement with SHELXL resulted in a well defined model of TonB–92 with an R–factor of 13.4% and an R_{free} of 18.5%. All amino acid residues except the first two N–terminal residues of the a–chain and the first four N–terminal residues of the b–chain were clearly visible in the electron density map.

Description of the experimental structure

TonB-92 presents an overall size for one molecule of approximately 50 Å by 20 Å by 20 Å and secondary structure elements in the order of α*-β1-β2-α - β3 (Figure 6.1). The strands β1, β2, and β3 are combined to a three–stranded β -sheet. The topology of the secondary structure elements is given in Figure 6.2. The C –terminal strand β3 is about 8 amino acid residues longer than β1 or β2 and interacts with the corresponding part of a second TonB–92 molecule by forming an intermolecular antiparallel β -sheet. The dimerization leads to a non–crystallographic two-fold symmetry (Figure 6.3).

Near the N–terminus a segment of eleven residues (Arg 154 – Pro 164, "ES1") possesses backbone conformation close to β-sheet followed by a short α-helix (Ala 165-Leu 170, "α*") which is part of a loop reversing the direction of the main-chain. The following strands β1 and β2 form a type I β -hairpin (Venkatachalam, 1968). The turn between β1 and β2 contains the conserved PDG motif (Pro184-Asp185-Gly186) for the TonB-family. This motif is a frequent sequence in β-hairpins (Gunasekaran et al., 1997) which confer high turn stability even in short peptides (Blandl et al., 2003). A segment "ES2" composed of four residues (Trp213-Glu216) with a conformation close to β-sheet is the adjacent part of segment ES1. Surprisingly, only four hydrogen bonds stabilize the orientation of the extended region ES1: the main chain of Arg154, Leu156 and Ser157 of ES1 form hydrogen bonds with the main chain of Arg214 and Glu216 of ES2 (Figure 6.4). Nevertheless, the electron density of residues of ES1 and of ES2 is well defined (Figure 6.5) and their B–factors do not deviate from the average value. The long C-terminal strand β3 protrudes out of the domain and assiciates with an antiparallel β3' of another TonB-92 molecule resulting in an intermolecular β-sheet.

Comparison with crystal structures of TonB-77 and TonB-85

In the following, the crystal structure of TonB-92 will be compared with the structures of TonB-77 and TonB-85. A superposition of one molecule of TonB-92 and TonB-77 (Figure 6.1 and 6.6) show that the secondary structure elements β1-β2-α-β3 are formed and arranged in a similar way in both structures. In the tight dimer of TonB-77 or TonB-85, respectively, two molecules are engaged by exchanging their β1-β2

hairpins as well as their β3 with one another resulting in the formation of a six-stranded intermolecular β-sheet. In contrast, the β1-β2 hairpin in TonB-92 does not exchange with another molecule and takes up the same place that is filled in the dimer of TonB-77 with the β1'-β2' hairpin of the second molecule (Figure 6.6). This backfolding of the β-hairpin in TonB-92 weakens its monomer-monomer interaction and leads to both a reduced length of β1 and the formation of a new helix α* (Figure 6.1). Strand β1 of TonB-85 starts with the residues Ala169, Leu170, and Arg171, whereas in case of Tonb-92 these residues are part of the helix α*. The presence of seven additional residues of TonB-92 as compared to TonB-85 thus seems to abolish the β1-β2 exchange leading to a remarkably different crystal structure but retaining the basic arrangement of the secondary structure elements (Figure 6.5). In the tight dimer of TonB-85, eleven N-terminal residues (res. 154-162) could not be modelled due to a high flexibility of this region. In the corresponding ES1 segment of TonB-92, residues 158-164 possess dihedral angles close to β-sheet but lack any hydrogen bonds of the backbone and the side-chains of other parts of the molecule. Interactions occur only more N-terminally between residues Arg154-Ser157 and the ES2 segment. TonB-77 and TonB-85 do not contain the helix α*, conversely, these residues show a β-like backbone conformation and are positioned close to the ES2 residues to which they form two hydrogen bonds (Gln168 NE2 and Arg166 NH1). The interaction partners of the ES2 residues are thus shifted by approximately ten residues from the N-terminal end of ES1 in the TonB-92 structure to its C-terminal end. This observation is surprising because TonB-77 and TonB-85 both contain most of the residues from the ES1 region.

Five aromatic amino acid residues were found to be conserved in TonB of several gram-negative bacteria, forming clusters in the TonB-85 dimer. Point mutants of these residues lead to reduced activity of TonB (Ghosh and Postle, 2004). In case of TonB-92 these aromatic residues have a similar orientation (Figure 6.3). Especially the cluster composed of Phe180, Trp213, and Tyr215, respectively, can be superimposed upon the corresponding residues of TonB-85 with low deviation (Figure 6.7). Phe180 resides on the exchangable β-hairpin. For this reason the aromatic cluster (Phe180, Trp213, Tyr215) is formed by residues of both molecules of the TonB-85 dimer, whereas in the structure of TonB-92 all three residues belong to one molecule.

Oligomerization of TonB-92 in solution and complex formation with FhuA

In contrast to the fact that TonB–92 forms a dimer in the crystal, we find a monomeric behaviour of TonB-92 in solution as determined by dynamic light scattering and analytical ultracentrifugation. Dynamic light scattering experiments show mono-dispersity and the autocorrelation function of scattered light intensity can be fitted by assuming a globular protein in solution with a calculated molecular weight of 13 kDa (data not shown). This finding is consistent with the results of the analytical ultra-centrifugation experiments presenting an average molecular weight of 12 kDa and a sedimentation coefficient of S_{20} =1.34. These experimentally determined molecular weights correspond well to the calculated molecular mass of 10.2 kDa for monomeric TonB–92.

In the process of TonB-dependent energy transduction a protein complex between TonB and the outer membrane receptor is necessary. We described in a recent publication the co-purification of several C-terminal fragments of TonB with ferrichrome loaded FhuA by size exclusion chromatography (Koedding et al., 2004a). We repeated this experiment with TonB-92 and found significant complex formation between TonB-92 and the siderophore receptor FhuA *in vitro* (data not shown).

6.5. Discussion

TonB of *E. coli* is known to be essential for the energy coupling between the proton motive force of the cytoplasmic membrane and TonB–dependent outer membrane transporters like FhuA and FepA. The structure of native TonB is not yet known. Recently, the crystal structures of two C–terminal fragments of TonB, TonB–77 (Koedding et al., 2004a) and TonB–85 (Chang et al., 2001), have been determined. Both fragments crystallized as an intertwined homodimer. Here we present the structure of TonB–92, a C–terminal fragment of TonB from *E. coli* containing 92 amino acid residues.

A major difference to the other TonB-fragments is the orientation of the β1/β2-hairpin. In the dimers of TonB–85 and TonB–77 it resides in an extended conformation that completes the 6 stranded intermolecular β - sheet. In the case of

TonB–92 the hairpin folds into one monomer and forms with β3 of the same monomer a three stranded antiparallel β -strand (Figure 6.3). The backfolding of the β -hairpin weakens the monomer – monomer interaction and leads to both a reduced length of β1 in TonB–92 and the formation of a new helix α*. This β -hairpin exchange is driven by the seven additional residues at the N–terminus of TonB–92. On the other hand, if we focus on hypothetical monomers, we can describe the stabilization of the dimeric form of the shorter fragments as a destabilization of the monomers. This theory is supported by the behavior of these TonB-fragments in solution. Results of dynamic light scattering and analytical ultracentrifugation experiments correlate with the monomeric state of TonB–92 in solution. A finding that corresponds to our earlier observations of shorter fragments being dimeric in solution, whereas TonB–96 and longer fragments behave monomeric in solution (Koedding et al., 2004a). It should be emphasized that we cannot rule out the possibility of dimer formation of TonB–92 in solution under conditions differing from those we have used. Nevertheless, the dimer-formation observed in the crystal structure might merely be an artifact of crystallization.

TonB transduces the energy that is used for specific transport processes across the outer membrane. The mechanism of energy transduction is completely unknown. Most likely the C–terminal domain of TonB and the outer membrane receptor build a complex. For this complex formation the region around amino acid residue 160 of TonB seem to be essential (Larsen et al., 1993; Larsen et al., 1997; Moeck et al., 1997; Cadieux and Kadner, 1999; Merianos et al., 2000; Ogierman and Braun, 2003). TonB–92 contains this binding region located at the so called ES1 segment which is stabilized by only few hydrogen bonds with the ES2 region (see chapter 6.4). The structure of TonB-85 gives us no information about this region due to its high flexibility.

We propose the hypothesis that these two TonB structures represent two possible conformations of native TonB during the process of energy transduction. We assume different functions of the C–terminal domain and the periplasmic part of TonB containing the proline-rich repeats. The C–terminal domain and the periplasmic domain fold into distinct domains. In accordance with its three dimensional crystal structure, TonB–92 represents a stable, monomeric and closed conformation of TonB. The transition to the second conformation of the C–terminal domain (represented by

TonB–85) can be achieved by a movement at the N–terminal side of TonB–92. This N–terminal movement has the same effect as the truncation of the first seven amino acid residues of TonB–92. The N–terminal residues Arg154, Leu156 and Ser157 of ES1 are no longer able to form hydrogen bonds (Figure 6.4) and initiate the transition to an open conformation that is represented by one monomer of the TonB–77 or the TonB–85 structure. In the presence of other TonB molecules the open monomers form very stable homodimers. In the absence of other TonB molecules the open monomers interact with the periplasmic side of their outer membrane receptor. Binding experiments of short C–terminal fragments of TonB with FhuA *in vitro* provided evidence for a weak interaction between TonB and FhuA that can be explained by the availability of free TonB in solution, since the association constant of dimerization is much higher than the formation constant of a heterogenic complex with FhuA. In the cell wall of gram–negative bacteria the low copy number of TonB compared to the number of TonB–dependent receptors ensures the complex formation with the outer membrane receptor *in vivo* (Ecker et al., 1986 and Higgs et al., 2002a/b). The lack of inhibition of the ferrichrome uptake by the short TonB-fragments *in vivo* (Koedding et al., 2004a) can also be explained with the dimerization of free TonB molecules in the periplasm during our experiments. The ability of the longer C–terminal fragments of TonB to bind to the outer membrane receptor in an iron-siderophore-dependent manner completes our image of the mechanism of energy translocation. The ligand binding to the receptor causes conformational changes at the periplasmic side of the receptor. This conformational transition like the unwinding of the “switch-helix” (Ferguson et al., 1998b) increases the affinity of the TonB-box of FhuA to bind to the ES1 region of TonB. According to our theory, at this step TonB acts at its ground state of energy, in a closed conformation represented by one monomer of TonB–92. The binding of TonB to the receptor is followed by some kind of energy transduction.

We propose that the tensible force leading to the movement of the N–terminal residues of TonB–92 is mediated by the ExbB/ExbD protein complex driven by the proton motive force. The stoichiometry for the TonB/ExbB/ExbD complex was determined to be 1 : 7 : 2 (Higgs et al., 2002a).

Two models for the energy transduction from the cytoplasmic membrane to the outer membrane receptor of gram-negative bacteria are discussed in the literature (Postle and Kadner, 2003). Our hypothesis of the conformational transition of the C-terminal domain of TonB is based on the transduction of mechanical energy. This kind of

energy transduction is more likely supported by the mechanistic propeller model than by the shuttle model. In case of the shuttle model, TonB crosses the periplasmic space in its excited state. According to our observations with TonB–77 and TonB–85, however, excited TonB immediately dimerizes. In agreement with the propeller model, TonB/ExbB/ExbD shares homologies with the protein complex MotA/MotB of the flagellar motor that uses the proton motive force for torque generation (DeRosier, 1998). The protein–protein interaction of MotA and MotB occurs between the α-helices in the cytoplasmic membrane. A bundle of five helices, four from MotA and one from MotB, forms a transmembrane channel in a larger protein complex with a stoichiometry of 4:2 for MotA / MotB (Braun et al., 2004). The major part of MotB resides in the periplasm with its C–terminal region folding into a peptidoglycan binding domain. According to this arrangement, the ExbB/ExbD/TonB complex is predicted to build five transmembrane α -helices forming a channel that enables a proton flow from the periplasmic space to the cytoplasmic side of the membrane (Zhai et al., 2003). ExbB, a protein predominantly composed of α -helices, provides three transmembrane helices for building the channel, whereas ExbD and TonB only contibute to the complex by one α -helix each. The major part of these two proteins resides in the periplasm. A hypothetical pathway for the proton–transport across the cytoplasmic membrane is based on eight strongly conserved amino acid residues carrying polar hydrogen atoms that face inward the transmembrane channel (Zhai et al., 2003). Although the ExbB/ExbD/TonB–complex and the MotA/MotB–channel share a considerable similarity in their tertiary structure, the ExbB/ExbD/TonB–complex has not been observed to be associated with a rotor protein complex as it is the case for the MotA/MotB–stator of the flagellar motor.

TolA, another energy transducing protein that belongs to the TolQ/R/A system, is known to connect the cytoplasmic membrane with the outer membrane (Cascales et al., 2001). The C–terminal domain of TolA has been successfully crystallized as a monomer (Witty et al., 2002) and shares the backfolding of the β1-β2 hairpin with TonB-92. A superposition of TonB–92 with the C–terminl fragment of TolA is given in Figure 6.8 and shows a very similar orientation of all β-strands and the large α-helix confirming the importance of the closed monomeric conformation for native TonB.

In the present work we report a new three dimensional structure of the C–terminal domain of TonB. The structural difference to other TonB–fragments is based on seven additional amino acid residues at the N–terminus of TonB–92. We consider this structure to be closer to native TonB than the shorter fragments which were determined earlier.

Acknowledgements

We thank the staff at the SLS/Switzerland synchrotron beamline for their support. We are grateful to Ariel Lustig from the Biozentrum Basel/Switzerland for performing the analytical ultracentrifugation of TonB-92. We also thank Ramon Kanaster for assisting us in purifying TonB-92 and Kinga Gerber for helpful discussions.

6.6. Tables

Table 6.1. Data collection and refinement statistics of TonB–92. (Part 1)

	native TonB-92		**SeMet TonB-92**	
Data processing:		**peak**	**inflection**	**remote high**
Wavelength (Å)	0.96862	0.97857	0.97919	0.97784
Unit cell parameters:				
a (Å)	22.58		22.49	
b (Å)	49.32		49.16	
c (Å)	72.22		71.40	
β (°)	97.99		99.36	
Unit cell volume ($Å^3$)	79600		77900	
Solvent content (%)	35.9		34.4	
Resolution (Å)	10 – 1.13			
No. of observed reflections	395729 [36472]	42065 [5668]	37950 [5121]	38020 [5138]
No. of unique reflections	58373 [5727]	20072 [2878]	19945 [2827]	20072 [2853]
Completeness (%)	99.8 [100]	96.9 [86.1]	96.5 [85.1]	96.2 [85.1]
R_{meas} (%) *	7.7 [34.7]	5.6 [17.0]	5.6 [16.9]	5.5 [18.3]
$R_{mrgd\text{-}F}$ (%)	5.4 [23.7]	6.3 [18.7]	6.5 [20.2]	6.8 [21.9]
I/σ_I**	14.0 [5.9]	13.3 [4.9]	12.7 [4.7]	12.9 [4.4]
S_{norm}/S_{ano}	—	1.25 [1.10]	1.12 [1.07]	1.24 [1.07]

Table 6.1. Data collection and refinement statistics of TonB–92. (Part 2)

Refinement statistics:	
Resolution range (Å)	10 – 1.13
R (%)	13.7 [19.9]
R_{free} (%)	18.5
No. of non-hydrogen atoms	1464
No. of residues with 2 conformations	14 (containing 110 atoms)
Residues with 2 conformations in molecule A	Ser157, Asn159, Gln160, Gln175, Asn190 Ser195, Glu216, Ser222, Val226, Ile228
Residues with 2 conformations in molecule B	Asn159, Arg171, Met201, Asn227
No. of solvent water molecules	201
r.m.s. deviation of bond length (Å)	0.015
r.m.s. deviation of bond angles (°)	2.966

Numbers in brackets correspond to the highest resolution shell.

* Diederichs and Karplus, 1997

** Size of anomalous signal as calculated in XDS/XSCALE

6.7. **Figures**

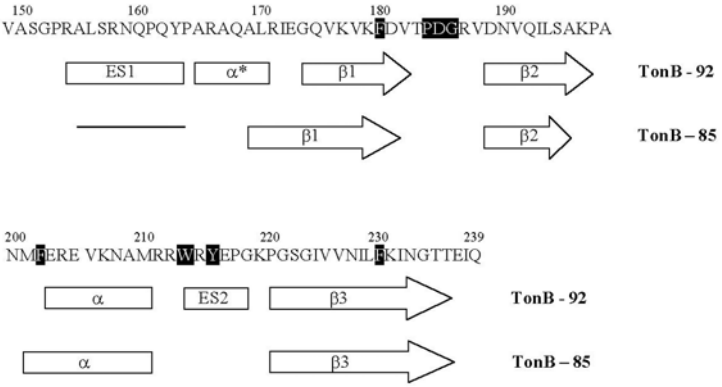

Figure 6.1. Amino acid sequence of the C–terminal fragments of TonB from *E. coli*. The amino acid regions forming secondary structure elements are indicated for TonB–77, TonB–85 (Chang et al., 2001 and Koedding et al., 2004a) and Ton–92 (this study) structures. The region of residues 155 to 164 that is not visible in the electron density map of TonB–85 is marked by a line, β-strands by arrows and α-helices by rectangles. Also indicated is the ES1 and the ES2 segment of TonB-92. Conserved residues are shown with black background.

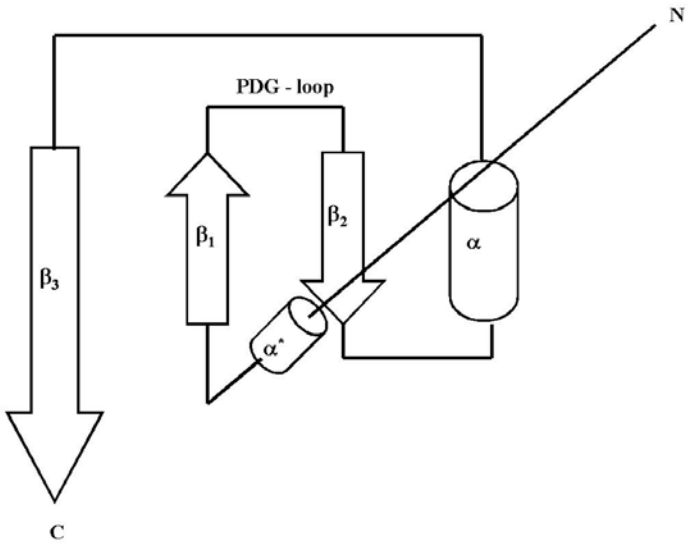

Figure 6.2. Topological diagram of TonB–92 showing secondary structure elements derived from the crystal structure. β-strands are indicated by arrows and α-helices by cylinders. Structure elements which were not observed in the structures of TonB–77 and TonB–85 are marked with a star. The C–terminal part of β3 is forming a β-sheet with another TonB–92 molecule of the homodimer.

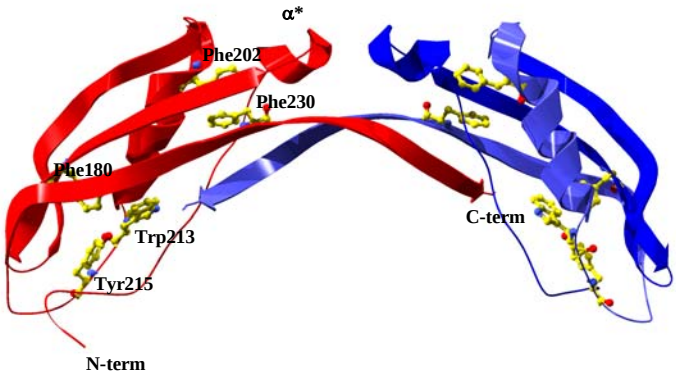

Figure 6.3. Three dimensional structure of the dimeric TonB–92. One molecule is shown in red and the other one in blue. The aromatic residues forming aromatic clusters are shown in ball–and–stick representation.

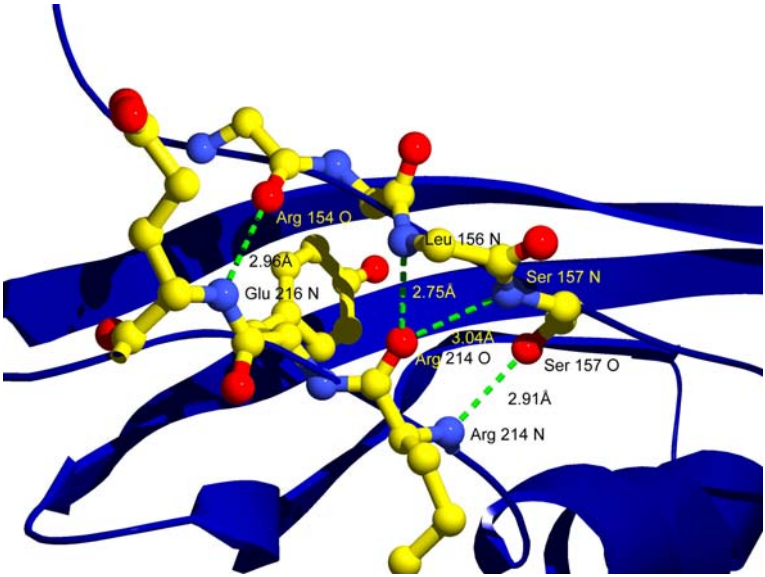

Figure 6.4. Bal–and–stick representation of the amino acid residues of Ton–92 which are involved in stabilizing the extended N–terminal ES1 segment by the formation of hydrogen bonds. The hydrogen bonds are shown as dotted green lines with the distances given in Angstoms (Å). The representation of the side–chain atoms is incomplete.

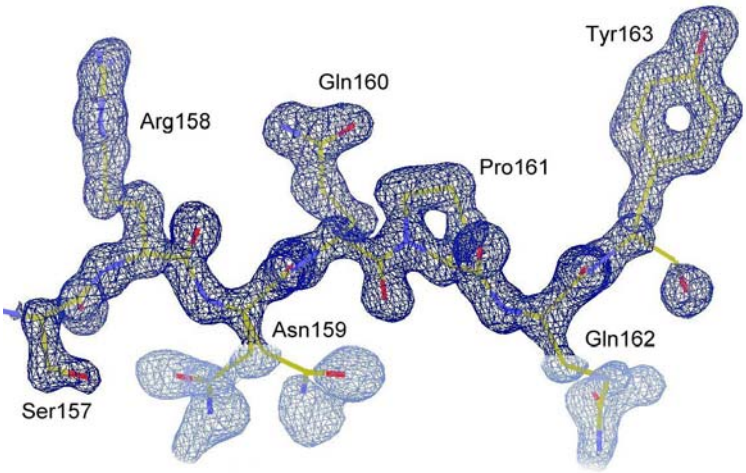

Figure 6.5. Electron density map ($2mF_0$-DF_C) at 3σ (dark blue) and at 2σ (light blue) around amino acid residue Gln160 of TonB–92. The side–chain of Asn159 and Gln162 show conformational changes.

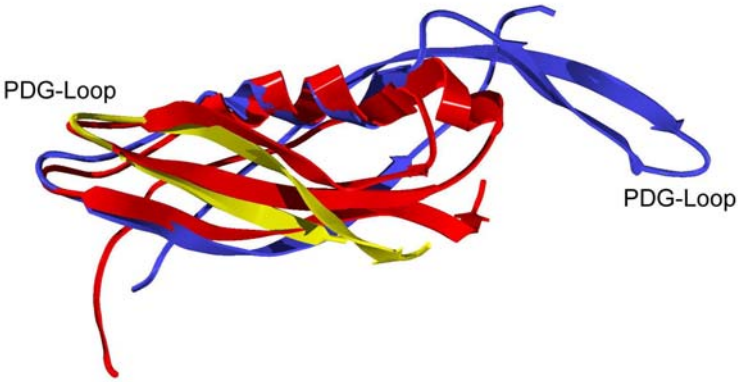

Figure 6.6. Superposition of the three dimensional structures of one molecule of TonB–92 (in red) with one molecule of the TonB–77 or TonB–85 dimer (in blue). The β1 - β2 hairpin of the a second molecule from the dimer of TonB–77 or TonB–85 is shown in yellow. The PDG–loop between β1 and β2 containing residues P184, D185 and G186 is indicated.

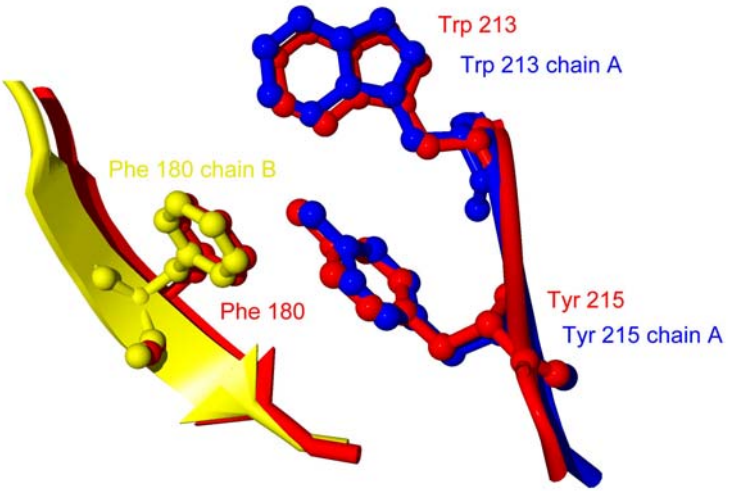

Figure 6.7. Closed view on a superposition of the aromatic residues F180, W213 and Y215 of TonB structures. The residues from TonB–92 are colored in red and the residues of TonB–77 or TonB–85 in blue and yellow depending on their location at the TonB monomers.

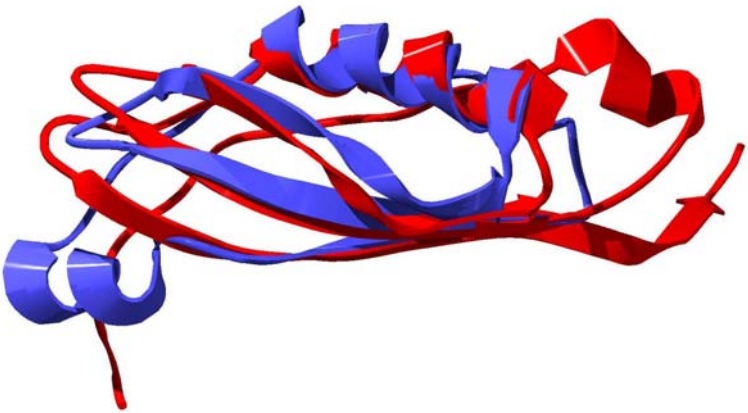

Figure 6.8. Superposition of the three dimensional structures of one molecule of TonB–92 (colored in red) and the C–terminal domain of TolA from *E. coli* (colored in blue) (pdb accession code: 1Tol, Lubkowski et al., 1999).

7. References

Ames, G.F. (1988) Structure and mechanism of bacterial periplasmic transport systems. *J. Bioenerg. Biomembr*. **20**, 1-18

Anderson, C., Bachmeyer, C., Tauber, H., Benz, R., Wang, J., Michel, V., Newton, S. M. C., Hofnung, M., and Charbit, A. (1999) In vivo and in vitro studies of major surface loop deletion mutants of the Escherichia coli K-12 maltoporin: contribution to maltose and maltooligosaccharide transport and binding. *Mol. Microbiol*. **32**, 851–867

Benz, R., Schmid, A., Greetje, H., and Vos-Scheperkeuter, H. (1987) Mechanism of sugar transport through sugar-specific LamB channel. *J. Membr.Biol*. **100**, 21–29

Blandl, T., Cochran, A.G., and Skelton, N.J. (2003) Turn stability in beta-hairpin peptides: Investigation of peptides containing 3:5 type I G1 bulge turns. *Protein Sci*. **12**, 237-247

Bonhivers, M., Ghazi, A., Boulanger, P., and Letellier, L. (1996) FhuA, a transporter of the *Escherichia coli* outer membrane is converted into a channel upon the binding of bacteriophage T5. *EMBO J*. **15**, 1850-1856

Bonhivers, M., Desmadril, M., Moeck, G., Boulanger, P., Colomer-Pallas, A., and Letellier, L. (2001) Stability studies of FhuA, a two-domain outer membrane protein from Escherichia coli. *Biochemistry* **40**, 2606–2613

Borths, E.L., Locher, K.P., Lee, A.T., and Rees, D.C. (2002) The structure of E. coli BtuF and binding to its cognate ATP binding cassette transporter. *Proc. Nat. Acad. Sci*. USA **99**, 16642–16647

Bös, C, Lorenzen, D., and Braun, V. (1998) Specific *in vivo* labelling of cell surface-exposed protein loops: reactive cysteines in the predicted gating loop mark a

ferrichrome binding site and a ligand-induced conformational change of the *Escherichia coli* FhuA protein. *J. Bacteriol*. **180**, 605-613

Bradbeer, C. (1993) The proton motive force drives outer membrane transport of cobalamine in Escherichia coli. *J. Bacteriol*. **175**, 3146–3150

Braun, V., Günther, K., Hantke, K., and Zimmermann, L. (1983) Intracellular activation of albomycin in *Escherichia coli* and *Salmonella typhimyrium*. *J. Bacteriol.* **156**, 308–315

Braun, V. (1989) The structurally related exbB and tolQ genes are interchangeable in conferring tonB-dependent colicin, bacteriophage, and albomycin sensitivity. *J. Bacteriol*. **171**, 6387–6390

Braun, V., Gunter, K., and Hantke, K. (1991) Transport of iron across the outer membrane. *Biol Met*. **4**, 14-22

Braun, V., and Herrmann, C. (1993) Evolutionary relationship of uptake systems for biopolymers in Escherichia coli: cross-complementation between the TonB-ExbB-ExbD and the TolA-TolQ-TolR proteins. *Mol. Microbiol*. **8**, 261–268

Braun, V., Hantke, K., and Köster, W. (1998) Iron transport and storage in microorganisms, plants, and animals. In: Sigel, A., Sigel, H. (eds.), *Metal Ions in Biological Systems*, (New York: Marcel Dekker Inc.) **35**, 67–145

Braun, M., Killmann, H., and Braun, V. (1999) The β-barrel domain of FhuAΔ5-160 is sufficient for TonB-dependent FhuA activities of *Escherichia coli*. *Mol. Microbiol*. **33**, 1037-1049

Braun, V., and Braun, M. (2002) Active transport of iron and siderophore antibiotics. *Curr. Opin. Microbiol*. **5**, 194-201

Braun, T.F., Al-Mawsawi, L.Q., Kojima, S., and Blair, D.F. (2004) Arrangement of core membrane segments in the MotA/MotB proton–channel complex of Escherichia coli, *Biochemistry* **43**, 35–45

Brewer, S., Tolley, M., Trayer, I.P., Barr, G.C., Dorman, C.J., Hannavy, K., Higgins, C.F., Evans, J.S., Levine, B.A., and Wormald, M.R. (1990) Structure and function of X-Pro dipeptide repeats in the TonB proteins of Salmonella typhimurium and Escherichia coli.
J. Mol. Biol. **216**, 883-895.

Briat, J.F. (1992) Iron assimilation and storage in prokaryotes. *J. Gen. Microbiol*. **138**, 2475-2483.

Bruenger, A.T., Adams P.D., Clore G.M., DeLano W.L., Gros P., Grosse-Kunstleve R.W., Jiang J.S., Kuszewski J., Nilges M., Pannu N.S., Readd R.J., Rice L.M., Simonson T., and Warren G.L. (1998) Crystallography and NMR system (CNS): a new software suite for macromolecular structure determination. *Acta Cryst*. **D54**, 905-921

Buchanan, S.K., Smith, B.S., Venkatramani, L., Xia, D., Esser, L., Palnitkar, M., Chakraborty, R., and van der Helm, D. (1999) Crystal structure of the active outer membrane transporter FepA of Escherichia coli. *Nat. Struc. Biol*. **6**, 56–63

Cadieux, N., and Kadner, R.J. (1999) Site-directed disulfide bonding reveals an interaction site between energy-coupling protein TonB and BtuB, the outer membrane cobalamine transporter. *Proc. Natl. Acad. Sci. U S A.* **96**, 10673-10678

Cascales, E., Gavioli, M., Sturgis, J., and Lloubès, R. (2000) Proton motive force drives the interaction of the inner membrane TolA and outer membrane Pal proteins in Escherichia coli. *Mol. Microbiol*. **38**, 904–915

Cascales, E., Lloubes, R., and Sturgis, J.N. (2001) The TolQ-TolR proteins energize TolA and shares homologies with the flagellar motor proteins MotA-MotB. *Mol. Microbiol*. **42**; 795–807

Chang, C., Mooser, A., Pluckthun, A., and Wlodawer, A. (2001) Crystal Structure of the C-terminal Domain of TonB Reveals a Novel Fold *J. Biol. Chem*. **276**, 27535–27540

Chimento, D.P., Mohanty, A.K., Kadner, R.J., and Wiener, M.C. (2003) Substrate-induced transmembrane signaling in the cobalamine transporter BtuB. *Nat. Struct. Biol*. **10**, 394-401

Clarke, T.E., Tari, L.W., and Vogel, H.J. (2001) Structural biology of bacterial iron uptake systems. *Curr. Top. Med. Chem*. **1**, 7-30

Clarke, T.E., Braun, V., Winkelmann, G., Tari, L.W., and Vogel, H.J. (2002) X-ray crystallographic structures of the Escherichia coli periplasmic protein FhuD bound to hydroxamate-type siderophores and the antibiotic albomycin. *J. Biol. Chem*. **277**, 13966-13972

Collaborative **C**omputational **P**roject, Number **4**. (1994) *Acta Cryst.* D50, 760-763

Coulton, J.W., Mason, P., Cameron, D.R., Carmel, G., Jean, R., and Rode, H.N. (1986) Protein fusions of galactosidase to the ferrichrome-iron receptor of Escherichia coli. *J. Bacteriol*. **165**, 181–192

Cowan, S. W., Schirmer, T., Rummel, G., Steiert, M., Ghosh, R., Pauptit, R. A., Jansonius, J. N., and Rosenbusch, J. (1992) Crystal structures explain functional properties of two *E.coli* porins *Nature* **358**, 727–733

Curtis, N.A., Eisenstadt, R.L., Turner, K.A., and White, A.J. (1985) Porin-mediated cephalosporin resistance in Escherichia coli K-12. *J. Antimicrobial. Chemother*. **15**, 642–644

DeRosier, D.J. (1998) The turn of the screw: the bacterial flagellar motor, *Cell* **93**, 17–20

de Veaux, L.C., Clevenson, D.S., Bradbeer, C., and Kadner, R.J. (1986) Identification of the btuCED polypeptides and evidence for their role in vitamin B12 transport in Escherichia coli. *J. Bacteriol*. **167**, 920-927

Diederichs, K., and Karplus, A. P. (1997) Improved R-factors for diffraction data analysis in macromolecular crystallography. *Nature Struct. Biol*. **4**, 269–275

Doublie, S. (1997) Preparation of selenomethionyl proteins for phase determination. *Methods. Enzymol*. **276**, 523 – 530. Academic Press

Ecker, D.J., Matzanke, B.F., and Raymond,K.N. (1986) Recognition and transport of ferric enterobactin in Escherichia coli. *J. Bacteriol*. **167**, 666–673

Edelstein, S.J., and Schachman H.K. (1973) Measurement of partial specific volume by sedimentation equilibrium in H2O-D2O solutions. *Methods Enzymol*. **27,** 82-98

Emsley, P., and Cowtan, K. (2004) Coot: Model-building Tools for molecular graphics. *Acta Cryst. D*, *in press*

Evans, J.S., Levine, B.A., Trayer, I.P., Dorman, C.J., and Higgins, C.F. (1986) Sequence imposed structural constraints in the TonB protein of Escherichia coli. *FEBS Lett.* **208,** 211-216

Ferguson, A.D., Breed, J., Diederichs, K., Welte, W. and Coulton, J.W. (1998a) An internal affinity-tag for purification and crystallization of the siderophore receptor FhuA, integral outer membrane protein from *Escherichia coli* K-12. *Prot. Sci*. **7**, 1636-1638

Ferguson, A.D., Hofmann, E., Coulton, J.W., Diederichs, K., and Welte, W. (1998b) Siderophore-Mediated Iron Transport: Crystal Structure of FhuA with bound Lipopolysaccharide. *Science.* **282**, 2215-2220

Ferguson, A.,D., Welte, W., Hofmann, E.,Lindner, B., Holst, O., Coulton, J.W., and Diederichs, K. (2000a) A conserved structural motif for lipopolysaccharide recognition by procaryotic and eucaryotic proteins. *Structure* **8**, 585–592

Ferguson, A.D., Braun, V., Fiedler, H.-P., Coulton, J.W., Diederichs, K., and Welte, W. (2000b) Crystal structure of the antibiotic albomycin in complex with the outer membrane transporter FhuA. *Protein Sci*. **9**, 956–963

Ferguson, A.D., Ködding, J., Walker, G., Bös, C., Coulton, J.W., Diederichs, K., Braun, V., and Welte, W. (2001) Active transport of an antibiotic rifamycin derivative by the outer-membrane protein FhuA. *Structure* **9**, 707–716

Ferguson, A.D., and Deisenhofer, J. (2002) TonB-dependent receptors–structural perspectives. *Biochimica et Biophysica Acta* **1565**, 318–332

Ferguson, A. D., Chakraborty, R., Smith, B.S., Esser, L., van der Helm, D., and Deisenhofer, J. (2002) Strucural basis of gating by the outer membrane transporter FecA. *Science* **295**, 1715-1719

Forst, D., Welte, W., Wacker, T., and Diederichs, K. (1998) Structure of the sucrose-specific porin ScrY from Salmonella typhimurium and its complex with sucrose. *Nature Struct. Biol*. **5**, 37–46

Fischer, E., Strelow, B., Hartz, D., and Braun, V. (1990) Soluble and membrane-bound ferrisiderophore reductases of Escherichia coli K-12. *Arch. Microbiol*. **153**, 329–336

Ghosh, J., and Postle, K. (2004) Evidence for dynamic clustering of carboxy-terminal aromatic amino acids in TonB-dependent energy transduction. *Mol. Microbiol*. **51**, 203–213

Günther, K., and Braun, V. (1990) In vivo evidence for FhuA outer membrane receptor interaction with the TonB inner membrane protein of Escherichia coli. *FEBS Lett.* **274**, 85–88

Gunasekaran, K., Ramakrishnan, C.,and Balaram, P. (1997) Beta-hairpins in proteins revisited: lessons for de novo design. *Protein Eng*. **10**, 1131-1141.

Hancock, R.E. (1997) The bacterial outer membrane as a drug barrier. *Trends Microbiol*. **5**, 37-42

Hantke, K., and Braun V. (1978) Functional interaction of the tonA/tonB receptor system in *Escherichia coli*. *J. Bacteriol*. **135,** 190-197

Hartmann, G.R., *et al*., Weiss, W. (1985) Molekulare Wirkungsweise des Antibioticums Rifampicin. *Angew. Chemie* **97**, 1011-1017

Heller, K., and Kadner, R.J. (1985) Nucleotide sequence of the gene for the vitamin B_{12} receptor protein in the outer membrane of *Escherichia coli*. *J. Bacteriol*. **161**, 904–908

Heller, K., Kadner, R.J., and Günter, K. (1988) Suppression of the btuB451 mutation by mutations in the tonB gene suggests a direct interaction between TonB and TonB-dependent receptor proteins in the outer membrane of Escherichia coli. *Gene* **64**, 147–153

Higgs, P.I., Larsen, R.A., and Postle, K. (2002a) Quantification of known components of the Escherichia coli TonB energy transduction system: TonB, ExbB, ExbD and FepA. *Mol. Microbiol.* **44**, 271–281

Higgs, P.L., Letain, T.F., Merriam, K.K., Burke, N.S., Park, H., Kang, C., and Postle, K. (2002b) TonB interacts with nonreceptor proteins in the outer membrane of Escherichia coli. *J. Bacteriol*. **184**, 1640–1648

Howard, S.P., Herrmann C., Stratilo C.W., and Braun V. (2001) In vivo synthesis of the periplasmic domain of TonB inhibits transport through the FecA and FhuA iron siderophore transporters of Escherichia coli. *J. Bacteriol*. **183,** 5885-5895

http://www.rcsb.org/pdb/cgi/explore.cgi?pid=70671060950031&page=0&pdbId=1IHR *(PDB for TonB-77)*

http://www.biozentrum.unibas.ch/personal/jseelig/AUC/software00.html *(SEGAL)*

Hussein, S., Hantke, K., and Braun, V. (1981) Citrate-dependent iron transport system in Escherichia coli K-12. *Eur. J. Biochem*. **117**, 431-437

Ingham, C., Buechner M., Adler J. (1990) Effect of outer membrane permeability on chemotaxis in Escherichia coli. *J. Bacteriol*. **172,** 3577-3583

Jancarik, J., Kim, S.-H. (1991) Sparse matrix sampling: a screening method for crystallization of proteins. *J. Appl. Cryst*. **24**, 409–411

Jones, T.A., Zou, J.Y., Cowan, S.W. and Kjeldgaard, M. (1991) Improved methods for building protein models in electron density maps and the location of errors in these models. *Acta Cryst. A* **47**, 110-119

Jurkevitch, E., Hadar, Y., Chen, Y., Libman, J. and Shanzer, A. (1992) Iron uptake and molecular recognition in *Pseudomonas putida*: Receptor mapping with ferrichrome and its biomimetic analogs. *J. Bacteriol*. **174**, 78-83

Kabsch, W. (1988) Evaluation of single crystal X-ray diffraction data from a position sensitive detector. *J. Appl. Crystallogr*. **21**, 916-924

Kabsch, W. (1993) Automated processing of rotation diffraction data from crystals of initially unknown symmetry and cell constants. *J. Appl. Cryst*. **26**, 795–800

Kadner, R.J., Heller, K., Coulton, J.W. and Braun, V. (1980) Genetic control of hydroxamate-mediated iron uptake in *Escherichia coli*. *J. Bacteriol*. **143**, 256-264

Kadner, R.J., and Heller, K.J. (1995) Mutual inhibition of cobalamine and siderophore uptake systems suggests their competition for TonB function. *J. Bacteriol*. **177**, 4829–4835

Kadner, R.J. (1996) Cytoplasmic membrane. In: *E.coli and Salmonella*, Cellular and Molecular Biology. Neidhardt, F.C. (ed.), Washington DC, ASM Press, pp.58–87

Khursigara, C.M., DeCrescenzo, G., Pawelek, P.D., and Coulton, J.W. (2004) Enhanced binding of TonB to a ligand-loaded outer membrane receptor: role of the oligomeric state of TonB in formation of a functional FhuA.TonB complex. *J. Biol. Chem*. **279**, 7405–7412

Killmann, H., Herrmann, C., Wolff, H., and Braun, V. (1998) Identification of a new site for ferrichrome transport of Escherichia coli, Salmonella paratyphi B, Salmonella typhimyrium, and Pantoea agglomerans. *J. Bacteriol*. **180**, 3845–3852

Killmann, H., Braun M., Herrmann C., Braun V. (2001) FhuA barrel-cork hybrids are active transporters and receptors. *J. Bacteriol*. **183,** 3476-3487

Killmann, H., Herrmann, C., Torun, A., Jung, G., and Braun, V. (2002) TonB of Escherichia coli activates FhuA through interaction with the beta-barrel. *Microbiology* **148**, 3497–3509

Koebnik, R. (1993) The molecular interaction between components of the TonB-ExbBD-dependent and of the TolQRA-dependent bacterial uptake systems. *Mol. Microbiol*. **9**, 219

Koedding, J., Howard, P., Kaufmann, L., Polzer, P., Lustig, A., and Welte, W. (2004a) Dimerization of TonB is not essential for its binding to the outer membrane siderophore receptor FhuA of Escherichia coli. *J. Biol. Chem*. **279**, 9978–9986

Koedding, J., Polzer, P., Killig, F., Howard, S.P., Gerber, K., Seige, P., Diederichs, K., and Welte, W. (2004b) Crystallization and preliminary X –ray analysis of a C –terminal TonB –fragment from Escherichia coli. *Acta Cryst.* **D60**, 1281–1283

Koedding, J., Killig, F., Polzer, P., Howard, S.P., Diederichs, K., and Welte, W. (2004c) Crystal structure of a 92-residue long C –terminal fragment of TonB from Escherichia coli reveals significant conformational changes compared to structures of smaller TonB-fragments. (manuscript pending submission)

Korteland, J., Tommassen, J., and Lugtenberg, B. (1982) PhoE protein pore of the outer membrane of E.coli K-12 is a particularly efficient channel for organic and inorganic phosphate. *Biochim. Biophys. Acta* **690**, 282–289

Koster, W., and Braun, V. (1990) Iron (III) hydroxamate transport into Escherichia coli. Substrate binding to the periplasmic FhuD protein. *J. Biol. Chem.* **265**, 21407-21410.

Koster, W. (1991) Iron(III) hydroxamate transport across the cytoplasmic membrane of Escherichia coli. *Biol. Met.* **4**, 23-32

Kraulis, P.J. (1991) MOLSCRIPT: a program to produce both detailed and schematic plots of protein structures. *J. Appl. Crystallogr*. **24**, 946-950

Krone, W.J.A., Stegehuis, F., Koningstein, G., van Dorn, C., Roosendaal, B., de Graaf, F.K., and Oudega, B. (1985) Characterization of the pColV-K30 encoded cloacin DF13/aerobactin outer membrane receptor protein of Escherichia coli: isolation and purification of the protein and analysis of its nucleotide sequence and primary structure. *FEMS Microbiol.Lett*. **26**, 153–161

Lalign server: http://www.ch.embnet.org/software/LALIGN_form.html

Larsen, R.A., Wood, G.E., and Postle, K. (1993) The conserved proline-rich motif is not essential for energy transduction by Escherichia coli TonB protein. *Mol. Microbiol.* **10**, 943–953

Larsen, R. A., Foster-Hartnett, D., McIntosh, M. A., and Postle, K. (1997) Regions of Escherichia coli TonB and FepA proteins essential for in vivo physical interactions. *J. Bacteriol.* **179**, 3213-3221

Larsen, R.A., Thomas, M.G., and Postle, K. (1999) Protonmotive force; ExbB and ligand-bound FepA drive conformational changes in TonB. *Mol. Microbiol*. **31**, 1809–1824

Larsen, R.A., and Postle, K. (2001) Conserved residues Ser(16) and His(20) and their relative positioning are essential for TonB activity, cross-linking of TonB with ExbB, and the ability of TonB to respond to proton motive force. *J. Biol. Chem.* **276**, 8111-8117

Larsen, R.A., Letain, T.E., and Postle, K. (2003) In vivo evidence of TonB shuttling between the cytoplasmic and outer membrane of E. coli. *Mol. Microbiol*. **49**, 211–218

Lebowitz, J., Lewis M.S., and Schuck P. (2002) Modern analytical ultracentrifugation in protein science: a tutorial review. *Protein Sci*. **11,** 2067-2079

Letain, T.E., and Postle, K. (1997) TonB protein appears to transduce energy by shuttling between the cytoplasmic membrane and the outer membrane of Escherichia coli. *Mol. Microbiol.* **24**, 271–283

Liu, Y., and Eisenberg D. (2002) 3D domain swapping: As domains continue to swap. Review. *Protein Science* **11,**1285-1299

Locher, K.P., and Rosenbusch, J.P. (1997) Oligomeric states and siderophore binding of the ligand-gated FhuA protein that forms channels across Escherichia coli outer membranes. *Eur. J. Biochem*. **247**, 770–775

Locher, K.P., Rees, B., Koebnik, R., Mitschler, A., Moulinier, L., Rosenbusch, J., and Moras, D. (1998) Transmembrane Signalling across the Ligand-Gated FhuA Receptor: Crystal Structures of Free and Ferrichrome-Bound States Reveal Allosteric Changes. *Cell* **95**, 771–778

Locher, K.P., Lee, A.T., and Rees, D.C. (2002) The *E. coli* BtuCD structure: a framework for ABC transporter architecture and mechanism. *Science* **296**, 1091–1098

Locher, K.P., and Borths, E. (2004) ABC transporter architecture and mechanism: implications from the crystal structures of BtuCD and BtuF. *FEBS Lett*. **564**, 264-268.

Lubkowski, J., Hennecke, F., Plückthun, A., and Wlodawer, A. (1999) Filamentous phage infection: crystal structure of g3p in complex with its coreceptor, the C-terminal domain of TolA. *Structure* **7**, 711–722

Lundrigen, M.L., and Kadner, R.J. (1986) Nucleotide sequence of the gene for the ferrienterocholin receptor FepA of Escherichia coli. *J. Biol. Chem*. **261**, 10797–10801

Matzanke, B.F., Anemuller, S., Schunemann, V., Trautwein, A.X., and Hantke, K. (2004) FhuF, part of a siderophore-reductase system. *Biochemistry* **43**, 1386-1392

Medzhitov, R., and Janeway, C.A. (1997) Innate Immunity: The virtues of a nonclonal system of recognition. *Cell* **91**, 295–298

Merianos, H.J., Cadieux, N., Lin, C.H., Kadner, R.J., and Cafiso, D.S. (2000) Substrate induced exposure of an energy-coupling motif of a membrane transporter. *Nature Struct. Biol*. **7**, 205–209

Merrit, E.A. and Bacon, D.J. (1997) Raster3D photorealistic molecular graphics. *Methods Enzymol*. **277**, 505-524

Miller, J.H. (1972) *Experiments in Molecular Genetics.* Cold Spring Harbour Laboratory Press, New York, NY

Moeck, G.S., Bazzaz B.S., Gras M.F., Ravi T.S., Ratcliffe M.J., and Coulton J.W. (1994) Genetic insertion and exposure of a reporter epitope in the ferrichrome-iron receptor of Escherichia coli K-12. *J. Bacteriol*. **176,** 4250-4259

Moeck, G.S., Tawa, P., Xiang, H., Ismail, A.A., Turnbull, J.L., and Coulton, J.W. (1996) Ligand-induced conformational change in the ferrichrome-iron receptor of Escherichia coli K-12. *Mol. Microbiol.* **22**, 459–471

Moeck, G.S., Coulton, J.W., and Postle, K. (1997) Cell envelope signalling in Escherichia coli. Ligand binding to the ferrichrome-iron receptor FhuA promotes interaction with the energy-transducing protein TonB. *J. Biol. Chem*. **272**, 28391–28397

Moeck, G.S., and Letellier L. (2001) Characterization of in vitro interactions between a truncated TonB protein from Escherichia coli and the outer membrane receptors FhuA and FepA . *J. Bacteriol*. **183,** 2755-2764

Muller, K., Matzanke, B.F., Schunemann, V., Trautwein, A.X., and Hantke, K. (1998) FhuF, an iron-regulated protein of Escherichia coli with a new type of [2Fe-2S] center. *Eur. J. Biochem*. **258**, 1001-1008

Murshudov, G. N., Vagin, A. and Dodson, E. J. (1997) Refinement of Macromolecular Structures by the Maximum-Likelihood Method. *Acta Cryst.* D53, 240-255

Nau, C.D., and Konisky, J. (1989) Evolutionary relationship between the TonB-dependent outer membrane transport proteins: nucleotide and amino acid sequences of the Escherichia coli colicin I receptor gene. *J. Bacteriol*. **171**, 1041–1047

Neilands, J.B., Konopka, K., Schwyn, B., Coy, M., Francis, R.T., Paw, B.H., and Bagg, A. (1987) Comparitive biochemistry of microbial iron assinilation. In: Winkleman, G., van der Helm, D., Neilands, J.B. (eds.), *Iron Transport in Microbes, Plants and Animals*. VCH Press, Weinheim, pp. 3–33

Nikaido, H. (1996) Outer membrane in: *E.coli and Salmonella*. Cellular and Molecular Biology. Neidhardt, F.C. (ed.), Washington DC, ASM Press, pp.29–49

Nikaido, H., and Hall, J.A. (1998) Overview of bacterial ABC transporters. *Methods Enzymol*. **292**, 3-21

Ogiermann, M., and Braun, V. (2003) Interactions between the outer membrane ferric citrate transporter FecA and TonB: studies of the FecA TonB box. *J. Bacteriol*. **185**, 1870–1885

Otwinowski, Z., and Minor W. (1997) Processing of X-ray diffraction data collected in oscillation mode. *Meth. Enzymol*. **276**, 307-326.

Plançon, L., Chami, M. and Letellier, L. (1997) Reconstitution of FhuA, an *Escherichia coli* outer membrane protein, into liposomes. Binding of phage T5 to FhuA triggers the transfer of DNA into the proteoliposomes. *J. Biol. Chem*. **272**,16868-16872

Postle, K., and Skare, J.T. (1988) Escherichia coli TonB protein is exported from the cytoplasm without proteolytic cleavage of its amino terminus. *J. Biol. Chem*. **263**, 11000–11007

Postle, K. (1990) TonB and the gram-negative dilemma. *Mol. Microbiol*. **4**, 2019–2025

Postle, K. (1993) TonB protein and energy transduction between membranes. *J. Bioenerg. Biomembr*. **25**, 591–601

Postle, K., and Kadner, R.J., (2003) Touch and go: tying TonB to transport. *Mol. Microbiol*. **49**, 869–882

Pressler, U., Staudenmaier, H., Zimmermann, L., and Braun, V. (1988) Genetics of the iron dicitrate transport system of Escherichia coli. *J. Bacteriol*. **170**, 2716–2724

Pugsley, A.P., Zimmermann, W., and Wehrli, W. (1987) Highly efficient uptake of a rifamycin derivative via the FhuA-TonB-dependent uptake route in Escherichia coli. *J. Gen. Microbiol*. **133**, 3505–3511

Raetz, C.R.H. (1996) *E.coli and Salmonella*, Cellular and Molecular Biology. Neidhardt, F.C. (ed.), Washington DC, ASM Press, pp.29–47

Sauer, M., Hantke, K., and Braun, V. (1990) Sequence of the *fhuE* outer-membrane receptor gene of Escherichia coli K-12 and properties of mutants. *Mol. Microbiol*. **4**, 427–437

Sauter, A., Howard, S.P., and Braun, V. (2003) In vivo evidence for TonB dimerization. *J. Bacteriol*. **185**, 5747–5754

Schirmer, T., Keller, T. A., Wang, Y. F., and Rosenbusch, J. (1995) Structural basis for sugar translocation through maltoporin channels at 3.1 Å resolution. *Science* **267**, 512–514

Schöffler, H. and Braun, V. (1989) Transport across the outer membrane of *Escherichia coli* K12 via the FhuA receptor is regulated by the TonB protein of the cytoplasmic membrane. *Mol. Gen. Genet*. **217**, 378-383

Scott, D.C., Cao Z., Qi Z., Bauler M., Igo J.D., Newton S.M., and Klebba P.E. (2001) Exchangeability of N termini in the ligand-gated porins of *Escherichia coli*. *J. Biol. Chem*. **276,** 13025-13033

Sheldrick, G.M., and Schneider, T.R. (1997) SHELXL: High resolution refinement. *Methods Enzymol*. **277**, 319–343

Skare, J.T., Ahmer, B.M.M., Seachord, C.L., Darveau, R.P., and Postle, K. (1993) Energy transduction between membranes – TonB, a cytoplasmic membrane protein,

can be chemically cross-linked in vivo to the outer membrane receptor FepA. *J. Biol. Chem*. **272**, 16302–16308

Sprencel, C., Cao, Z., Qi, Z., Scott, D.C., Montague, M.A., Ivanoff, N., Xu, J., Raymond, K.M., Newton, S.M., and Klebba, P.E. (2000) Binding of ferric enterobactin by the Escherichia coli periplasmic protein FepB. *J. Bacteriol*. **182**, 5359-5364.

Stephens, D.L., Choe, M.D., and Earhart, C.F. (1995) Escherichia coli periplasmic protein FepB binds ferrienterobactin. *Microbiology*. **141**, 1647-1654

Terwilliger, T.C., and Berendzen, J. (1999) Automated MAD and MIR structure solution. *Acta Cryst*. **D55**, 849–861

Terwilliger, T.C. (2000) Maximum likelihood density modification. Acta Cryst. **D56**, 965-972

Terwilliger, T.C. (2002) Automated main – chain model – building by template – matching and iterative fragment extension. *Acta Cryst* **D59**, 34–44

Traub, I., Gaisser, S., and Braun, V. (1993) Activity domains of the TonB protein. *Mol. Microbiol*. **8**, 409–423

Usher, K.C., Ozkan E., Gardner K.H., and Deisenhofer J. (2001) The plug domain of FepA, a TonB-dependent transport protein from Escherichia coli, binds its siderophore in the absence of the transmembrane barrel domain. *Proc. Natl. Acad. Sci. U S A.* **98,** 10676-10681

Vagin, A., Teplyakov, A. (1997) Molrep: an automated program for molecular replacement. *J. Appl. Cryst*. **30**, 1022–1025

Vakharia, H.L., and Postle K. (2002) FepA with Globular Domain Deletions Lacks Activity. *J. Bacteriol*. **184**, 5508-5512

Venkatachalam, C.M. (1968) Related Stereochemical criteria for polypeptides and proteins. V. Conformation of a system of three linked peptide units. *Biopolymers* **6**, 1425-1436

Wehrli, W., *et al*., Zak, O. (1987) CGP 4832, a semisynthetic rifamycin derivative highly active against some Gram-negative bacteria. *J. Antibiotics* **40**, 1733-1739

Welte, W., Weiss, M.S., Nestel, U., Weckesser, J., Schiltz, E., and Schulz, G.E. (1991) Prediction of the general structure of OmpF and PhoE from the sequence and structure of porin from Rhodobacter capsulatus. Orientation of porin in the membrane. *Biochim. Biophys. Acta* **1080**, 271–274

Welte, W., Nestel, U., Wacker, T., and Diederichs, K. (1995) Structure and function of the porin channel. *Kidney Int*. **48**, 930–940

Witty, M., Sanz, C., Shah, A., Grossmann, J.G., Mizuguchi, K., Perham, R.N., and Luisi, B. (2002) Structure of the periplasmic domain of Pseudomonas aeruginosa TolA: evidence for an evolutionary relationship with the TonB transporter protein *EMBO J*. **21**, 4207–4218

Zhai, Y.F., Heijne, W., and Saier, M.H. (2003) Molecular modeling of the bacterial outer membrane receptor energizer, ExbBD/TonB, based on homology with the flagellar motor, MotAB *Biochim. Biophys. Acta* **1614**, 201–210

Single–letter abbreviations for the amino acid residues are as follows: A, Ala; C, Cys; D, Asp; E, Glu; F, Phe; G, Gly; H, His; I, Ile; K, Lys; L, Leu; M, Met; N, Asn; P, Pro; Q, Gln; R, Arg; S, Ser; T, Thr; V, Val; W, Trp; and Y, Tyr.